# 無線通訊系統
# (Wireless Communications Systems)

國立清華大學電機系暨通訊工程研究所
蔡育仁
台達館 821 室
Tel: 62210
E-mail: yrtsai@ee.nthu.edu.tw



# Chapter 2
# Propagation Effects

# Path Loss and Shadowing

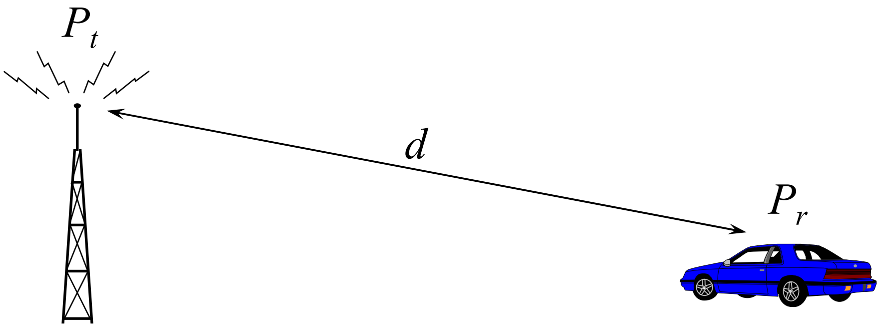


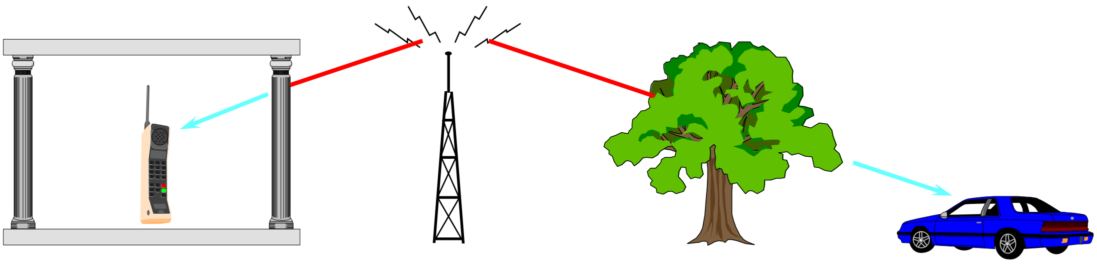



# Multipath Propagation

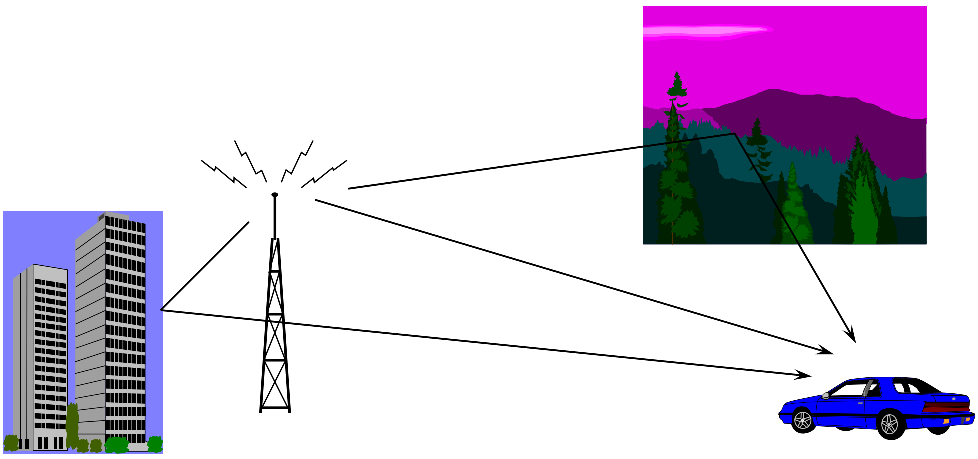

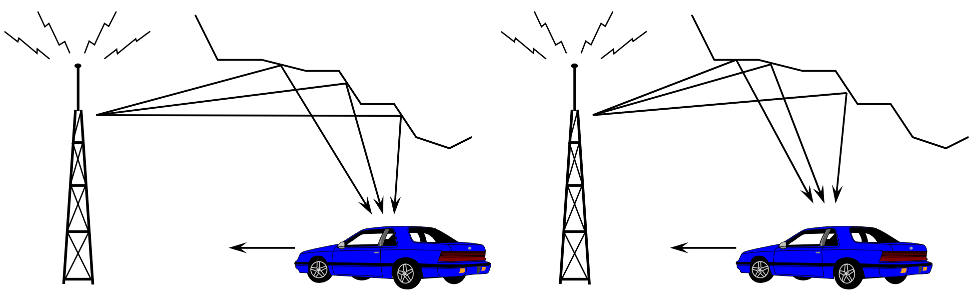

# Fast Multipath Fading

- The variation of propagation channel results in the change of the received signal strength
- For the same propagation environment, **different frequency components** may experience different fading characteristics

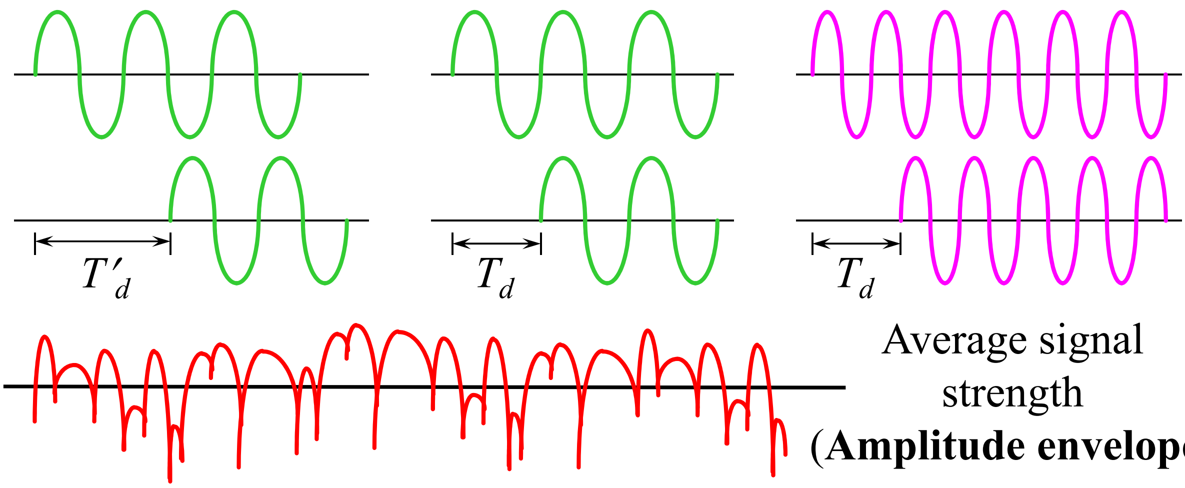


Average signal strength (**Amplitude envelope**)



# Radio Propagation

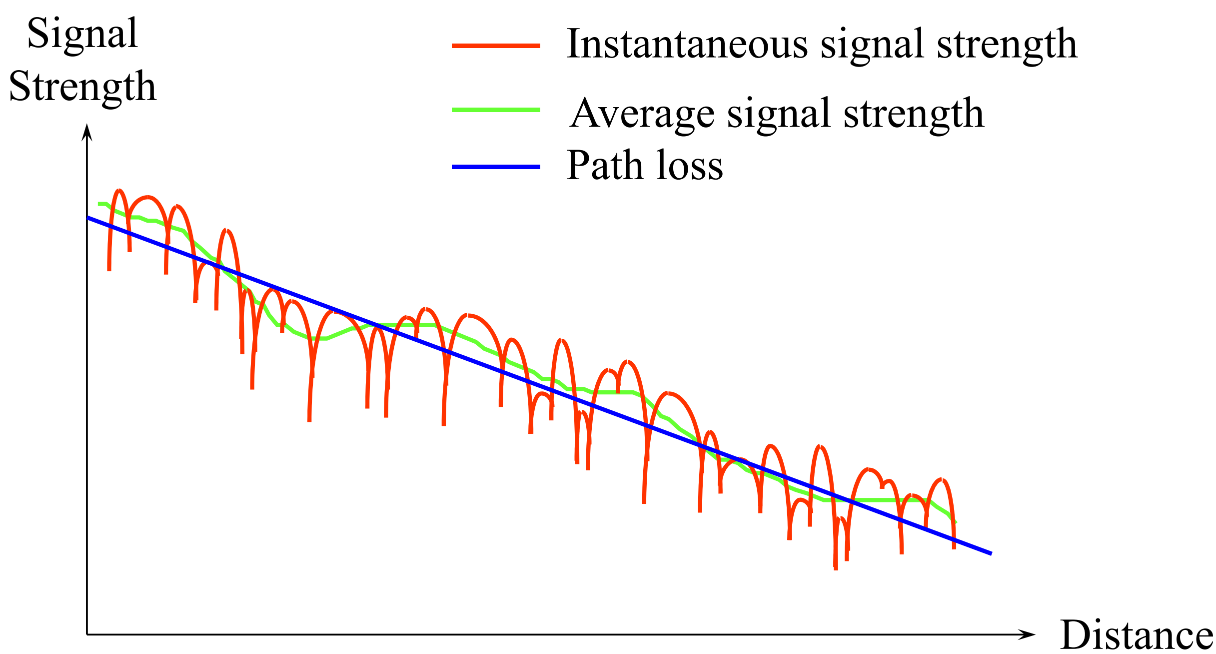

# Basic Concepts of Propagation Modeling



# Radio Propagations

- **Reciprocity Theorem :** If a propagation path exists, it carries energy equally well in **both directions**
- An MS in a typical macrocellular environment is usually surrounded by local scatterers
  - The plane waves arrive from many directions without a direct **LOS (Line-Of-Sight)** component

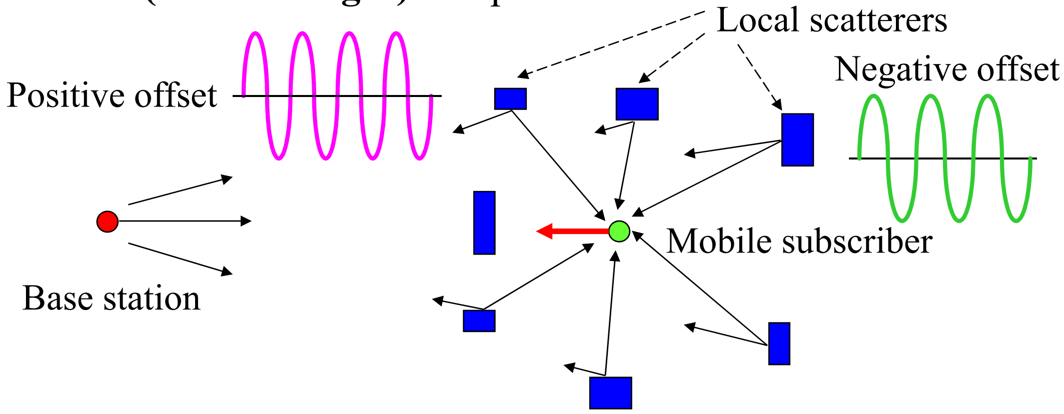

# Radio Propagations (Cont.)

- **MS** in a **macrocellular** system: **isotropic scattering**
  - The arriving plane waves arrive from **all directions** with **equal probability**
  - In general, no direct LOS path exists between an MS and the BS
- **BS** in a **macrocellular** system: relatively free from local scatterers
  - The plane waves tend to arrive from **one general direction**
  - The cell radius is from 0.5km to several kilometers
- In a **microcellular** environment:
  - The BS antennas are only moderately elevated above the local scatterers
  - The cell radius is from 100m to several hundred meters
  - **A direct LOS path** may exist between an MS and the desired BS



# Doppler (Frequency) Shift

- **Doppler (frequency) shift** is introduced for a mobile user
  - MS velocity: $v$
  - The **incidence angle** of the incoming wave: $\theta_n(t)$

$$f_{D,n}(t) = f_m \cos\theta_n(t) \quad \text{Hz}$$

  - where $f_m = v/\lambda_c$ and $\lambda_c$ is the wavelength

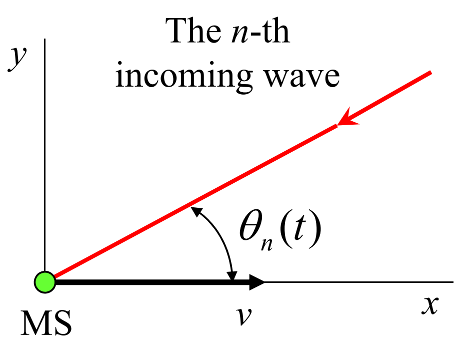

# Multipath Fading Channel

- Consider the transmission of the band-pass signal $s(t)$:

$$s(t) = \Re\left\{ \tilde{s}(t) e^{j2\pi f_c t} \right\}$$

  – $\tilde{s}(t)$ is the complex envelope and $f_c$ is the carrier frequency
- The received band-pass signal is:

$$r(t) = \Re\left\{ \tilde{r}(t) e^{j2\pi f_c t} \right\}$$

  – $\tilde{r}(t)$ is the complex envelope

$$\boxed{\alpha_n(t);\ \tau_n(t);\ f_{D,n}(t)}$$

$$r(t) = \Re\left\{ \sum_{n=1}^{N} \alpha_n(t)\, e^{j2\pi\left(f_c + \underline{f_{D,n}(t)}\right)\left(t - \underline{\tau_n(t)}\right)}\ \tilde{s}(t - \tau_n(t)) \right\}$$

$$= \Re\left\{ \sum_{n=1}^{N} \alpha_n(t)\, e^{-j2\pi\left[\left(f_c + f_{D,n}(t)\right)\tau_n(t) - f_{D,n}(t)t\right]}\ \tilde{s}(t - \tau_n(t)) e^{j2\pi f_c t} \right\}$$

$$= \Re\left\{ \tilde{r}(t) e^{j2\pi f_c t} \right\}$$



# Multipath Fading Channel (Cont.)

- The received complex low-pass signal (for an $N$-path channel):

$$\tilde{r}(t) = \sum_{n=1}^{N} \alpha_n(t)\, e^{-j2\pi\left[\left(f_c + f_{D,n}(t)\right)\tau_n(t) - f_{D,n}(t)t\right]}\ \tilde{s}(t - \tau_n(t))$$

  – $\alpha_n(t)$ is the amplitude gain and $\tau_n(t)$ is the time delay

$$\Rightarrow \tilde{r}(t) = \sum_{n=1}^{N} \alpha_n(t)\, e^{-j\phi_n(t)}\ \tilde{s}(t - \tau_n(t))$$

  – The phase associated with the $n$-th path is

$$\phi_n(t) = 2\pi\left[\left(f_c + f_{D,n}(t)\right)\tau_n(t) - f_{D,n}(t)t\right]$$

- The phase can be regarded as a **uniformly random** phase
  – Since $f_c \times \tau_n(t) >> 1$

# Channel Modeling as a Filter

- The channel is modeled as a time-variant linear filter

$$g(\tau,t)=\sum_{n=1}^{N}\alpha_n(t)e^{-j\phi_n(t)}\delta(\tau-\tau_n(t))$$

  - A small change in path delay $\tau_n(t)$ causes a large change in phase $\phi_n(t)$ (due to a very large $f_c+f_{D,n}(t)$)
  - Random **amplitude and phase** for each received path

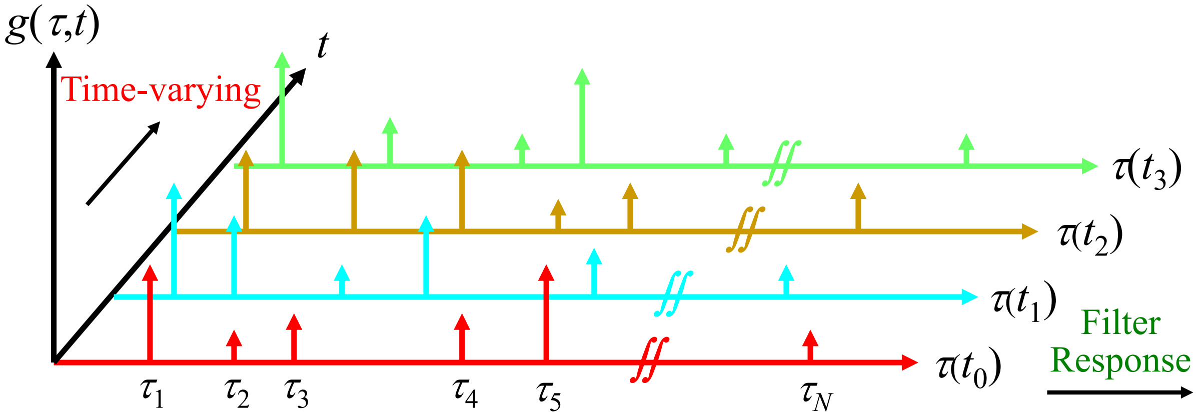




# Channel Modeling as a Filter (Cont.)

- If multiple impulse signals are transmitted at $t_0$, $t_1$, …

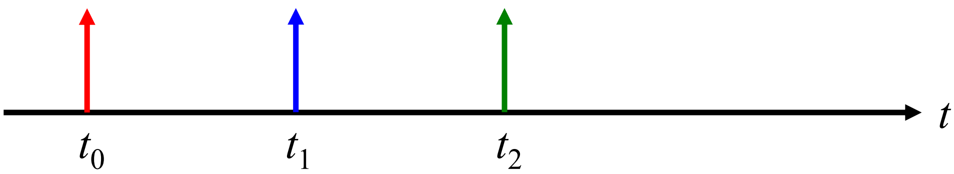


- The signal received at a receiver is

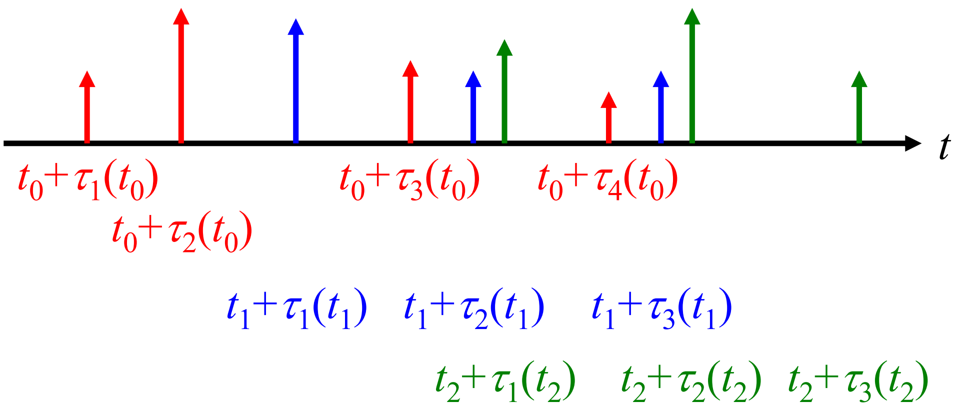

# Freq.-Selective & -Non-Selective Fading

- **Frequency-non-selective:** if the differential of path delays $\tau_i - \tau_j$ are small compared to the duration of a modulated symbol, $\tau_n$ are all approximately equal to $\hat{\tau}$

$$g(\tau,t) \cong \sum_{n=1}^{N} \alpha_n(t) e^{-j\phi_n(t)} \delta(\tau - \hat{\tau}) = g(t)\delta(\tau - \hat{\tau})$$

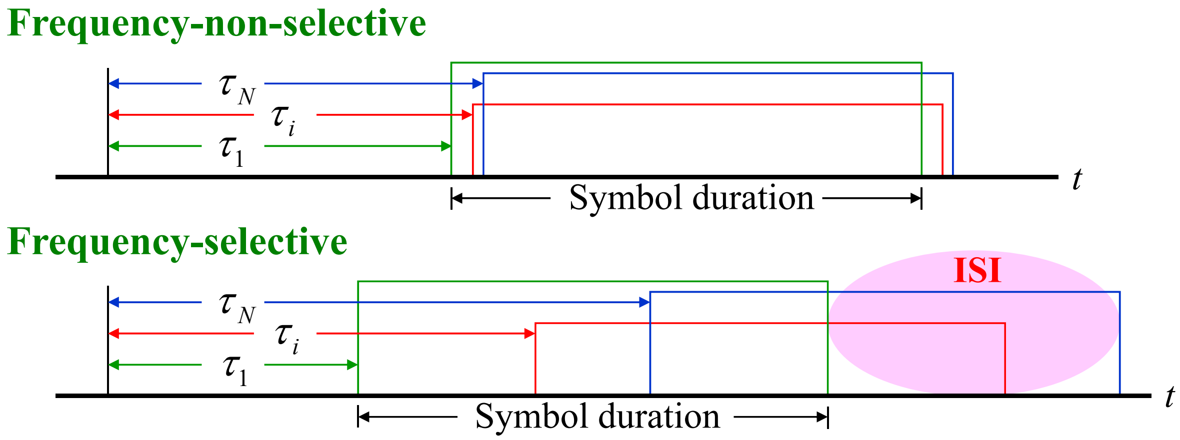




# Freq.-Selective & -Non-Selective Fading (Cont.)

- **Frequency-selective:** if the differential of path delays $\tau_i - \tau_j$ are comparable to the duration of a modulated symbol

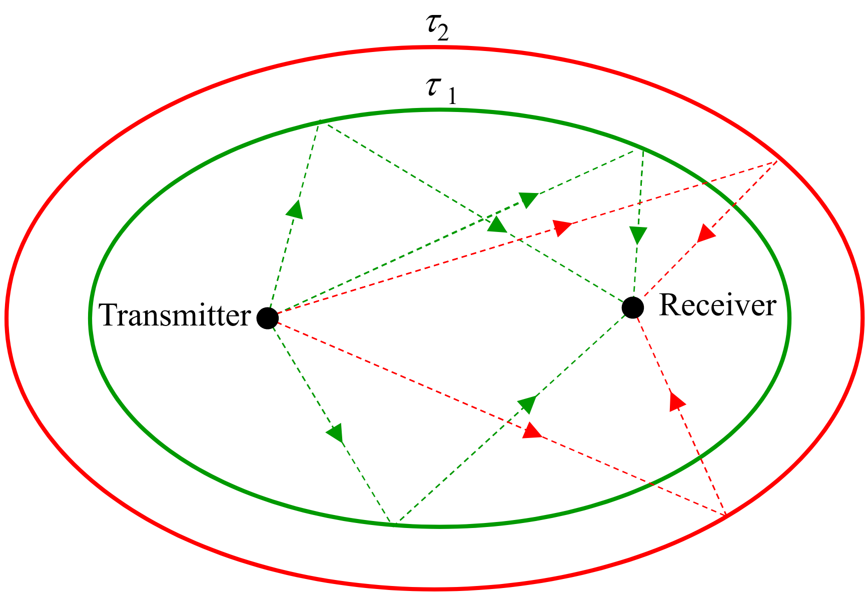

# Frequency-Non-Selective Multipath Fading

- **Frequency-non-selective multipath fading:**
  - Narrow-band transmission
  - Signal bandwidth << coherence bandwidth
  - The inverse of the signal bandwidth >> time spread of the propagation path delay
  - Modulated symbol duration >> time spread of the propagation path delay
  - All frequency components experience **the same random attenuation and a linear phase shift**
  - Very little or no distortion ⇒ **no ISI**, do not need equalization

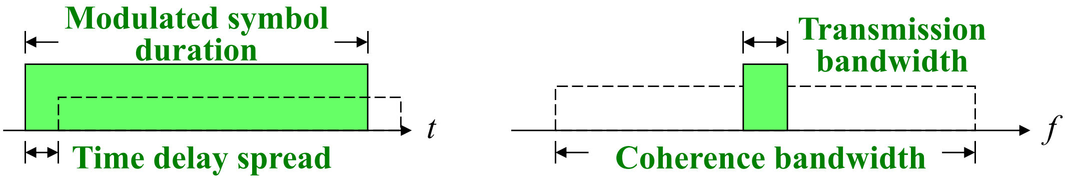




# Frequency-Selective Multipath Fading

- **Frequency-selective multipath fading:**
  - Wide-band transmission
  - Signal bandwidth >≈ coherence bandwidth
  - The inverse of the signal bandwidth ≈< the time spread of the propagation path delay
  - Modulated symbol (or chip) duration ≈< time spread of the propagation path delay
  - Different frequency components may experience **different random attenuation and a non-linear phase shift**
  - Significant distortion ⇒ ISI, **equalization or RAKE is need**

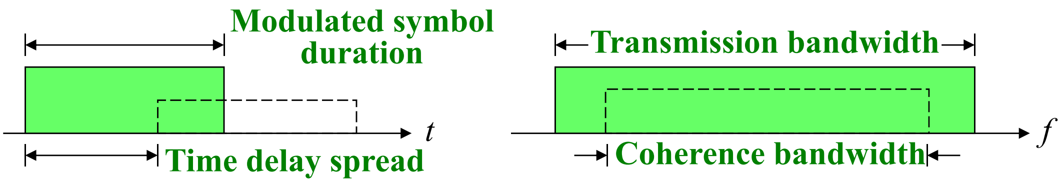

# Question

- The multipath delay profiles of two propagation channels are shown as follows:

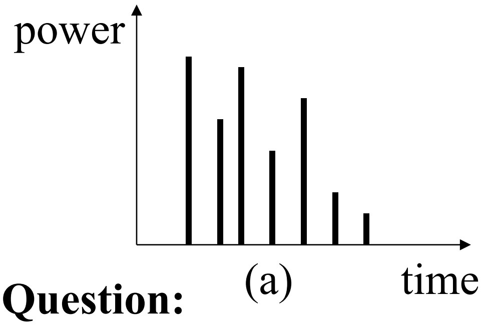


(a)

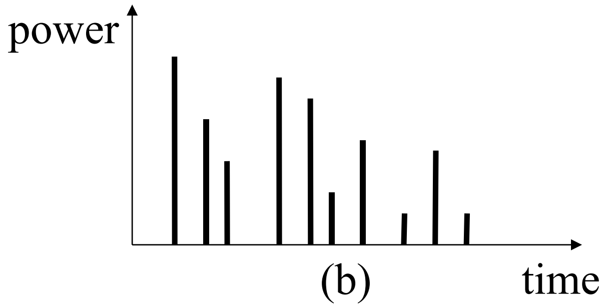


(b)

- **Question:**
  - These two channels are **Frequency-selective or Frequency-non-selective**?
  - How to determine the environment is **Frequency-selective or Frequency-non-selective**?
  - Can we say that an environment is **Frequency-selective or Frequency-non-selective** for all communication systems?



# Frequency-Non-Selective (Flat) Multipath Fading

# Freq.-Non-Selective Multipath Fading

- At any time $t$, the random phase $\phi_n(t)$ may result in the **constructive** or **destructive** addition of the $N$ components
- If the differential of path delays $\tau_i - \tau_j$ is small compared to the duration of a modulated symbol, for all $i \neq j$, all the path delays are approximately equal to $\hat{\tau}$
- Since the carrier frequency is very high, small differences in the path delays will correspond to **large differences** in $\phi_n(t)$

  $\Rightarrow$ The received signal still experiences fading
- The channel impulse response can be approximated as

$$g(\tau,t) = \sum_{n=1}^{N} \alpha_n(t) e^{-j\phi_n(t)} \delta(\tau - \tau_n(t)) \approx g(t)\delta(\tau - \hat{\tau})$$

- The corresponding channel transfer function is

Impulse response

$$T(t,f) = \mathbb{F}\{g(t,\underline{\tau})\} = \mathbb{F}\{g(t)\delta(\tau - \hat{\tau})\} = \underline{g(t)} e^{-j2\pi f \hat{\tau}}$$



# Freq.-Non-Selective Multipath Fading (Cont.)

- The amplitude response is $|T(t,f)| = |g(t)|$
- **All frequency components** in the received signal are subject to the **same complex gain** $g(t)$
  - The phase is linear with respect to $f \Rightarrow$ **constant delay** for all $f$ $\Rightarrow$ **no distortion**
- The received signal is said to exhibit **flat fading**
  - It holds for the corresponding frequency components only, i.e., the frequency components in the transmission bandwidth

# Doppler Power Spectrum



# Received Signal Correlation

- By assuming the transmission of an **unmodulated carrier**
- The received band-pass signal is

**Narrow band signal**
**Freq.-Non-Selective**

$$\boxed{\tilde{s}(t)=1}$$

$$r(t)=\mathrm{Re}\left\{\ \tilde{r}(t)e^{j2\pi f_c t}\right\}$$

$$\tilde{r}(t)=\sum_{n=1}^{N}\alpha_n(t)\,e^{-j\phi_n(t)}\tilde{s}(t-\tau_n(t))=\sum_{n=1}^{N}\alpha_n(t)\,e^{-j\phi_n(t)}$$

$$=g_I(t)+jg_Q(t)$$

  – where

$$g_I(t)=\sum_{n=1}^{N}\alpha_n(t)\cos\phi_n(t) \qquad g_Q(t)=-\sum_{n=1}^{N}\alpha_n(t)\sin\phi_n(t)$$

$$\boxed{e^{j\theta}=\cos\theta+j\sin\theta}$$

- The band-pass signal can be expressed as

$$r(t)=g_I(t)\cos 2\pi f_c t-g_Q(t)\sin 2\pi f_c t$$

# Received Signal Correlation (Cont.)

- It is assumed that these random processes are all wide sense stationary (WSS)
  - $f_{D,n}(t) = f_{D,n}$, $\alpha_n(t) = \alpha_n$, and $\tau_n(t) = \tau_n$
- The autocorrelation of $r(t)$: (for an arbitrary **time difference τ**)

$$\phi_{rr}(\boldsymbol{\tau}) = E\left[r(t)r(t+\boldsymbol{\tau})\right] \leftarrow \boxed{\text{Auto-correlation time separation}}$$

$$= E\left[g_I(t)g_I(t+\boldsymbol{\tau})\right]\cos 2\pi f_c\boldsymbol{\tau} - E\left[g_Q(t)g_I(t+\boldsymbol{\tau})\right]\sin 2\pi f_c\boldsymbol{\tau}$$

$$= \phi_{g_I g_I}(\boldsymbol{\tau})\cos 2\pi f_c\boldsymbol{\tau} - \phi_{g_Q g_I}(\boldsymbol{\tau})\sin 2\pi f_c\boldsymbol{\tau}$$

$$\boxed{\begin{aligned}\phi_{g_I g_I}(\boldsymbol{\tau}) &= \phi_{g_Q g_Q}(\boldsymbol{\tau});\\ \phi_{g_I g_Q}(\boldsymbol{\tau}) &= -\phi_{g_Q g_I}(\boldsymbol{\tau})\end{aligned}}$$

$$\boxed{\begin{aligned}\sin x \sin y &= \tfrac{1}{2}\left[\cos(x-y) - \cos(x+y)\right]\\ \cos x \cos y &= \tfrac{1}{2}\left[\cos(x-y) + \cos(x+y)\right]\\ \sin x \cos y &= \tfrac{1}{2}\left[\sin(x+y) + \sin(x-y)\right]\\ \cos x \sin y &= \tfrac{1}{2}\left[\sin(x+y) - \sin(x-y)\right]\end{aligned}}$$



# Received Signal Correlation (Cont.)

- According to $\phi_n(t) = 2\pi\left[\left(f_c + f_{D,n}(t)\right)\tau_n(t) - f_{D,n}(t)t\right]$, $\tau_n(t) \approx \hat{\tau}$ and $g_I(t) = \sum_{n=1}^{N}\alpha_n(t)\cos\phi_n(t)$, we have

$$\phi_{g_I g_I}(\boldsymbol{\tau}) = E\left[g_I(t)g_I(t+\boldsymbol{\tau})\right] = \Omega_p \times E_{\hat{\tau},\theta_n}\left[\cos\phi_n(t)\cos\phi_n(t+\boldsymbol{\tau})\right]$$

$$= \frac{\Omega_p}{2}\left\{E_{\hat{\tau},\theta_n}\left[\underbrace{\overset{x-y}{\cos 2\pi f_{D,n}\boldsymbol{\tau}}}_{\text{A constant for } \hat{\tau}}\right] + E_{\hat{\tau},\theta_n}\left[\overset{x+y}{\cos 2\pi[2(f_c + f_{D,n})\hat{\tau} - 2f_{D,n}t - f_{D,n}\boldsymbol{\tau}]}\right]\right\}$$

$$= \frac{\Omega_p}{2}E_{\theta_n}\left[\cos\left(2\pi f_m\boldsymbol{\tau}\cos\theta_n\right)\right] + 0 \quad \left(\because f_c\hat{\tau} >> 1 \text{ and } f_{D,n}(t) = f_m\cos\theta_n(t)\right)$$

  - where the total received envelope power is

$$\Omega_p = E\left[g_I^2(t)\right] + E\left[g_Q^2(t)\right] = \sum_{n=1}^{N}E\left[\alpha_n^2\right]$$

$$\boxed{\phi_n(t) \text{ is uniformly distributed over } [-\pi, \pi]}$$

- Similarly, we have

$$\phi_{g_I g_Q}(\boldsymbol{\tau}) = E_{\hat{\tau},\theta_n}\left[g_I(t)g_Q(t+\boldsymbol{\tau})\right] = \frac{\Omega_p}{2}E_{\theta_n}\left[\sin\left(2\pi f_m\boldsymbol{\tau}\cos\theta_n\right)\right]$$

## Received Signal Correlation – IS

- For **isotropic scattering (IS)**: $\theta_n$ is uniformly distributed over $[-\pi, \pi]$

**Even function**

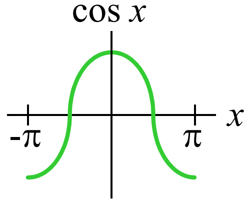


$$\phi_{g_I g_I}(\boldsymbol{\tau}) = \frac{\Omega_p}{2}\frac{1}{2\pi}\int_{-\pi}^{\pi}\cos(2\pi f_m \boldsymbol{\tau}\cos\theta)\,d\theta$$

$$= \frac{\Omega_p}{2}\frac{1}{\pi}\int_{0}^{\pi}\cos(2\pi f_m \boldsymbol{\tau}\sin\theta)\,d\theta = \frac{\Omega_p}{2}J_0(2\pi f_m \boldsymbol{\tau})$$

– $J_0(x)$ is the zero-order Bessel function of the first kind

**Odd function**

$$\phi_{g_I g_Q}(\boldsymbol{\tau}) = \frac{\Omega_p}{2}\frac{1}{2\pi}\int_{-\pi}^{\pi}\sin(2\pi f_m \boldsymbol{\tau}\cos\theta)\,d\theta = 0$$

$$\boxed{\because \sin(x) = -\sin(-x)}$$

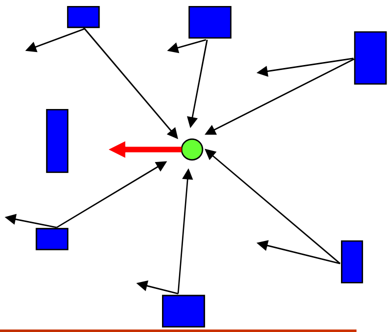

- $g_I(t)$ and $g_Q(t)$ are uncorrelated



## Received Signal Correlation – IS (Cont.)

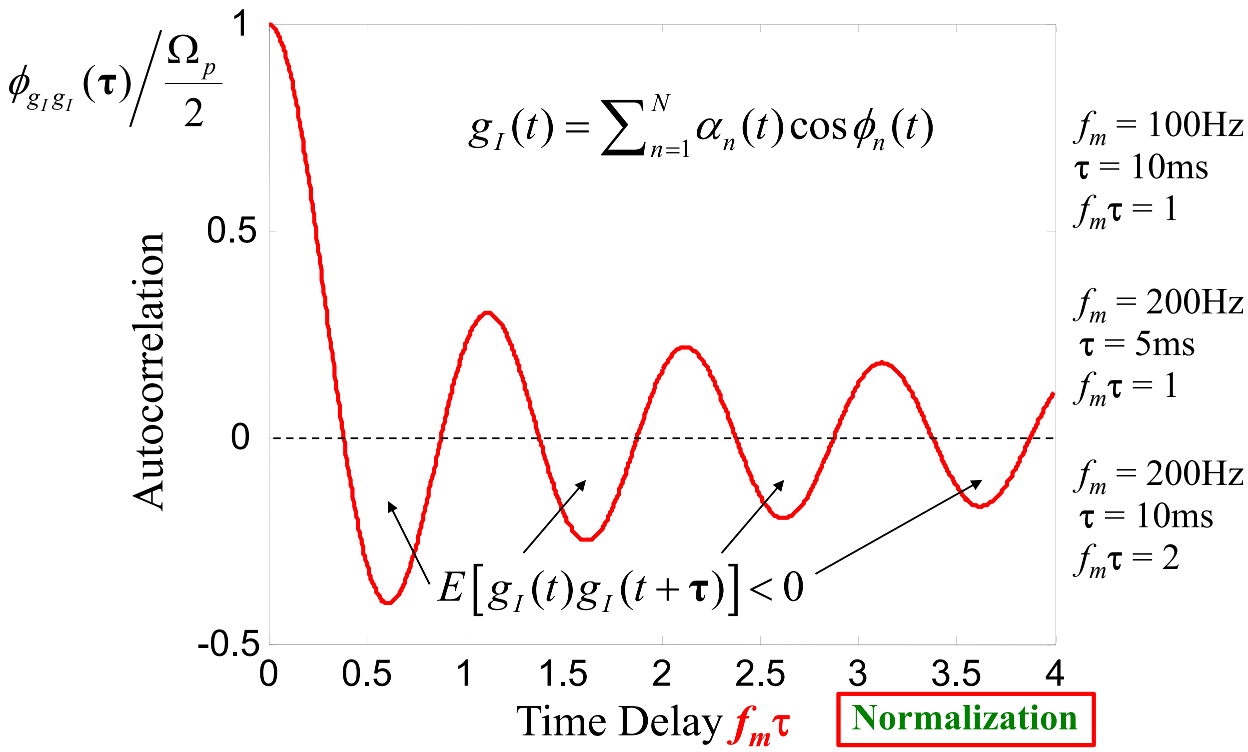

# Received Signal Spectrum – IS (Cont.)

- The power spectral density of $g_I(t)$ is

$$S_{g_I g_I}(f) = \mathbb{F}\left\{\phi_{g_I g_I}(\boldsymbol{\tau})\right\} = \begin{cases} \dfrac{\Omega_p}{2\pi f_m} \dfrac{1}{\sqrt{1-\left(f/f_m\right)^2}} & |f| \le f_m \\ 0 & \text{otherwise} \end{cases}$$

- The received complex envelope of $r(t)$ is

$$\tilde{r}(t) = g(t) = g_I(t) + jg_Q(t)$$

$$\Rightarrow \phi_{gg}(\boldsymbol{\tau}) = \frac{1}{2}E\left[g^*(t)g(t+\boldsymbol{\tau})\right] = \phi_{g_I g_I}(\boldsymbol{\tau}) + j\phi_{g_I g_Q}(\boldsymbol{\tau})$$

- The power spectral density of $g(t)$ (**Doppler power spectrum**) is

$$S_{gg}(f) = S_{g_I g_I}(f) + jS_{g_I g_Q}(f)$$



# Received Signal Spectrum – IS (Cont.)

- For the received band-pass signal $r(t)$, we have

$$\phi_{rr}(\boldsymbol{\tau}) = \Re\,[\phi_{gg}(\boldsymbol{\tau})e^{j2\pi f_c \tau}]$$

- Since $\phi_{g_I g_Q}(\boldsymbol{\tau}) = 0$, we have the PSD of $r(t)$ as

$$\begin{aligned} S_{rr}(f) &= \frac{1}{2}\left[S_{gg}(f-f_c) + S_{gg}(-f-f_c)\right] \\ &= \frac{1}{2}\left[S_{g_I g_I}(f-f_c) + S_{g_I g_I}(-f-f_c)\right] \\ &= \frac{\Omega_p}{4\pi f_m}\frac{1}{\sqrt{1-\left(|f-f_c|/f_m\right)^2}}, \qquad |f-f_c| \le f_m \end{aligned}$$

- $S_{rr}(t)$ is limited to $|f-f_c| \le f_m$

# Received Signal Spectrum – IS (Cont.)

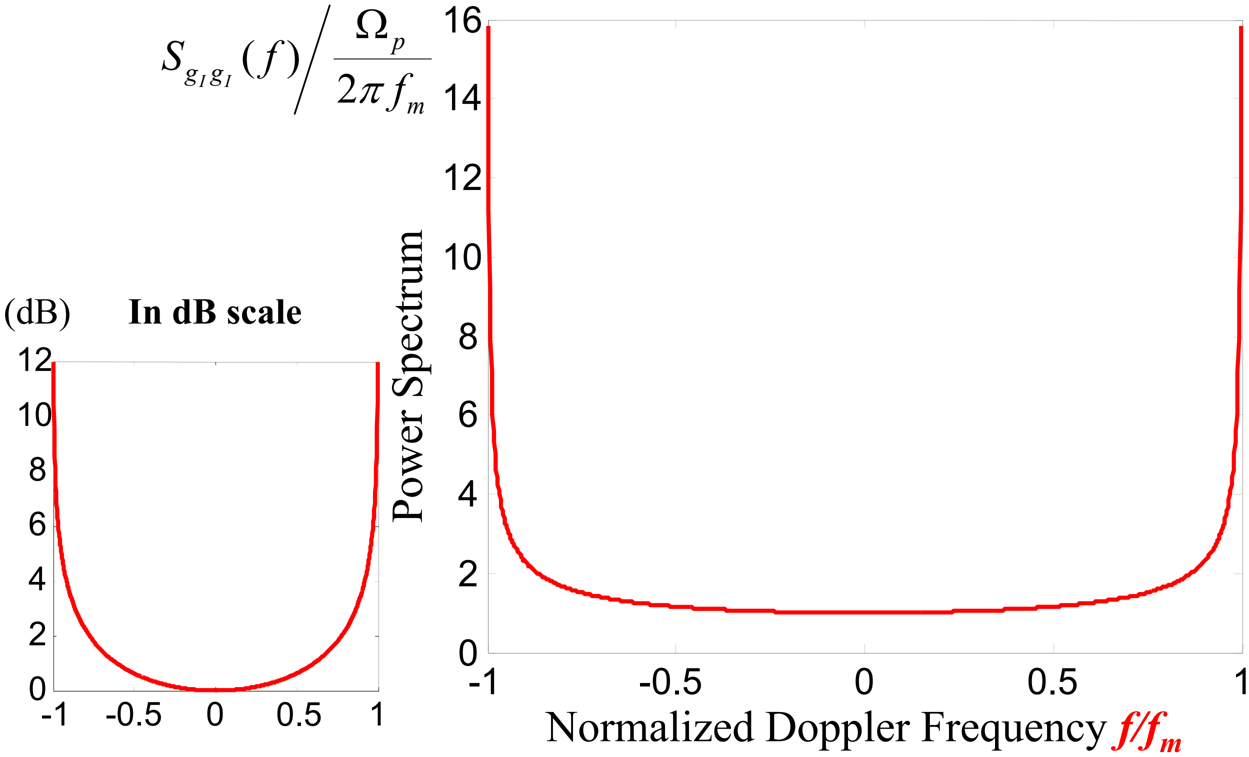




# Question

- **Question:**
  - Why the power spectral density of an unmodulated carrier is limited to $|f-f_c| \le f_m$ ?
  - For a transmission with the transmission bandwidth $B$, what is the frequency range of the received power spectrum?

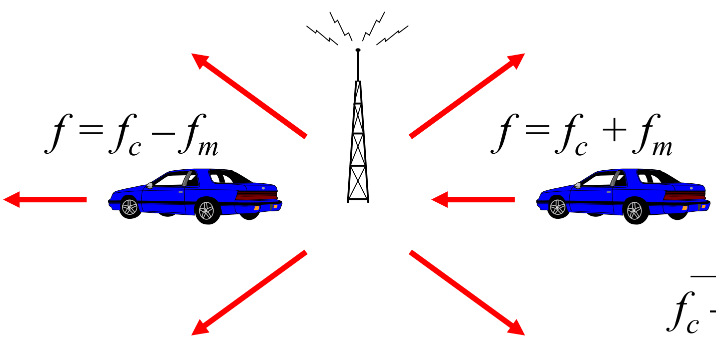


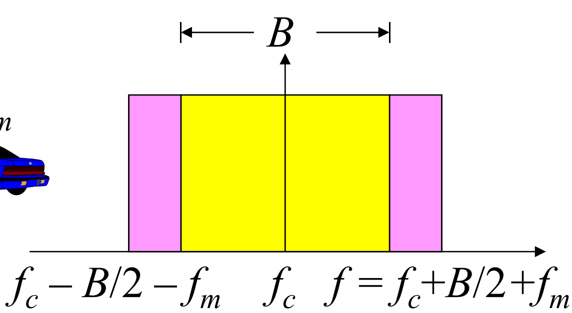

# Received Signal Spectrum with LOS – IS

- If an **LOS** or a **strong specular component** is present in the received signal and arrives at angle $\theta_0$: **Ricean／Rician fading**

$$S_{gg}(f)=\begin{cases}\frac{1}{K+1}\frac{\Omega_p}{2\pi f_m}\frac{1}{\sqrt{1-(f/f_m)^2}}+\frac{K}{K+1}\frac{\Omega_p}{2}\delta(f-f_m\cos\theta_0), & 0\le|f|\le f_m\\ 0, & \text{otherwise}\end{cases}$$

  - where $K$ is the **Rice factor**: the ratio of the power in the **specular** and **scatter** components of the received signal
- The PSD is the same as Fig. 2.4, except for an additional **discrete tone** at $f_c+f_m\cos\theta_0$

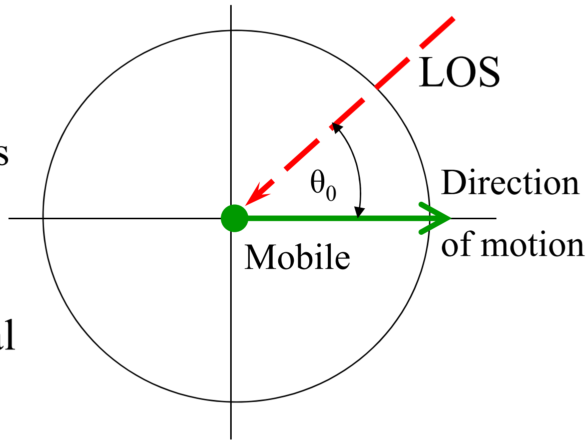




# Received Signal Correlation (Microcellular)

- In microcellular environment, the plane waves may be **channeled by the buildings** along the streets and arrive at the receiver from just **one direction**
  - The scattering is **non-isotropic**

$$p(\theta)=\begin{cases}\frac{\pi}{4|\theta_m|}\cos\left(\frac{\pi}{2}\times\frac{\theta}{\theta_m}\right), & |\theta|\le|\theta_m|\le\pi/2\\ 0, & \text{elsewhere}\end{cases}$$

  - $\theta_m$: the directivity of the incoming waves

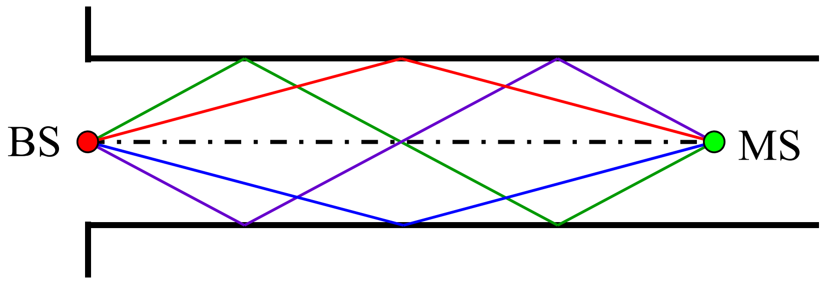

## Received Signal Correlation (Microcell) (Cont.)

- According to

$$\phi_{g_I g_I}(\boldsymbol{\tau}) = \frac{\Omega_p}{2} E_{\theta_n}\left[\cos\left(2\pi f_m \boldsymbol{\tau} \cos\theta_n\right)\right]$$

$$\phi_{g_I g_Q}(\boldsymbol{\tau}) = \frac{\Omega_p}{2} E_{\theta_n}\left[\sin\left(2\pi f_m \boldsymbol{\tau} \cos\theta_n\right)\right]$$

- We have

$$\phi_{g_I g_I}(\boldsymbol{\tau}) = \frac{\Omega_p}{2} \int_{-\pi}^{\pi} \cos(2\pi f_m \boldsymbol{\tau} \cos\theta) \underline{p(\theta)}\, d\theta \neq \frac{\Omega_p}{2} J_0(2\pi f_m \boldsymbol{\tau})$$

$$\phi_{g_I g_Q}(\boldsymbol{\tau}) = \frac{\Omega_p}{2} \int_{-\pi}^{\pi} \sin(2\pi f_m \boldsymbol{\tau} \cos\theta) \underline{p(\theta)}\, d\theta \neq 0$$



# Fading Characteristics (Received Envelope/Power Distribution)

# Rayleigh Fading

- **Rayleigh Fading:** the received complex low-pass signal is modeled as a complex Gaussian random process
  - $g_I(t)$ and $g_Q(t)$ are independent **zero-mean** Gaussian RVs
  - The received **complex envelope** $\alpha(t) = |\,g(t)\,|$ has a Rayleigh distribution

$$p_\alpha(x) = \frac{x}{\sigma^2}\exp\left[-\frac{x^2}{2\sigma^2}\right], \quad x \ge 0$$

$$\boxed{\begin{aligned} g_I(t) &= \sum_{n=1}^{N}\alpha_n(t)\cos\phi_n(t) \\ g_Q(t) &= -\sum_{n=1}^{N}\alpha_n(t)\sin\phi_n(t) \end{aligned}}$$

- The average power is

$$E[\alpha^2] = \Omega_p = 2\sigma^2$$

- The squared-envelope (power) $\alpha^2(t) = |\,g(t)\,|^2$ has an exponential distribution

$$p_{\alpha^2}(x) = \frac{1}{\Omega_p}\exp\left[-\frac{x}{\Omega_p}\right], \quad x \ge 0$$



# Rayleigh Fading (Cont.)

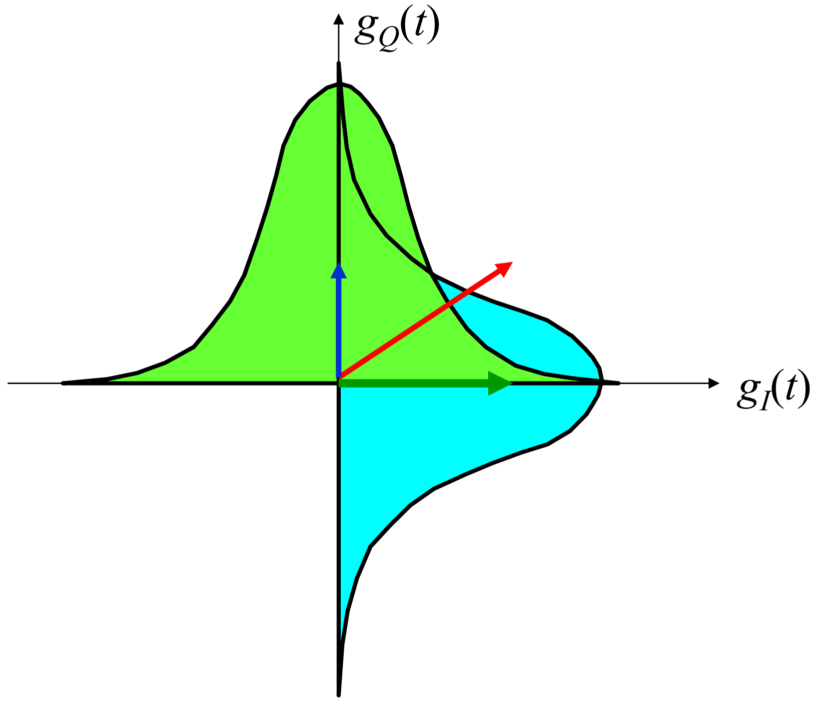

# Ricean Fading

- **Ricean Fading:** the received complex low-pass signal contains a LOS or a strong specular component
  - $g_I(t)$ and $g_Q(t)$ are independent Gaussian RVs with **non-zero mean** $m_I(t)$ and $m_Q(t)$ ($m_I(t)$ and $m_Q(t)$ depend on the LOS and $\theta_0$)
  - The complex envelope $\alpha(t) = |\, g(t)\,|$ has a Ricean distribution

$$p_\alpha(x) = \frac{x}{\sigma^2}\exp\left[-\frac{x^2+s^2}{2\sigma^2}\right] I_0\left(\frac{xs}{\sigma^2}\right) \quad x \ge 0$$

Power of the LOS component

$$s^2 = m_I^2(t) + m_Q^2(t), \qquad K = s^2 / 2\sigma^2$$

  - The modified Bessel function of the first kind of zero order

$$I_0(x) = \int_0^{2\pi} \exp(x\cos\psi)\, d\psi \Big/ 2\pi$$

  - Rice factor $K = 0$: Rayleigh fading
  - Rice factor $K = \infty$: the channel does not exhibit fading



# Ricean Fading (Cont.)

- The average power is

$$E[\alpha^2] = \Omega_p = s^2 + 2\sigma^2$$

$$s^2 = \frac{K\Omega_p}{K+1}, \qquad 2\sigma^2 = \frac{\Omega_p}{K+1}$$

- The squared-envelope $\alpha^2(t) = |\, g(t)\,|^2$ has a non-central chi-square distribution

$$p_{\alpha^2}(x) = \frac{(K+1)}{\Omega_p}\exp\left[-K - \frac{(K+1)x}{\Omega_p}\right] I_0\left(2\sqrt{\frac{K(K+1)x}{\Omega_p}}\right), \quad x \ge 0$$

- The phase is not uniformly distributed over $[-\pi, \pi]$ for $K \ne 0$

$$\phi(t) = \tan^{-1}\left(x_Q(t)/x_I(t)\right)$$

  - For $K = 0$: Rayleigh fading $p_\phi(x) = 1/2\pi, \quad -\pi \le x \le \pi$

# Ricean Fading (Cont.)

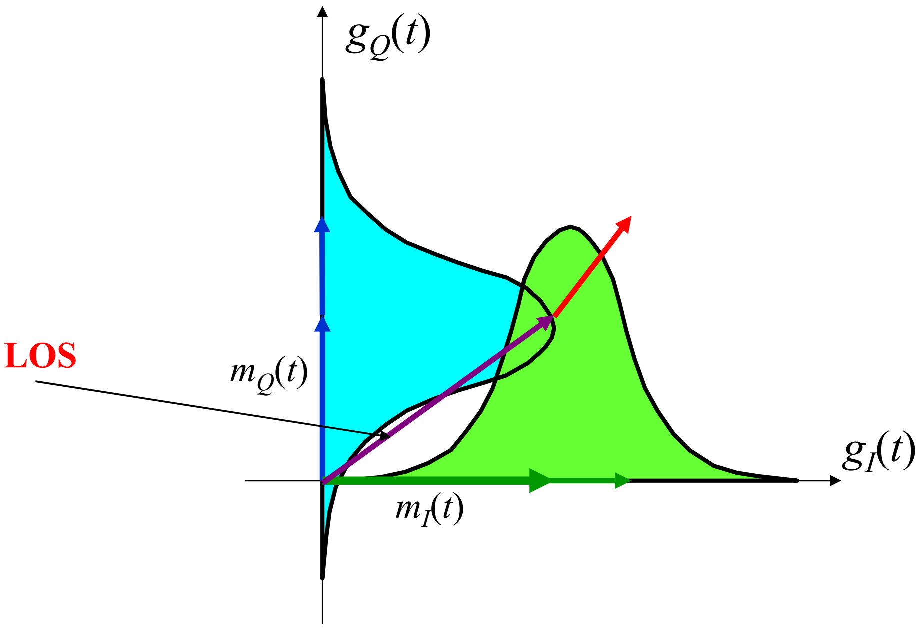




# Rayleigh and Ricean Distributions

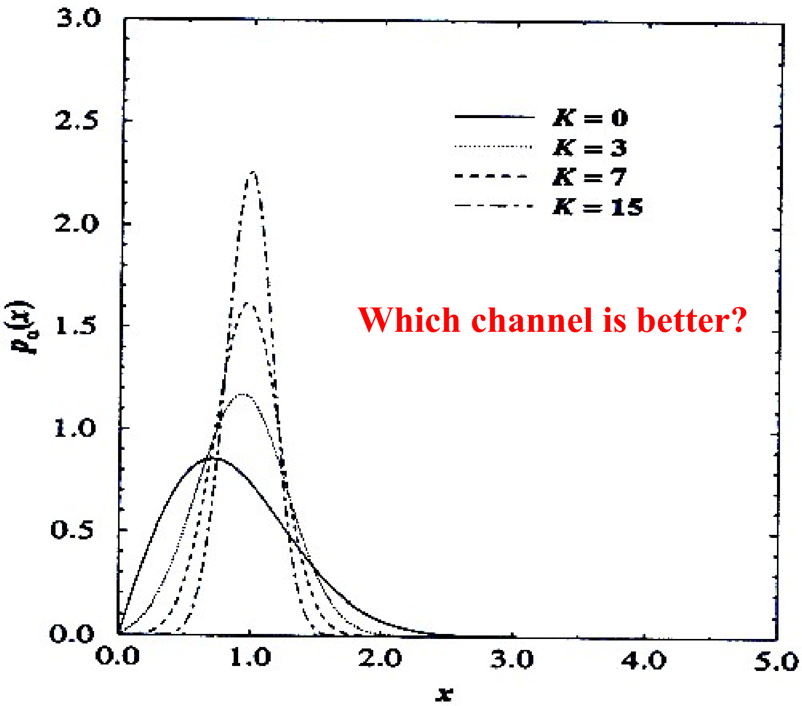

# Nakagami Fading

- **Nakagami Fading:** provides a closer match to some experimental data
  - The received complex envelope $\alpha(t) = |g(t)|$ has a Nakagami distribution

$$p_\alpha(x) = \frac{2m^m x^{2m-1}}{\Gamma(m)\Omega_p^m} \exp\left[-\frac{mx^2}{\Omega_p}\right], \quad m \geq \frac{1}{2}$$

    - where $\Gamma(m)$ is the Gamma function defined as

$$\Gamma(m) = \int_0^\infty u^{m-1} e^{-u}\, du$$
$$= (m-1)!, \quad \text{if } m \text{ is a positive integer}$$

  - $m$ = 1: Rayleigh fading
  - $m$ = 1/2: one-sided Gaussian
  - $m = \infty$: no fading



# Nakagami Fading (Cont.)

- Nakagami distribution can model fading conditions that are **either more or less** severe than Rayleigh fading
- Ricean fading can be closely approximated by

$$K = \frac{\sqrt{m^2 - m}}{m - \sqrt{m^2 - m}} \qquad m \geq 1; \qquad m = \frac{(K+1)^2}{(2K+1)}$$

- The Nakagami distribution often leads to closed form analytical expressions
- The squared-envelope $\alpha^2(t) = |g(t)|^2$ has a Gamma density

$$p_{\alpha^2}(x) = \left(\frac{m}{\Omega_p}\right)^m \frac{x^{m-1}}{\Gamma(m)} \exp\left[-\frac{mx}{\Omega_p}\right]$$

# Nakagami Fading (Cont.)

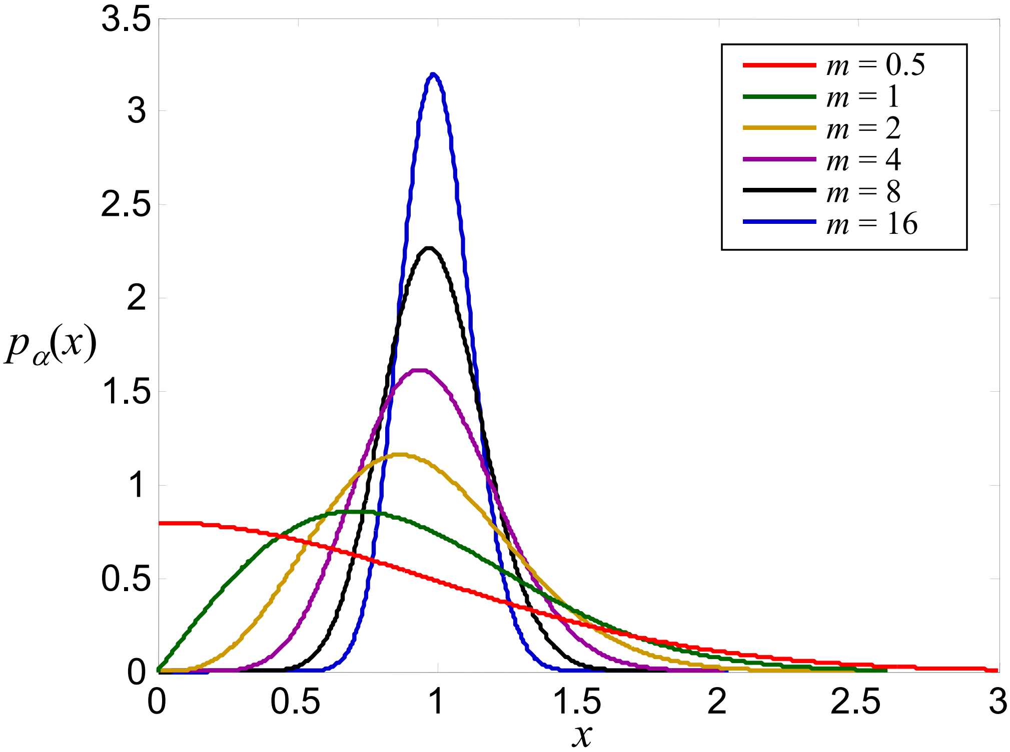




# Nakagami and Ricean Distributions

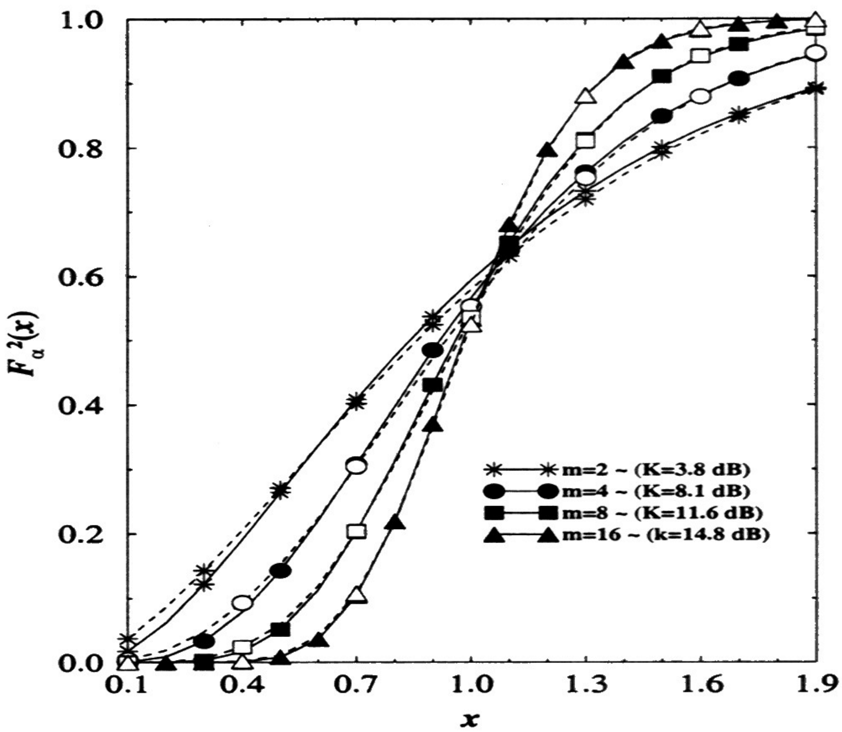

# Envelope Correlation

- The autocorrelation of the envelope $\alpha(t) = |g(t)|$:

$$\phi_{\alpha\alpha}(\tau) = E[\alpha(t)\alpha(t+\tau)] = \frac{\pi}{2}\left|\phi_{gg}(0)\right| F\left[-\frac{1}{2}, -\frac{1}{2}; 1, \frac{|\phi_{gg}(\tau)|^2}{|\phi_{gg}(0)|^2}\right]$$

  – where $\left|\phi_{gg}(\tau)\right|^2 = \phi^2_{g_I g_I}(\tau) + \phi^2_{g_I g_Q}(\tau)$

$$= \phi^2_{g_I g_I}(\tau) \quad \text{(isotropic scattering)}$$

$$F\left[-\tfrac{1}{2}, -\tfrac{1}{2}; 1, x\right] = 1 + \tfrac{1}{4}x + \tfrac{1}{64}x^2 + \cdots \text{(Hypergeometric Function)}$$

$$\phi_{\alpha\alpha}(\tau) \approx \frac{\pi}{2}\left|\phi_{gg}(0)\right|\left[1 + \frac{1}{4}\frac{|\phi_{gg}(\tau)|^2}{|\phi_{gg}(0)|^2}\right]$$

- The autocovariance function:

$$\mu_{\alpha\alpha}(\tau) = E[\alpha(t)\alpha(t+\tau)] - E[\alpha(t)]E[\alpha(t+\tau)]$$

$$= \frac{\pi}{8|\phi_{gg}(0)|}\left|\phi_{gg}(\tau)\right|^2 = \frac{\pi\Omega_p}{16} J_0^2(2\pi f_m \tau)$$



# Envelope Correlation (Cont.)

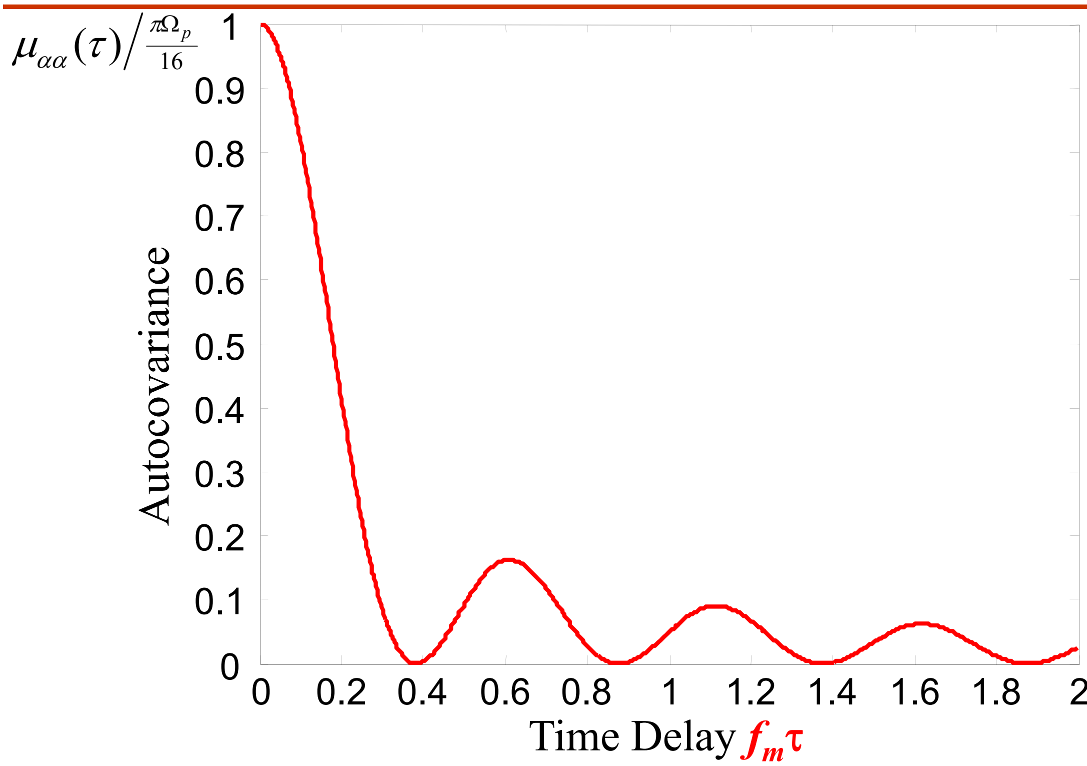

# Envelope Level Crossing Rate and Average Envelope Fade Duration



# The Impact of Multipath Fading

- The receive performance is severely degraded in a **deep fade region**.
  - For example, the received signal level is below a threshold $R$
- We care the following two things:
  - How often will deep fading occur?
    - **Envelope Level Crossing Rate**
  - How long will the deep fading last?
    - **Average Envelope Fade Duration**

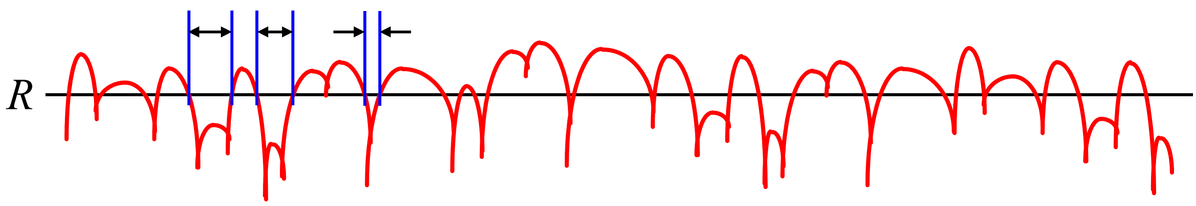

# Envelope Level Crossing Rate

- $L_R$: the rate at which the envelope crosses level $R$ in the positive (or negative) going direction
- $\dot{\alpha}$: the envelope slope
  - $\dot{\alpha}$ is either **positive** (for positive going direction) or **negative** (for negative going direction)
- $p(\alpha, \dot{\alpha})$: the join pdf of $\alpha$ and $\dot{\alpha}$
- $dt$: the observation time interval
- For given values of $\alpha = R$ and $\dot{\alpha}$, the probability is

$$p(R,\dot{\alpha})\, d\alpha\, d\dot{\alpha}$$

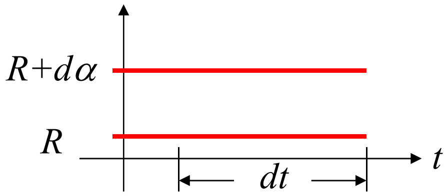




# Envelope Level Crossing Rate (Cont.)

- The expected amount of time spent in the interval $(R, R+d\alpha)$ for given values of $\dot{\alpha}$ and $dt$ is

$$p(R,\dot{\alpha})\, d\alpha\, d\dot{\alpha}\, dt$$

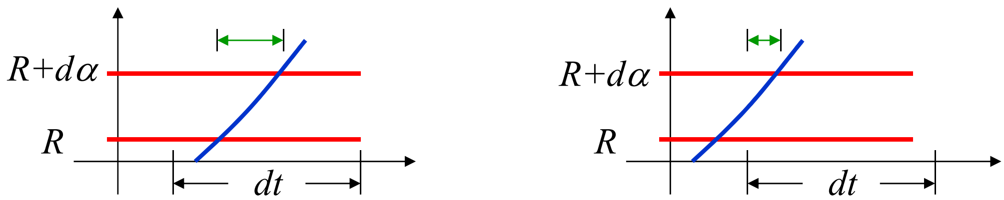


- The time required to cross the interval $d\alpha$ once for a given $\dot{\alpha}$ is $d\alpha / \dot{\alpha}$
  - The time spent in $(R, R+d\alpha)$ for one positive going direction cross

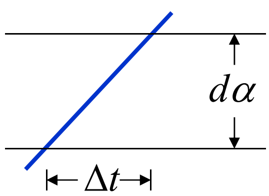


$$\dot{\alpha} = d\alpha / \Delta t$$

# Envelope Level Crossing Rate (Cont.)

- The expected number of crossings of the envelope $\alpha$ within the interval $(R, R+d\alpha)$ for a given $\dot{\alpha}$ is

$$\left(p(R,\dot{\alpha})\,d\alpha\,d\dot{\alpha}\,dt\right)/\left(d\alpha/\dot{\alpha}\right)=\dot{\alpha}\;p(R,\dot{\alpha})\,d\dot{\alpha}\,dt$$

- The expected number of crossings in a time interval $T$ for a given $\dot{\alpha}$ is

$$\int_0^T \dot{\alpha}\,p(R,\dot{\alpha})\,d\dot{\alpha}\,dt=\dot{\alpha}\,p(R,\dot{\alpha})\,d\dot{\alpha}\,T$$

- The excepted number of positive going direction crossings:

$$N_R = T\int_0^{\infty}\dot{\alpha}\,p(R,\dot{\alpha})\,d\dot{\alpha}$$

**All slopes are counted.**

- The envelope level crossing rate:

$$L_R = \int_0^{\infty}\dot{\alpha}\,p(R,\dot{\alpha})\,d\dot{\alpha}$$



# Envelope Level Crossing Rate – Ricean

- For Ricean fading:

$$p(\alpha,\dot{\alpha})=\sqrt{\frac{1}{2\pi b_2}}\exp\left\{-\frac{\dot{\alpha}^2}{2b_2}\right\}\times\frac{\alpha}{b_0}\exp\left\{-\frac{(\alpha^2+s^2)}{2b_0}\right\}I_0\left(\frac{\alpha s}{b_0}\right)=p(\dot{\alpha})p(\alpha)$$

  – where $b_2 = b_0(2\pi f_m)^2/2$ and $2b_0$ is the power of the scatter component of the received signal

- The envelope level crossing rate is

$$L_R=\sqrt{2\pi(K+1)}\,f_m\rho e^{-K-(K+1)\rho^2}I_0\left(2\rho\sqrt{K(K+1)}\right)$$

  – where $\rho=\frac{R}{\sqrt{\Omega_p}}=\frac{R}{R_{rms}}$

  – $\sqrt{\Omega_p}\triangleq R_{rms}$ : the rms envelope level

# Envelope Level Crossing Rate – Rayleigh

- For Rayleigh fading ($K = 0$):

$$L_R = \sqrt{2\pi} f_m \rho e^{-\rho^2}$$

- Maximum LCR: around $\boldsymbol{\rho} = \mathbf{0}$ **dB** (nearly independent of $K$)
  - For Rayleigh fading channel:

$$\frac{dL_R}{d\rho} = \sqrt{2\pi} f_m \left(e^{-\rho^2} - 2\rho^2 e^{-\rho^2}\right) = \sqrt{2\pi} f_m \left(1 - 2\rho^2\right) e^{-\rho^2} = 0$$

$$\Rightarrow \rho = 1/\sqrt{2}$$



# Envelope Level Crossing Rate (Cont.)

- The fades are shallower when the Rice factor, $K$, is larger

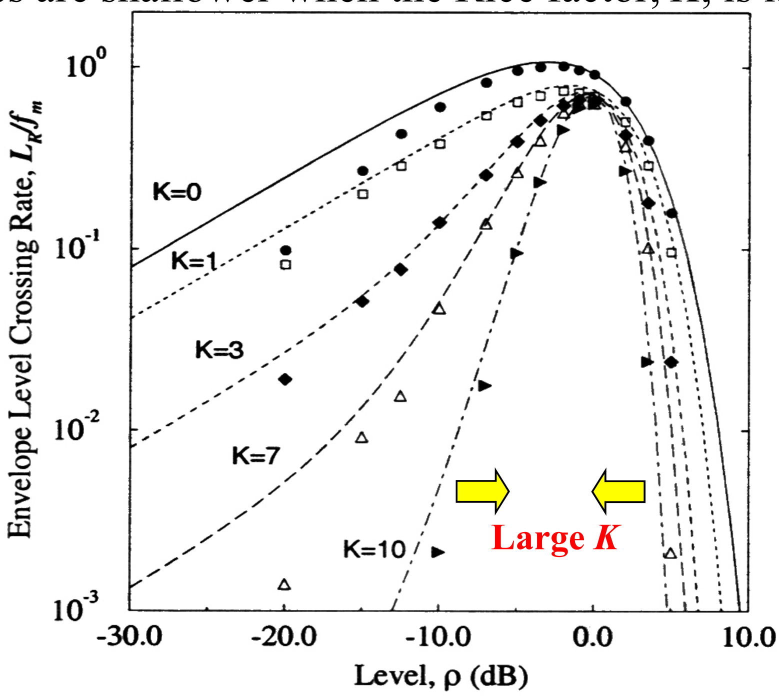

# Envelope Level Crossing Rate (Cont.)

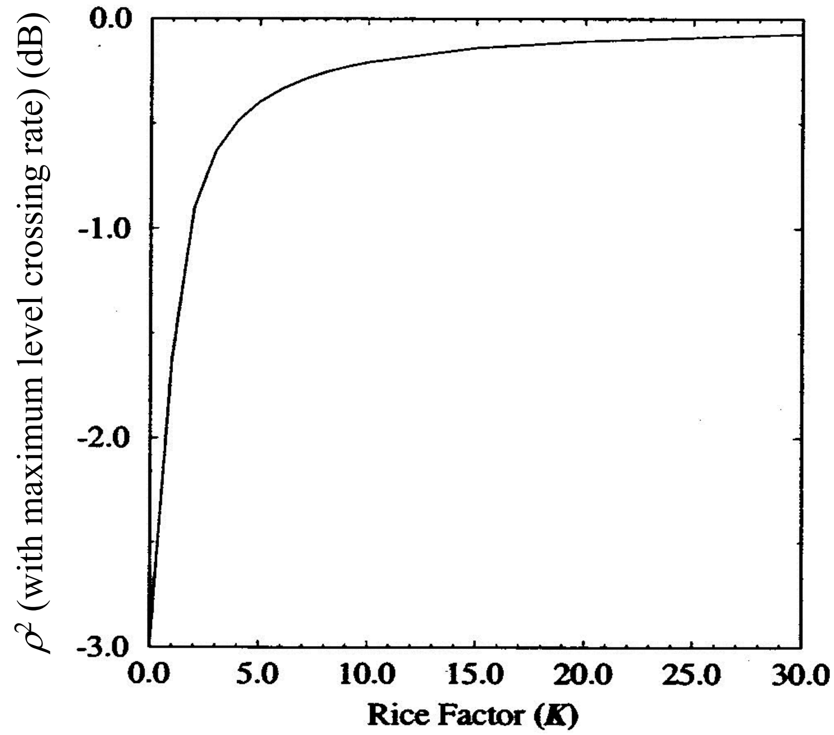




# Average Envelope Fade Duration

- Consider a very long observation time interval $T$
- The probability that the received envelope level is less than $R$ can be expressed as

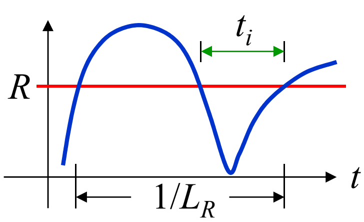


**Can be obtained based on the envelope distribution, i.e., Rayleigh/Ricean distribution**

$$P(\alpha \le R) = \frac{1}{T}\sum_i t_i$$

- The average envelope **fade duration** is

$$\bar{t} = \frac{1}{TL_R}\sum_i t_i = \frac{P(\alpha \le R)}{L_R}$$

  - $1/L_R$ is the mean time interval between two adjacent level-crossings
  - $P(\alpha \le R)$: the probability of $\alpha \le R$
  - Only one interval less than $R$ in the $1/L_R$ duration

# Average Envelope Fade Duration (Cont.)

- **Ricean:** $P(\alpha \le R) = \int_0^R p(\alpha) d\alpha = 1 - Q\left(\sqrt{2K}, \sqrt{2(K+1)\rho^2}\right)$
  - where $Q(a,b)$ is the Marcum Q function

$$Q(a,b) \triangleq \int_b^\infty \alpha \exp\left[-\tfrac{1}{2}\left(\alpha^2 + a^2\right)\right] I_0(a\alpha)\, d\alpha$$

- The average envelope fade duration is

$$\bar{t} = \frac{1 - Q\left(\sqrt{2K}, \sqrt{2(K+1)\rho^2}\right)}{\sqrt{2\pi(K+1)}\, f_m \rho e^{-K-(K+1)\rho^2} I_0\left(2\rho\sqrt{K(K+1)}\right)}$$

- **Rayleigh:** $P(\alpha \le R) = \int_0^R p(\alpha)\, d\alpha = 1 - e^{-\rho^2}$
- The average envelope fade duration is

$$\bar{t} = \frac{e^{\rho^2} - 1}{\rho f_m \sqrt{2\pi}}, \qquad L_R = \sqrt{2\pi} f_m \rho e^{-\rho^2}$$



# Average Envelope Fade Duration (Cont.)

- The average level crossing rate, zero crossing rate and average fade duration all depend on the velocity of MS
  - $f_m = v/\lambda_c$ and 1 mile = 1.609 km
  - Example:

$$v = 60 \text{ mile/hr} = 97 \text{ km/hr} = 27 \text{ m/sec};$$
$$f_c = 900 \text{ MHz} \Rightarrow f_m = 81 \text{ Hz}$$

  - Rayleigh:

$$L_R = 74 \text{ fades/sec at } \rho = 0 \text{ dB}; \quad \bar{t} = 8.5 \text{ ms}$$
$$L_R = 2.0 \text{ fades/sec at } \rho = -20 \text{ dB}; \quad \bar{t} = 50\ \mu\text{s}$$

# Average Envelope Fade Duration (Cont.)

- The average fade duration tends to be larger with the Rice factor *K*

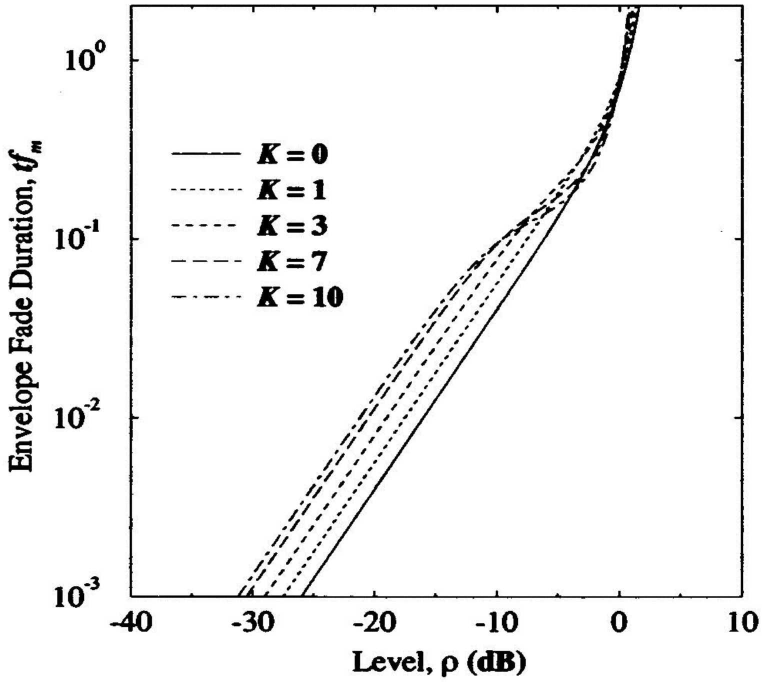




# Spatial Correlation

# Spatial Correlation

- **Diversity reception:** use two separate receiving antennas to provide uncorrelated diversity branches
- The antenna separation: $\ell$
  - By distance-time transformation

$$\ell = v\tau, \quad \ell/\lambda_c = v\tau/\lambda_c = f_m\tau$$

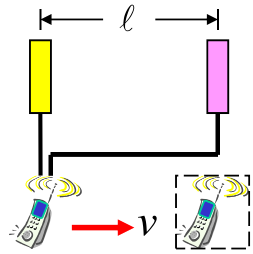


- For the case of **isotropic scattering**:
  - Autocorrelation: $\phi_{g_I g_I}(\ell) = \frac{\Omega_p}{2} J_0(2\pi\,\ell/\lambda_c)$
  - Autocovariance: $\mu_{\alpha\alpha}(\ell) = \frac{\pi\Omega_p}{16} J_0^2(2\pi\,\ell/\lambda_c)$
- The normalized envelope autocovariance is zero at $\ell = 0.38\lambda_c$
  - Less than 0.3 for $\ell > 0.38\lambda_c$



# Spatial Correlation (Cont.)

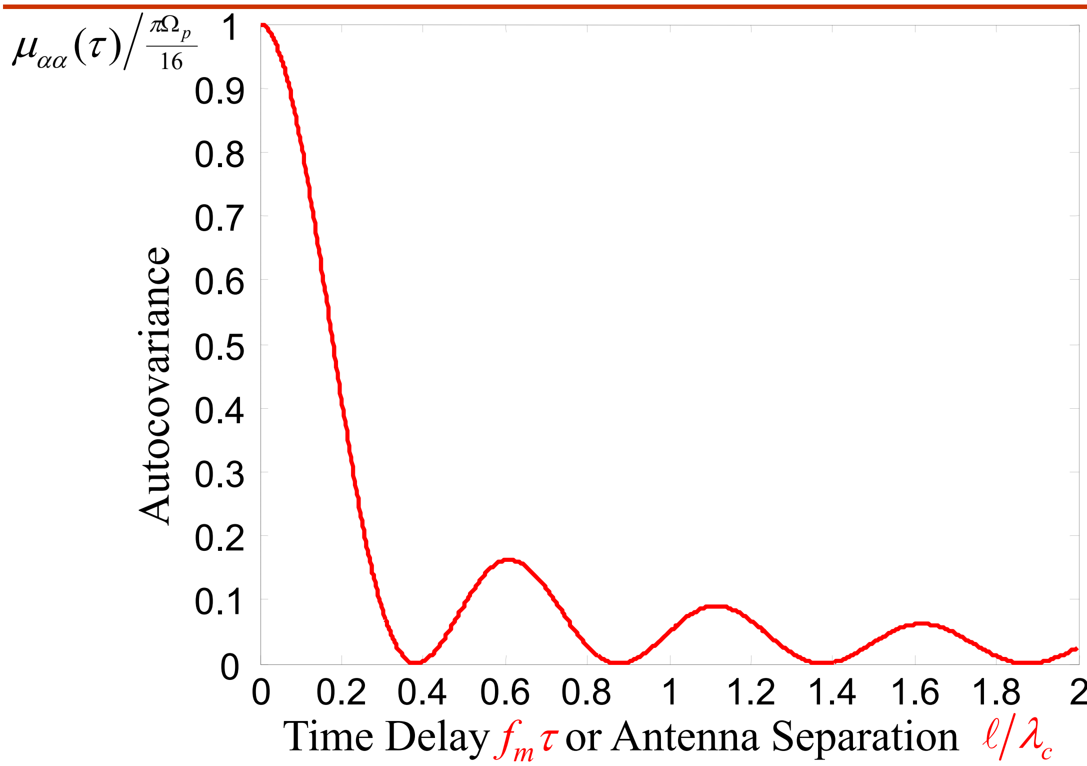

# Spatial Correlation (Cont.)

- $r_s$: the radius of primary scatterers
- $d$: the distance between BS and MS
- $\phi_{BS}$: arriving angle

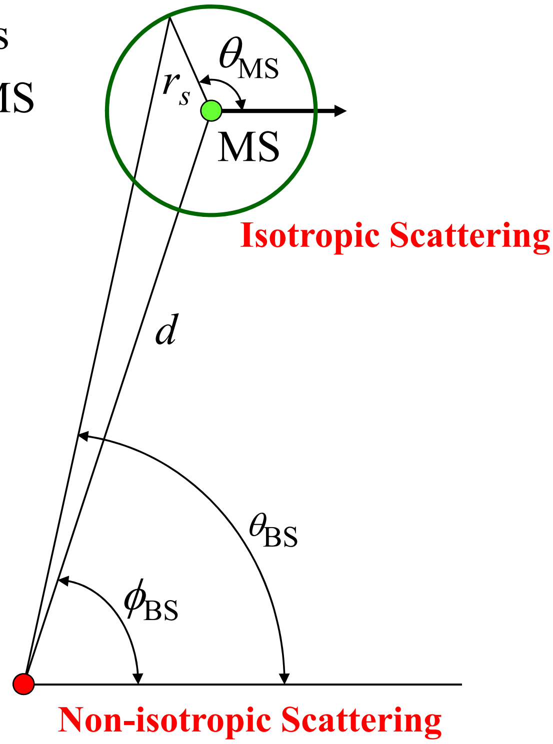




# Spatial Correlation (Cont.)

- For an MS (isotropic scattering), the antenna elements should space about **a half-wavelength apart**
- For a BS, the antenna elements separate about $\mathbf{20\lambda_c}$ to obtain a correlation of about 0.7
  – The location of BS antennas is highly above the buildings
  – The arriving plane waves at the BS tend to be concentrated in **a narrow angle** of arrival (non-isotropic scattering)
  – The two antennas located at the BS will view the MS from only a slightly different angle
  – The spatial correlation is higher than isotropic scattering
- Another scheme of diversity reception: **polarization reception**

# Spatial Correlation for BS

- Almost like a single incoming wave

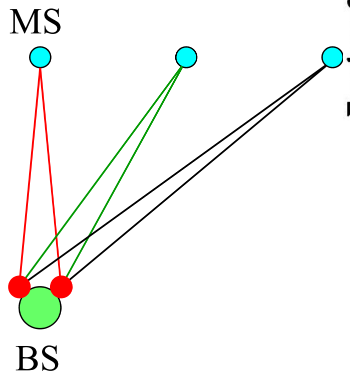


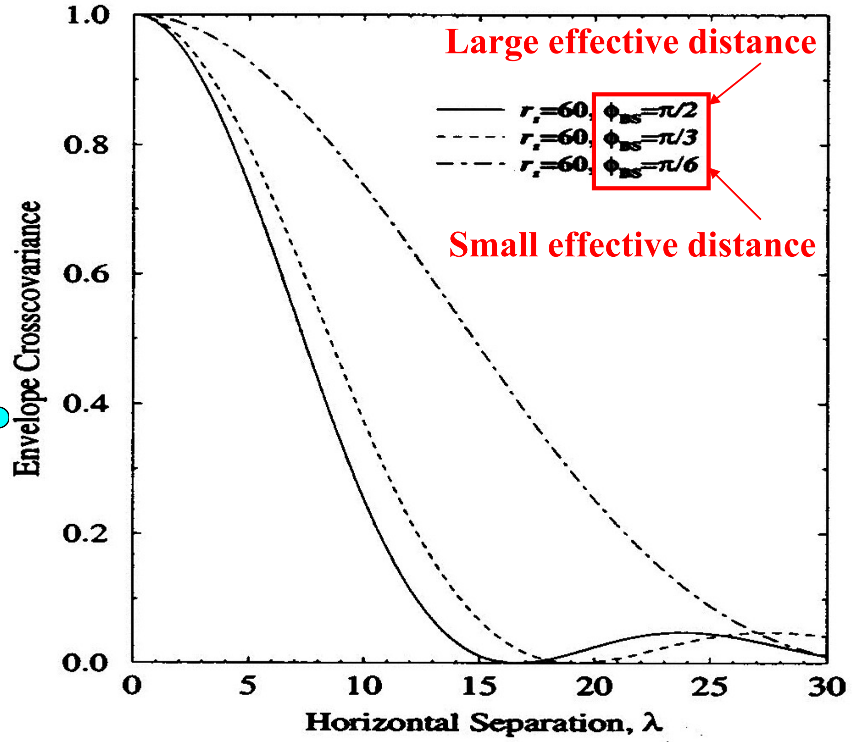




# Spatial Correlation for BS (Cont.)

- $r_s\uparrow \Rightarrow$ isotropic scattering
- $d\downarrow \Rightarrow$ isotropic scattering

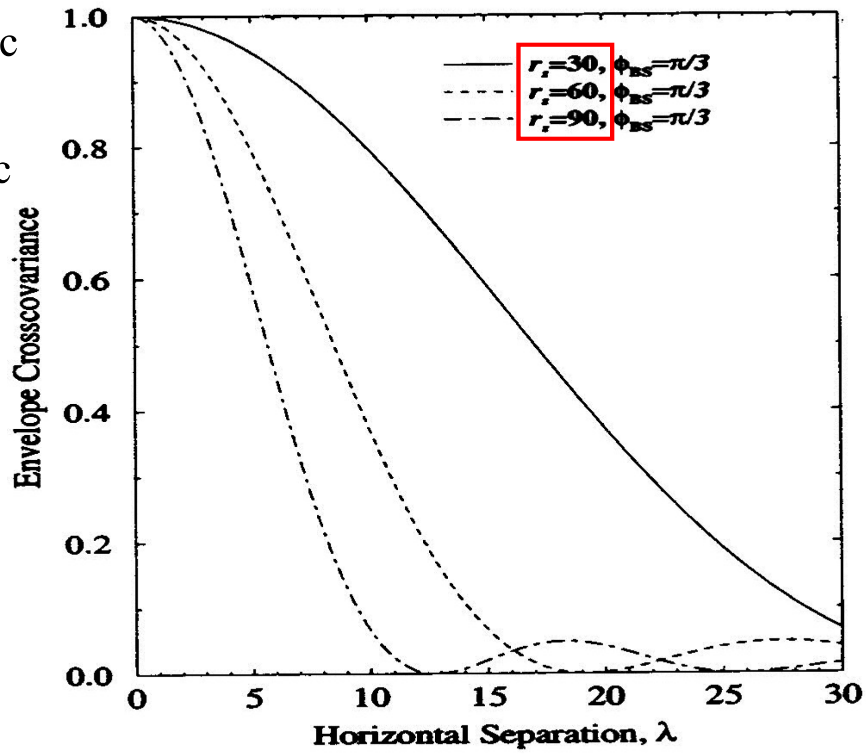

# Question

- For modern wireless cellular systems, the allocated frequency bands are around 900 MHz and 2 GHz.
- **Question:**
  - Is it possible to implement the spatial diversity reception in an MS? Why?
  - Is it possible to implement the spatial diversity reception in a BS? Why?



# Frequency-Selective Multipath Fading

# Transmission Functions

- The multipath fading channels can be modeled as **time-variant linear filters**

$\Rightarrow$ Four transmission functions are used for representation

  - Input delay-spread function $g(\tau, t)$
  - Output Doppler-spread function $H(f, v)$
  - Time-variant transfer function $T(f, t)$
  - Delay Doppler-spread function $S(\tau, v)$

- The parameters:
  - $t$: time domain
  - $f$: frequency domain
  - $\tau$: time delay
  - $v$: Doppler frequency shift



# Transmission Functions (Cont.)

- The time delay (delay spread) determines the channel frequency response
  - The time delay $\tau$ can be viewed as the impulse response of the filter $\Rightarrow$ corresponding to the frequency response of the filter
  - The distributions of $\tau$ and $f$ vary with time $t$
  - $\tau$ relates to $f$ in different domains
- The varying of time corresponds to the change in the scattering environment (the change of Doppler frequency shift)
  - $t$ relates to $v$ in different domains
- $t \leftrightarrow v$
- $\tau \leftrightarrow f$

# Transmission Functions (Cont.)

$$g(\tau,t) \underset{\tau\leftrightarrow f}{\overset{Fourier}{\Leftrightarrow}} T(f,t)$$

$$T(f,t) \underset{t\leftrightarrow v}{\overset{Fourier}{\Leftrightarrow}} H(f,v)$$

$$S(\tau,v) \underset{\tau\leftrightarrow f}{\overset{Fourier}{\Leftrightarrow}} H(f,v)$$

$$g(\tau,t) \underset{t\leftrightarrow v}{\overset{Fourier}{\Leftrightarrow}} S(\tau,v)$$



# Classification of Channels

- Three channel types:
  – Wide Sense Stationary (WSS) channel
  – Uncorrelated Scattering (US) channel
  – Wide Sense Stationary Uncorrelated Scattering (WSSUS) channel

# Wide Sense Stationary (WSS) Channel

- The fading statistics **remain constant** over short periods of time
- The channel correlation functions depend on the **time difference** $\Delta t$
- $t \leftrightarrow v$: the fading characteristics are constant in the time domain $\leftrightarrow$ a delta function in the **correlation** of Doppler frequency shift
  - WSS channels give rise to scattering with **uncorrelated Doppler shifts**
  - The attenuations and phase shifts, associated with signal components **having different Doppler shifts**, are uncorrelated
- **The fading statistics remain constant**
- **Signal components having different Doppler shifts are uncorrelated**



# Uncorrelated Scattering (US) Channel

- The attenuations and phase shifts, associated with the paths of **different delays**, are uncorrelated
- $\tau \leftrightarrow f$: the fading characteristics are uncorrelated (delta function) in the delay time domain $\leftrightarrow$ **constant** characteristics in the frequency domain
  - WSS in the frequency variable
  - The correlation functions depend on the frequency difference $\Delta f$
- **WSS in the frequency variable**
- **Signal components having different delays are uncorrelated**

# WSSUS Channel

- Wide Sense Stationary Uncorrelated Scattering Channel
- The channel displays uncorrelated scattering in both the **time-delay** and **Doppler shift**
- Most of the radio channels can be modeled as WSSUS channels

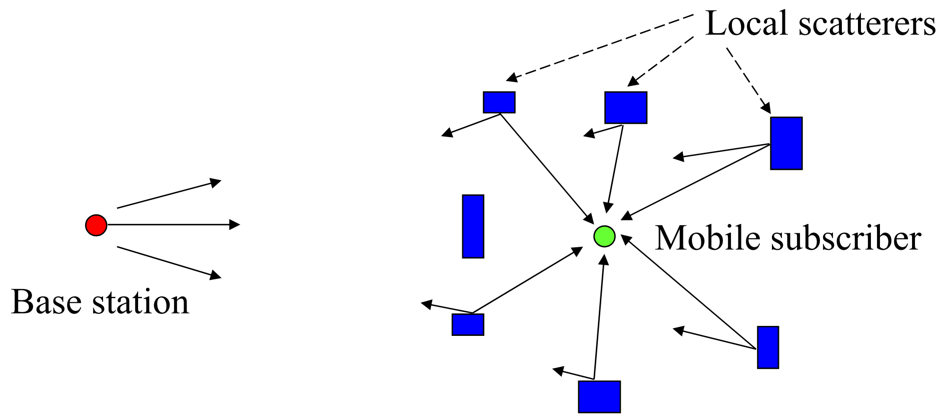




# Multipath Intensity Profile

- For WSSUS, the autocorrelation function of $g(\tau, t)$: $\phi_g(\Delta t; \tau)$
- Multipath intensity profile: For $\Delta t = 0$, $\phi_g(0;\tau) = \phi_g(\tau)$ shows the power profile
  - The average power at channel output of time delay $\tau$
  - It can be viewed as the scattering function averaged over all Doppler shifts
- Average delay: $$\mu_\tau = \frac{\int_0^\infty \tau\, \phi_g(\tau)\, d\tau}{\int_0^\infty \phi_g(\tau)\, d\tau}$$
- RMS delay spread: $$\sigma_\tau = \sqrt{\frac{\int_0^\infty (\tau - \mu_\tau)^2 \phi_g(\tau)\, d\tau}{\int_0^\infty \phi_g(\tau)\, d\tau}}$$

# Multipath Intensity Profile (Cont.)

- Middle profile: $W_x$
  - Contains $x$% of the total power in the profile

$$W_x = \tau_3 - \tau_1$$

$$\int_0^{\tau_1} \phi_g(\tau)\, d\tau = \int_{\tau_3}^{\infty} \phi_g(\tau)\, d\tau$$

$$\int_{\tau_1}^{\tau_3} \phi_g(\tau)\, d\tau = x\% \int_0^{\infty} \phi_g(\tau)\, d\tau$$

- Difference in delay: $W_P$
  - The delay profile rises to a value $P$ dB below the maximum value: $\tau_1$
  - The delay profile drops to a value $P$ dB below the maximum value: $\tau_2$

$$W_P = \tau_2 - \tau_1$$



# Multipath Intensity Profile (Cont.)

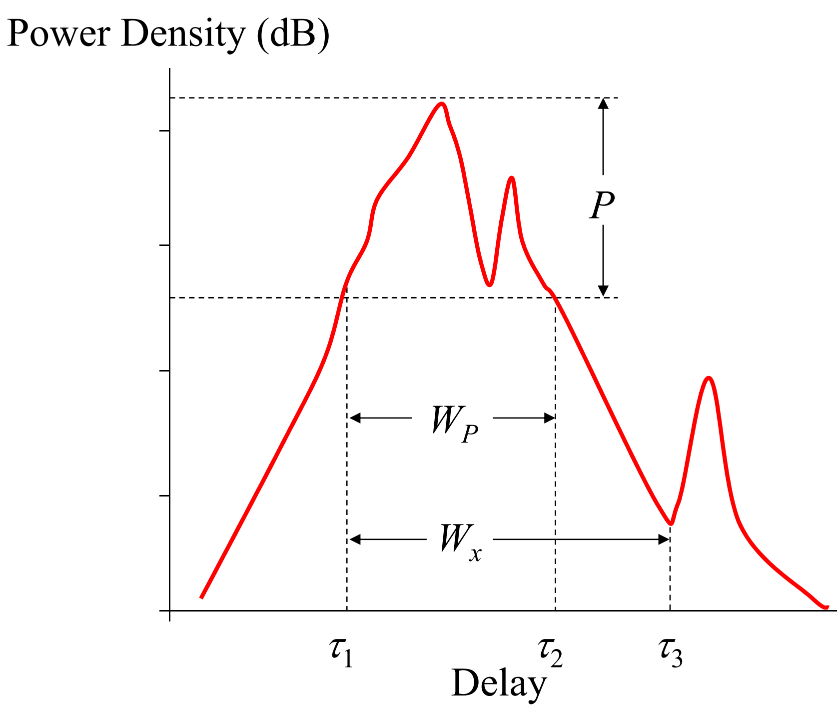

# Multipath Intensity Profile (Cont.)

- The power delay profiles play a key role in determining the need of an adaptive equalizer
- If the delay spread exceeds **10% to 20%** of the symbol duration
  - An adaptive equalizer is required
- Delay spread diminish (↓) with the decrease in cell size (↓)
- The delay spread strongly depends on the environment (and frequency):
  - Urban, suburban, open area
  - Macrocellular: 1 ~ 10 $\mu$s
  - In building: 30 ~ 60 *n*s

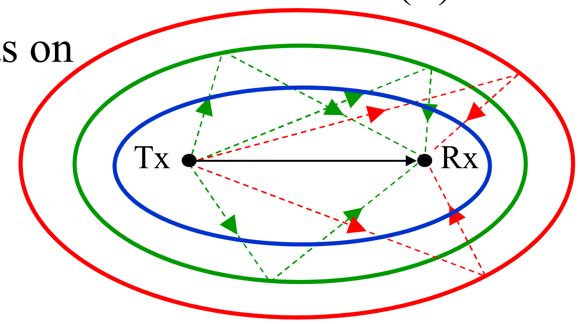


- The value of delay spread impacts on the transmission rate
  - Under the considerations of **complexity** and **performance**



# Coherence Bandwidth

- For WSSUS, the autocorrelation function of $T(t, f)$ is $\phi_T(\Delta t;\Delta f)$: spaced-frequency spaced-time correlation function
- For $\Delta t = 0$, $\phi_T(0;\Delta f) = \phi_T(\Delta f)$ measures the frequency correlation of the channel (depending on the multipath intensity profile)
- **Coherence Bandwidth** $B_c$:
  - The smallest value of $\Delta f$ for which $\phi_T(\Delta f)$ equals some suitable correlation coefficient, such as 0.5
- $\phi_g(\tau)$ and $\phi_T(\Delta f)$ are Fourier transform pair

$$B_c \propto \frac{1}{\sigma_\tau}$$

  - $\sigma_\tau$: the rms delay spread

## Coherence Bandwidth (Cont.)

- For frequency non-selective fading:
  - The transmission bandwidth ($1/T_s$) is smaller than $B_c$
  - The symbol duration $T_s >> \sigma_\tau$
- For frequency selective fading:
  - The transmission bandwidth ($1/T_s$) is larger than or equivalent to $B_c$
  - The symbol duration $T_s \cong \sigma_\tau$ or $T_s < \sigma_\tau$



## Doppler Spread and Coherence Time

- For WSSUS, the autocorrelation function of $H(\nu, f)$: $\phi_H(\nu\,; \Delta f)$
- Doppler power spectral density: For $\Delta f = 0$, $\phi_H(\nu\,; 0) = \phi_H(\nu)$ shows the power density
  - The average power at the channel output as a function of Doppler frequency $\nu$
- **Doppler Spread** $B_d$:
  - The range of values over which $\phi_H(\nu)$ is significant
- $\phi_H(\nu)$ and $\phi_T(\Delta t)$ are Fourier transform pair
  - The inverse of the Doppler spread $B_d$ gives a measure of the coherence time $T_c$

$$T_c \approx \frac{1}{B_d}$$

# Doppler Spread and Coherence Time (Cont.)

- **Coherence time** (corresponding to the average fade duration):
  - Can be used to evaluate the performance of coding and interleaving techniques
  - Coding and interleaving ⇒ **time diversity**
- The duration of interleaving should much larger than the coherence time
- The Doppler spread and the coherence time depend directly on the **velocity** of a moving MS



# Fading Channel

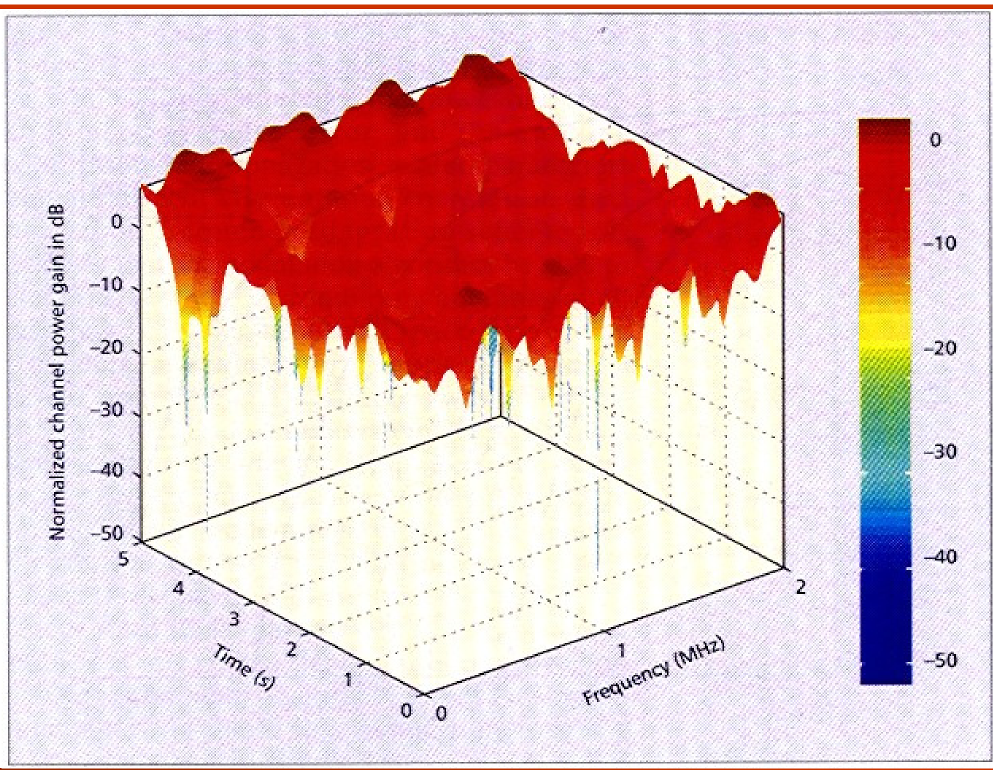

# Question

- **Question:**
  - For what characteristics will a channel have a flat frequency response?
  - For what characteristics will a channel have a large time domain fading correlation?
  - What decides the frequency-domain/time-domain fading characteristics?
- Small delay spread $\Rightarrow$ Large coherence bandwidth $B_c$
  - A simple propagation environment
- Small Doppler spread $B_d \Rightarrow$ Large coherence time $T_c$
  - Low user mobility
- Frequency-domain: propagation environments
- Time-domain: user mobility



# Laboratory Simulation

# Simulation of Multipath-Fading Channels

- The multipath fading channel simulator:
  - Filtered Gaussian Noise Method
  - Jakes' Method
  - Wide-band multipath-fading channels



# Filtered Gaussian Noise Method

- Gaussian noise sources:
  - Zero mean: Rayleigh fade envelope
  - Non-zero mean: Ricean fade envelope
  - The two different noise sources must have the same PSD
- Low-pass filter: the output PSD should have the actual Doppler PSD of the multipath fading channel

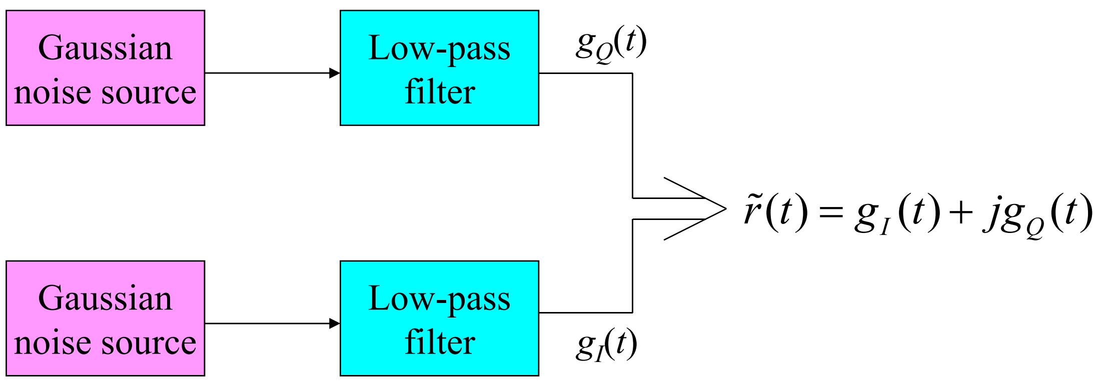

# Doppler Spectrum of Multipath Fading Channel

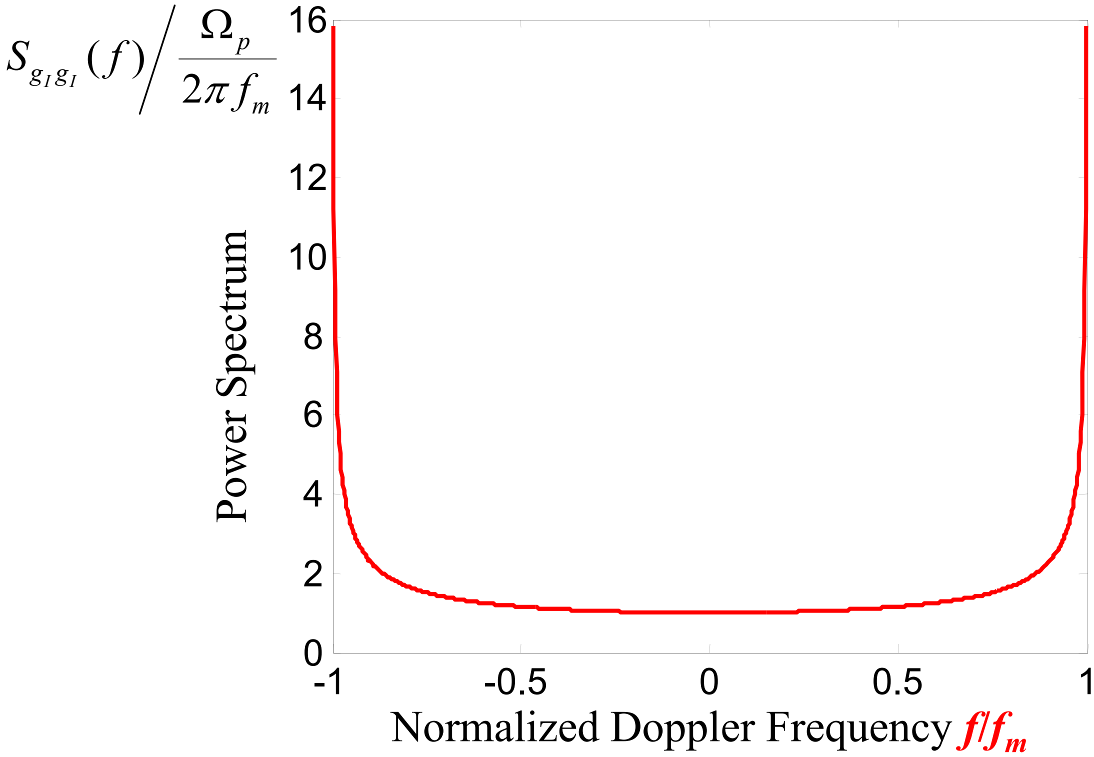




# Filtered Gaussian Noise Method (Cont.)

- In order to approximate the Doppler spectrum of the multipath fading channel, a **high order filter** is required
  - $\Rightarrow$ Long impulse response
  - $\Rightarrow$ Significantly increase the run times
- Advantage: different paths are uncorrelated (if the Gaussian noise sources are uncorrelated)
- Disadvantage: hard to provide correct autocorrelation (a high order filter is required)
- If the noise sources have power spectral densities of $\Omega_p/2$ and the low-pass filters have transfer function $H(f)$
  - We have $S_{g_I g_I}(f) = S_{g_Q g_Q}(f) = \frac{\Omega_p}{2} |H(f)|^2$

$$S_{g_I g_Q}(f) = S_{g_Q g_I}(f) = 0$$

## Filtered Gaussian Noise Method (Cont.)

- Let $g_{I,k} \equiv g_I(kT)$ and $g_{Q,k} \equiv g_Q(kT)$ represent the real and imaginary parts of the complex envelope at epoch $k$, where $T$ is the simulation step size
- Using a **first-order** low-pass digital filter

$$(g_{I,k+1}, g_{Q,k+1}) = \zeta(g_{I,k}, g_{Q,k}) + (1-\zeta)(w_{1,k}, w_{2,k})$$

  - where $w_{1,k}$ and $w_{2,k}$ are **independent** zero-mean Gaussian random variables

$$E\left[g_{I,k}g_{I,k}\right] = \zeta^2 E\left[g_{I,k-1}g_{I,k-1}\right] + (1-\zeta)^2\sigma^2 \Rightarrow \sigma_{g_I}^2 = \sigma_{g_Q}^2 = \frac{1-\zeta}{1+\zeta}\sigma^2$$

  - $\sigma^2$: the variance of $w_{1,k}$ and $w_{2,k}$, and

**Auto-correlation**

$$\phi'_{g_I g_I}(n) = \phi'_{g_Q g_Q}(n) = E[g_{I,k}g_{I,k+n}] = \frac{1-\zeta}{1+\zeta}\sigma^2\zeta^{|n|}$$

**Cross-correlation**

$$\phi'_{g_I g_Q}(n) = \phi'_{g_Q g_I}(n) = 0$$



## Filtered Gaussian Noise Method (Cont.)

- The values of $\sigma^2$ and $\zeta$ should be specified
- For isotropic scattering, the ideal auto-correlation is

$$\phi_{g_I g_I}(n) = \frac{\Omega_p}{2}J_0(2\pi f_m nT)$$

$$\boxed{u[n] = \begin{cases} +1, & n \geq 0 \\ 0, & n < 0 \end{cases}}$$

- Taking DFT on $\phi'_{g_I g_I}(n)$

**Different**

$$\phi'_{g_I g_I}(n) = \frac{1-\zeta}{1+\zeta}\sigma^2\zeta^{|n|} = \frac{1-\zeta}{1+\zeta}\sigma^2\left(\zeta^n u[n] + \zeta^{-n}u[-n] - \delta[n]\right)$$

$$\zeta^n u[n] \xleftrightarrow{\mathbb{F}} \frac{1}{1-\zeta e^{-j2\pi f t}},\ \zeta^{-n}u[-n] \xleftrightarrow{\mathbb{F}} \frac{1}{1-\zeta e^{j2\pi f t}},\ \delta[n] \xleftrightarrow{\mathbb{F}} 1$$

$$S'_{g_I g_I}(f) = \mathbb{F}\left\{\phi'_{g_I g_I}(n)\right\} = \frac{(1-\zeta)^2\sigma^2}{1+\zeta^2 - 2\zeta\cos 2\pi fT}$$

# Filtered Gaussian Noise Method (Cont.)

$$S'_{g_I g_I}(f) = \frac{(1-\zeta)^2 \sigma^2}{1+\zeta^2 - 2\zeta \cos 2\pi f T}$$

- Set the 3 dB point of $S'_{g_I g_I}(f)$ to $f_m/4$, $\boxed{S'_{g_I g_I}(f_m/4) = S'_{g_I g_I}(0)/2}$ we have

$$\zeta^2 - 2\zeta\left(2 - \cos\left(\pi f_m T/2\right)\right) + 1 = 0$$

$$\zeta = 2 - \cos(\pi f_m T/2) - \sqrt{(2 - \cos(\pi f_m T/2))^2 - 1}$$

- To normalized the mean square envelope to $\Omega_p$

$$\sigma_{g_I}^2 = \frac{1-\zeta}{1+\zeta}\sigma^2 = \frac{\Omega_p}{2} \Rightarrow \sigma^2 = \frac{1+\zeta}{(1-\zeta)}\frac{\Omega_p}{2}$$



# Filtered Gaussian Noise Method (Cont.)

$S'_{g_I g_I}(f)$

Obtained by Filtered Gaussian Noise method

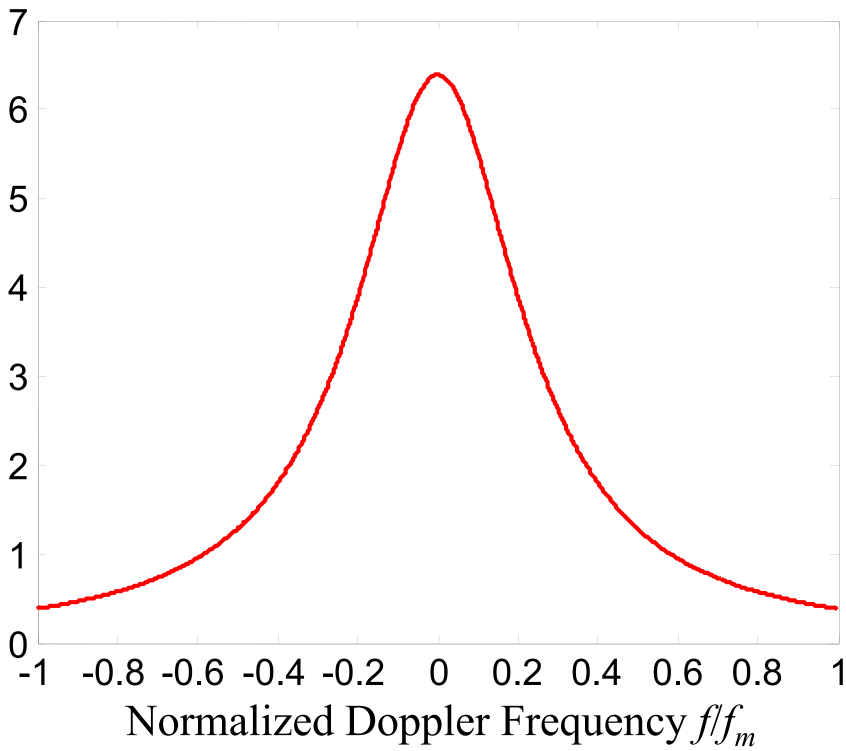

# Filtered Gaussian Noise Method (Cont.)

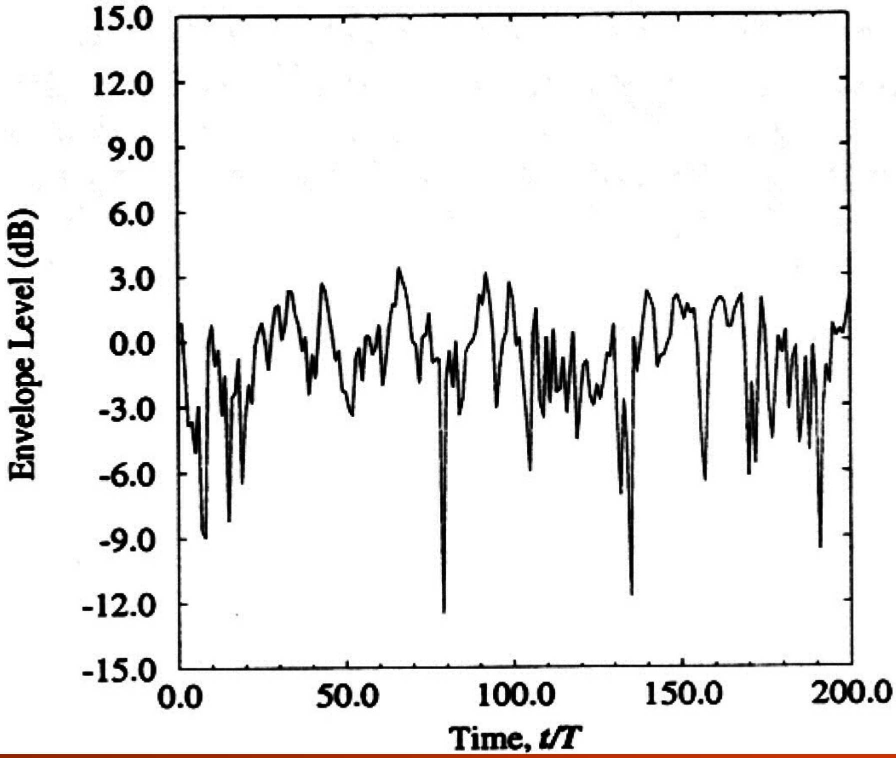




# Sum of Sinusoids Method

- From

$$g(t) = \sum_{n=1}^{N} \alpha_n(t)\, e^{-j\phi_n(t)}$$

$$\phi_n(t) = 2\pi\left\{\left(f_c + f_{D,n}(t)\right)\tau_n(t) - f_{D,n}(t)t\right\}$$

- Assume that
  - The channel is stationary ($f_{D,n}(t) = f_{D,n}$, $\tau_n(t) = \tau_n$, $\alpha_n(t) = \alpha_n$)
  - Equal strength of multipath components ($\alpha_n = 1, \forall n$)

$$g(t) = \sum_{n=1}^{N} e^{j2\pi\left[f_m t\cos\theta_n - \left(f_c + f_m\cos\theta_n\right)\tau_n\right]} = \sum_{n=1}^{N} e^{j(2\pi f_m t\cos\theta_n + \hat{\phi}_n)}$$

- For an isotropic scattering environment, we can assume that the **incident angles** are uniformly distributed

$$\theta_n = \frac{2\pi n}{N}, \quad n = 1, 2, \cdots, N$$

# Sum of Sinusoids Method (Cont.)

- Choose $N/2$ to be an odd integer, we can rewrite $g(t)$ as

$$g(t)=\sum_{n=1}^{N/2-1}\Big[\underbrace{e^{j(2\pi f_m t\cos\theta_n+\hat{\phi}_n)}}_{\mathbf{A}}+\underbrace{e^{-j(2\pi f_m t\cos\theta_n+\hat{\phi}_{-n})}}_{\mathbf{A'}}\Big]+e^{j(2\pi f_m t+\hat{\phi}_N)}+e^{-j(2\pi f_m t+\hat{\phi}_{-N})}$$

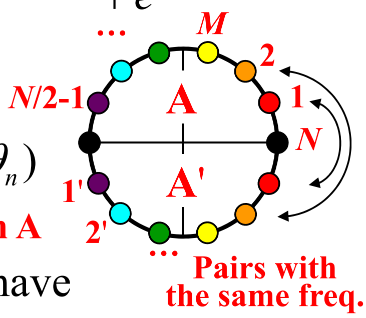


- Some terms have the same freq. components

$$2\pi f_m t\cos(\theta_n+\pi)=-2\pi f_m t\cos\theta_n=2\pi f_m t\cos(\pi-\theta_n)$$

**Term $N/2+n$** **Term $n$ in A'** $\xleftrightarrow{\text{same freq.}}$ **Term $N/2-n$ in A**

- Combining the terms with the same freq., we have

$$g(t)=\sqrt{2}\sum_{n=1}^{M}\Big[e^{j(2\pi f_m t\cos\theta_n+\hat{\phi}_n)}+e^{-j(2\pi f_m t\cos\theta_n+\hat{\phi}_{-n})}\Big]+e^{j(2\pi f_m t+\hat{\phi}_N)}+e^{-j(2\pi f_m t+\hat{\phi}_{-N})}$$

**Maintain the same total power**

$$M=\frac{1}{2}\left(\frac{N}{2}-1\right)$$

- For the same freq. components, the phases are now set to be the same ⇒ Correlation is introduced into the phases



# Sum of Sinusoids Method (Cont.)

$$g(t)=\sqrt{2}\sum_{n=1}^{M}\Big[e^{j(2\pi f_m t\cos\theta_n+\hat{\phi}_n)}+e^{-j(2\pi f_m t\cos\theta_n+\hat{\phi}_{-n})}\Big]+e^{j(2\pi f_m t+\hat{\phi}_N)}+e^{-j(2\pi f_m t+\hat{\phi}_{-N})}$$

- If we further adopt the constraint that $\hat{\phi}_n=-\hat{\phi}_{-n}$, we have

$$\boxed{\begin{aligned}\cos(x+y)&=\cos(x)\cos(y)-\sin(x)\sin(y)\\ \sin(x+y)&=\sin(x)\cos(y)+\cos(x)\sin(y)\end{aligned}}$$

$$\boxed{2\pi f_n t=2\pi f_m t\cos\theta_n}$$

$$\begin{aligned}g(t)&=g_I(t)+jg_Q(t)\\ &=\sqrt{2}\Big\{\Big[2\sum_{n=1}^{M}\cos\beta_n\cos\underline{2\pi f_n t}+\sqrt{2}\cos\alpha\cos 2\pi f_m t\Big]\\ &\qquad+j\Big[2\sum_{n=1}^{M}\sin\beta_n\cos 2\pi f_n t+\sqrt{2}\sin\alpha\cos 2\pi f_m t\Big]\Big\}\end{aligned}$$

  - where $\alpha=\hat{\phi}_N=-\hat{\phi}_{-N}$, $\beta_n=\hat{\phi}_n=-\hat{\phi}_{-n}$
- Only **($M$+1)** independent frequency oscillators are required
  - There are ($M$+1) different frequencies

## Sum of Sinusoids Method (Cont.)

- Considering the channel statistics

$$E\left[g_I^2(t)\right] = 2\sum_{n=1}^{M}\cos^2\beta_n + \cos^2\alpha = M + \cos^2\alpha + \sum_{n=1}^{M}\cos 2\beta_n$$

$$E\left[g_Q^2(t)\right] = 2\sum_{n=1}^{M}\sin^2\beta_n + \sin^2\alpha = M + \sin^2\alpha - \sum_{n=1}^{M}\cos 2\beta_n$$

$$E\left[g_I(t)g_Q(t)\right] = 2\sum_{n=1}^{M}\sin\beta_n\cos\beta_n + \sin\alpha\cos\alpha$$

- It is desirable that

$$E\left[g_I^2(t)\right] = E\left[g_Q^2(t)\right], \quad E\left[g_I(t)g_Q(t)\right] = 0$$

- Choose the parameters $\beta_n = \dfrac{\pi n}{M}, \quad \alpha = 0$

$$E\left[g_I^2(t)\right] = M + 1, \quad E\left[g_Q^2(t)\right] = M, \quad E\left[g_I(t)g_Q(t)\right] = 0$$



## Sum of Sinusoids Method (Cont.)

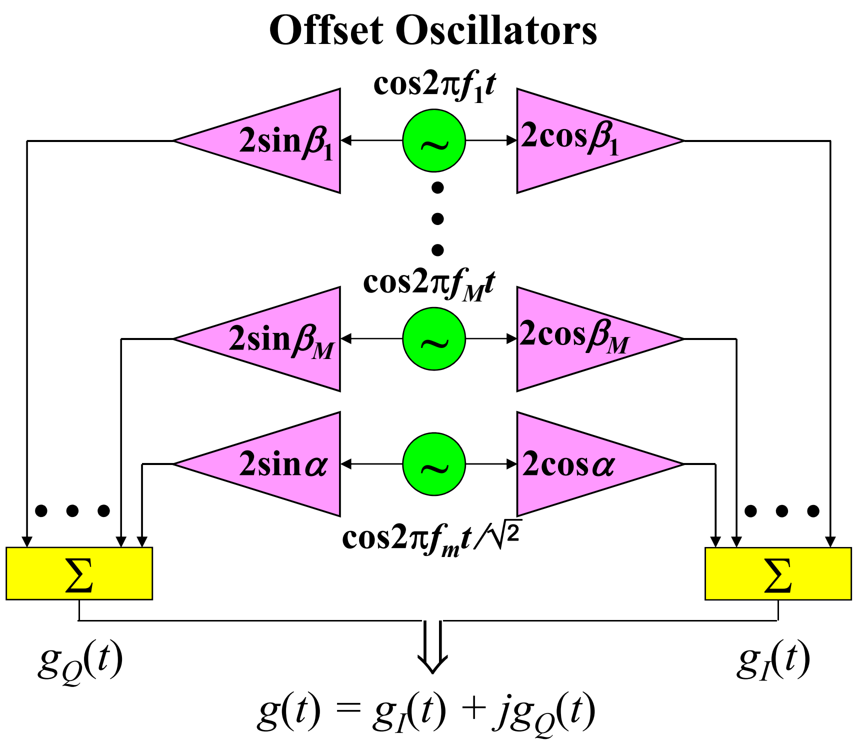


$$f_n = f_m \cos\frac{2\pi n}{N}$$

$$\beta_n = \frac{\pi n}{M}$$

$$\alpha = 0$$

Uniform incoming direction

Uniform phase

# Sum of Sinusoids Method (Cont.)

- If the last term of $g_I(t)$ is ignored, we have

$$E\left[g_I^2(t)\right]=M,\quad E\left[g_Q^2(t)\right]=M,\quad E\left[g_I(t)g_Q(t)\right]=0$$

  – when $\beta_n=\dfrac{\pi n}{M},\quad \alpha=0$
- Advantage: the **autocorrelation** of inphase and quadrature components reflect an **isotropic scattering** environment with a reasonable complexity
- The channel model output is a **deterministic process**
  – No random number generator is applied



# Sum of Sinusoids Method (Cont.)

- $M = 8$

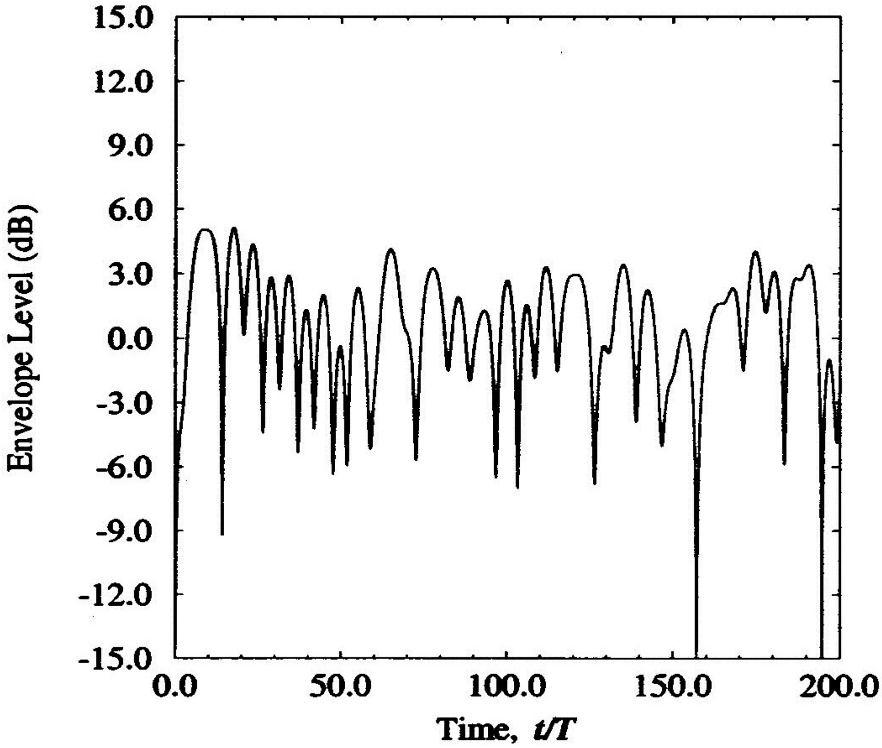

# Sum of Sinusoids Method (Cont.)

- $M = 8$

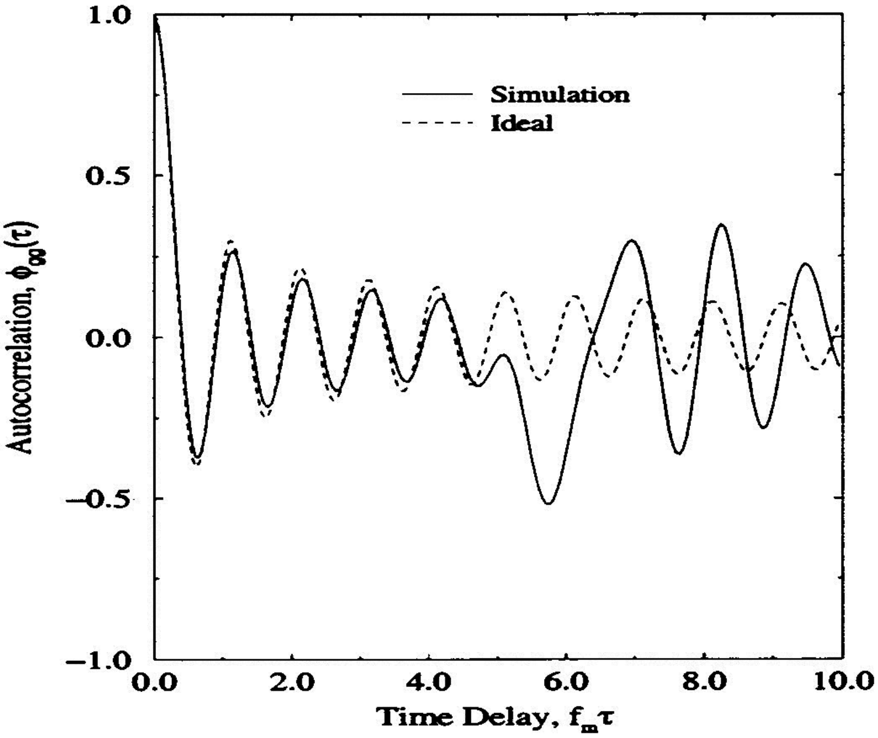




# Sum of Sinusoids Method (Cont.)

- $M = 16$

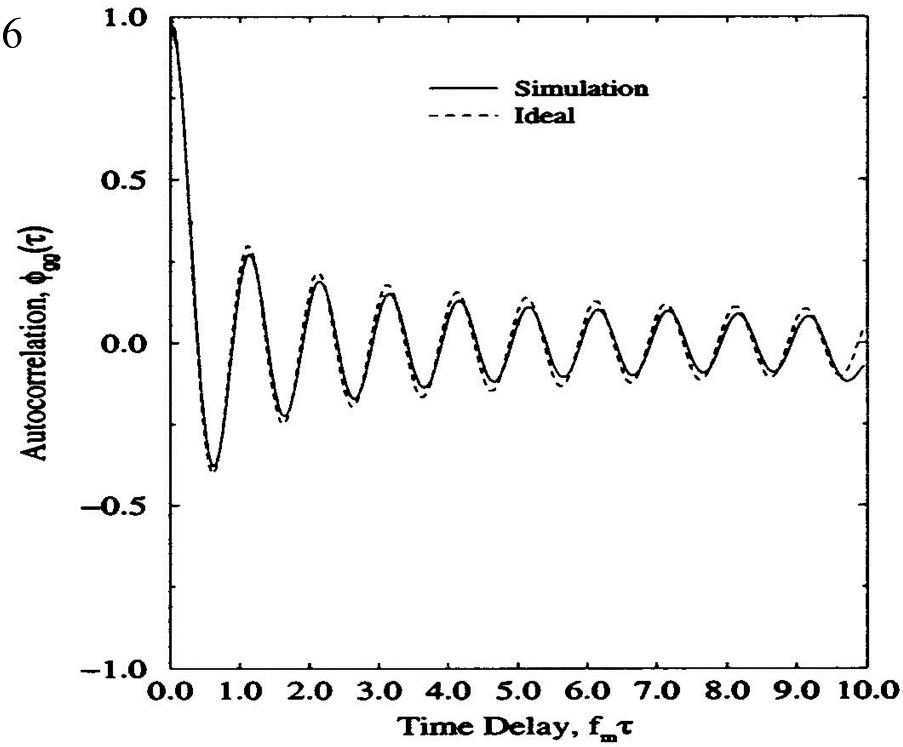

# Wide-Band Multipath-Fading Channels

- For wide-band communication systems, the time-domain resolution is increased and multiple paths can be resolved
- $\tau$–spaced model:
  - Model the channel by a tapped delay line
  - Assume a number of discrete paths at different delays

$$\tilde{r}(t) = \sum_{i=1}^{\ell} g_i(t)\tilde{s}(t-\tau_i)$$

  - $g_i(t)$ and $\tau_i$ are the tap gain and delay of the $i$-th path

$$g(t,\tau) = \sum_{i=1}^{\ell} g_i(t)\delta(t-\tau_i)$$

  - The tap gain and tap delay vectors

$$\mathbf{g}(t) = \left(g_1(t),\, g_2(t),\, \cdots,\, g_\ell(t)\right)$$
$$\boldsymbol{\tau} = \left(\tau_1,\, \tau_2,\, \cdots,\, \tau_\ell\right)$$



# Wide-Band Multipath-Fading Channels (Cont.)

- The path delays are multiples of some small number $\tau$

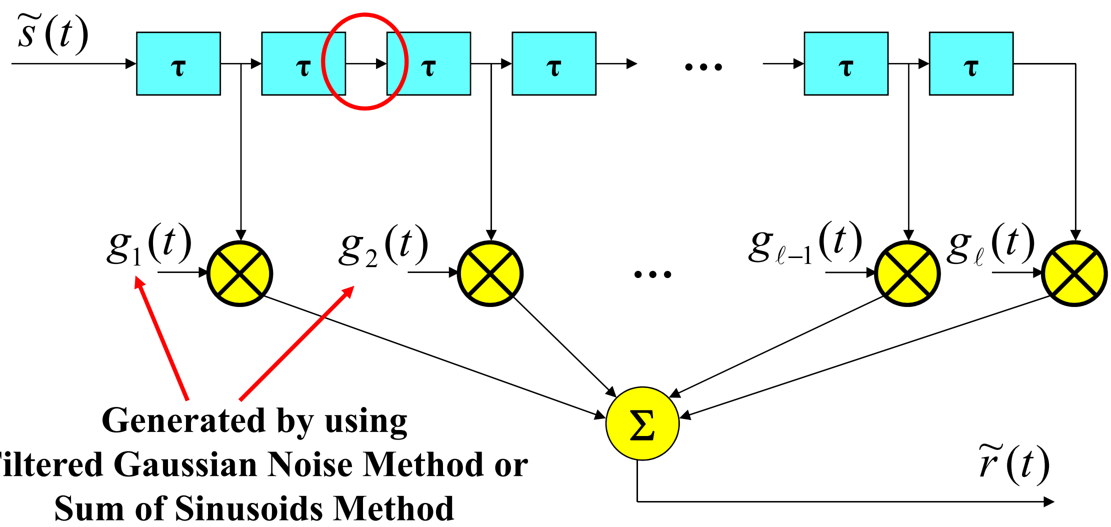

# Multiple Faded Envelopes

- In many cases, it is desirable to generate multiple envelopes with **uncorrelated fading** (i.e., different paths with resolvable delays)
  - Generate up to ***M*** fading envelopes by using the same ***M*** frequency oscillators
- Give the $n$-th oscillator, $1 \le n \le M$, an additional phase shift $\theta_{nk} = \gamma_{nk} + \beta_n$, $1 \le k \le M$, where $k$ is the index of fading envelopes
- An additional constraint: the multiple faded envelopes should be **uncorrelated**
  - Choose appropriate values of $\gamma_{nk}$ and $\beta_n$
- The $k$-th fading envelope is (ignore the last term of $g_I(t)$)

$$g_k(t) = 2\sqrt{2}\sum_{n=1}^{M}\left(\cos\beta_n + j\sin\beta_n\right)\underline{\cos\left(2\pi f_n t + \theta_{nk}\right)}$$



# Multiple Faded Envelopes (Cont.)

- By using two quadrature frequency oscillators

**Actually, only one oscillator is needed**

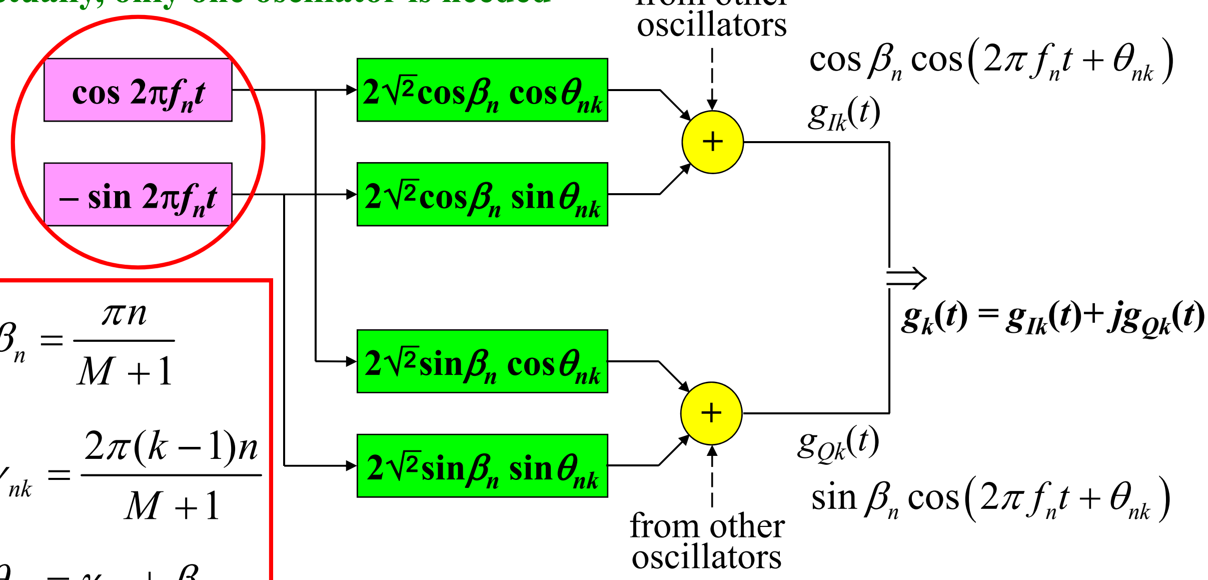


$$\beta_n = \frac{\pi n}{M+1}$$

$$\gamma_{nk} = \frac{2\pi(k-1)n}{M+1}$$

$$\theta_{nk} = \gamma_{nk} + \beta_n$$

# Multiple Faded Envelopes (Cont.)

- Choose the parameters with the objective yielding uncorrelated waveforms

$$\beta_n = \frac{\pi n}{M+1}, \quad \gamma_{nk} = \frac{2\pi(k-1)n}{M+1}, \quad n = 1, 2, \cdots, M$$

- Significant cross-correlation between the different generated fading envelopes (**without modification**)
- A modification that uses orthogonal **Walsh-Hadamard** codewords to decorrelate the fading envelopes is applied
  - $A_k(n)$: the $k$-th row of Hadamard matrix $\mathbf{H}_M$
  - **$A_k(n)$: +1 (“0”) or –1 (“1”)**

$$g_k(t) = 2\sqrt{2}\sum_{n=1}^{M} A_k(n)\left(\cos\beta_n + j\sin\beta_n\right)\cos\left(2\pi f_n t + \theta_{nk}\right)$$



# Multiple Faded Envelopes (Cont.)

- Walsh-Hadamard codes:
  - It is an **orthogonal code set**
  - The cross-correlation between different codes is zero
- The code period of Walsh codes must be a power of 2
  - The code length must be 2, 4, 8, 16, …

$$\mathbf{H}_1 = [0] \quad \mathbf{H}_{2^n} = \begin{bmatrix} \mathbf{H}_{2^{(n-1)}} & \mathbf{H}_{2^{(n-1)}} \\ \mathbf{H}_{2^{(n-1)}} & \overline{\mathbf{H}_{2^{(n-1)}}} \end{bmatrix}$$

$$\mathbf{H}_2 = \begin{bmatrix} 0 & 0 \\ 0 & 1 \end{bmatrix}; \quad \mathbf{H}_4 = \begin{bmatrix} 0 & 0 & 0 & 0 \\ 0 & 1 & 0 & 1 \\ 0 & 0 & 1 & 1 \\ 0 & 1 & 1 & 0 \end{bmatrix}; \quad \mathbf{H}_8 = \begin{bmatrix} 0 & 0 & 0 & 0 & 0 & 0 & 0 & 0 \\ 0 & 1 & 0 & 1 & 0 & 1 & 0 & 1 \\ 0 & 0 & 1 & 1 & 0 & 0 & 1 & 1 \\ 0 & 1 & 1 & 0 & 0 & 1 & 1 & 0 \\ 0 & 0 & 0 & 0 & 1 & 1 & 1 & 1 \\ 0 & 1 & 0 & 1 & 1 & 0 & 1 & 0 \\ 0 & 0 & 1 & 1 & 1 & 1 & 0 & 0 \\ 0 & 1 & 1 & 0 & 1 & 0 & 0 & 1 \end{bmatrix};$$

# Multiple Faded Envelopes (Cont.)

- $M = 8$
- Without modification

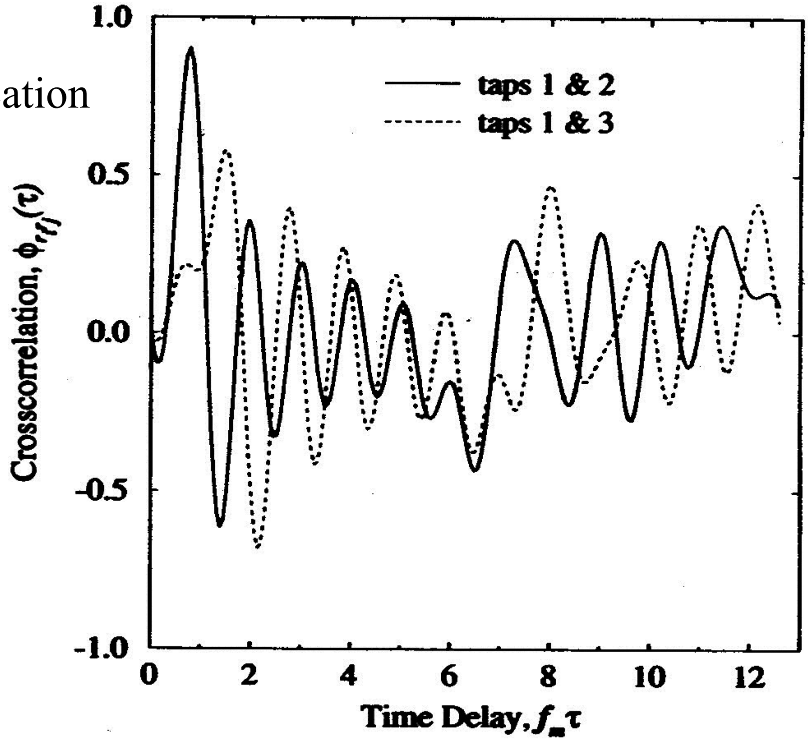




# Multiple Faded Envelopes – Modified

- $M = 8$
- With modification

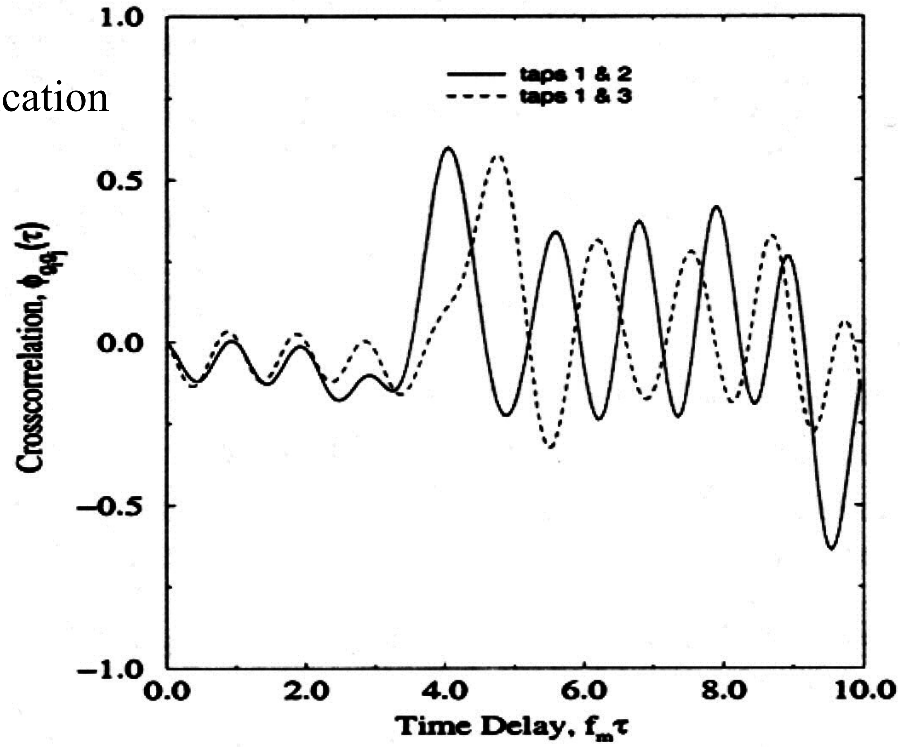

# Multiple Faded Envelopes – Modified (Cont.)

- $M = 16$
- With modification

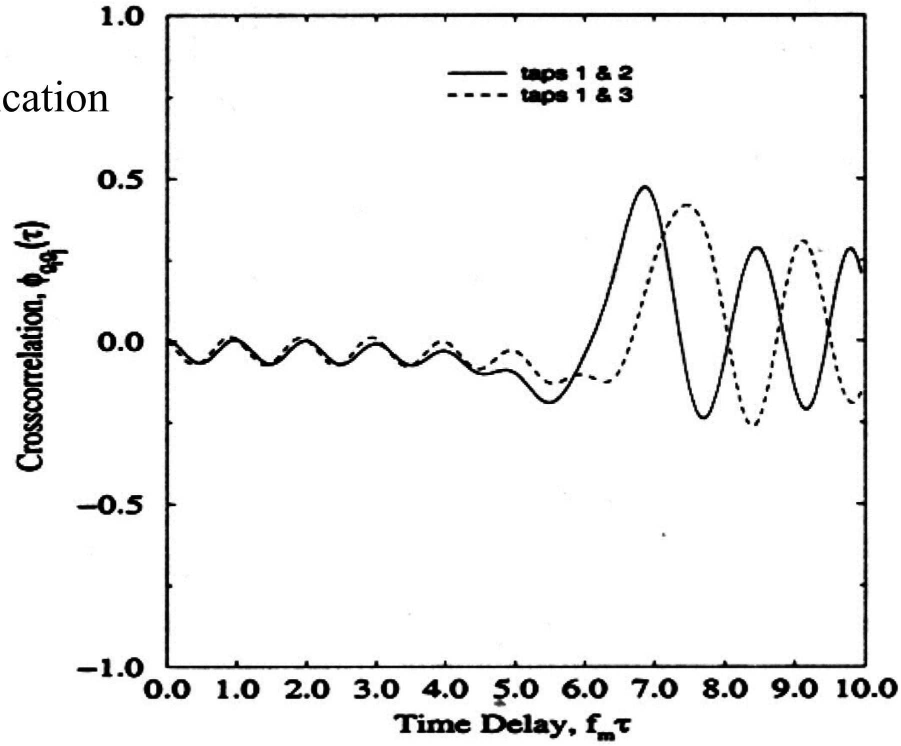




# Shadowing

# Shadowing

- $\Omega_v$: the mean envelope level, $\Omega_v = E[\alpha(t)]$
  – where $\alpha(t)$ is Rayleigh or Ricean distributed
  – The local mean: averaged over a few wavelengths
- $\Omega_p$: the mean squared envelope level, $\Omega_p = E[\alpha^2(t)]$
- $\Omega_v$ and $\Omega_p$ are random variables due to shadow variations that caused by
  – **Macrocell:** large terrain features (buildings, hills)
  – **Microcell:** small objects (vehicles, human)
- $\Omega_v$ and $\Omega_p$ follow the log-normal distributions

**Linear Scale**

$$p_{\Omega_v}(x) = \frac{2}{x\sigma_\Omega \xi \sqrt{2\pi}} \exp\left[ -\frac{(10\log_{10} x^2 - \mu_{\Omega_v(\text{dBm})})^2}{2\sigma_\Omega^2} \right]$$

$$p_{\Omega_p}(x) = \frac{1}{x\sigma_\Omega \xi \sqrt{2\pi}} \exp\left[ -\frac{(10\log_{10} x - \mu_{\Omega_p(\text{dBm})})^2}{2\sigma_\Omega^2} \right]$$



# Shadowing (Cont.)

– where $\xi = \ln 10/10$ and

$$\mu_{\Omega_v(\text{dBm})} = 30 + 10E[\log_{10}\Omega_v^2]; \quad \mu_{\Omega_p(\text{dBm})} = 30 + 10E[\log_{10}\Omega_p]$$

- $\Omega_{v(\text{dBm})}$ and $\Omega_{p(\text{dBm})}$ have the Gaussian densities
  – The mean is determined by the propagation **path loss**

**dB Scale**

$$p_{\Omega_v(\text{dBm})}(x) = \frac{1}{\sqrt{2\pi}\sigma_\Omega} \exp\left[ -\frac{(x - \mu_{\Omega_v(\text{dBm})})^2}{2\sigma_\Omega^2} \right]$$

$$p_{\Omega_p(\text{dBm})}(x) = \frac{1}{\sqrt{2\pi}\sigma_\Omega} \exp\left[ -\frac{(x - \mu_{\Omega_p(\text{dBm})})^2}{2\sigma_\Omega^2} \right]$$

- The standard deviation of log-normal shadowing ranges:
  – Macrocell: **5 ~ 12 dB** with typical value $\sigma_\Omega = 8$ dB
    - $\sigma_\Omega$ increases slightly with frequency ($\sigma_{1.8\text{GHz}} = \sigma_{900\text{MHz}} + 0.8\text{dB}$)
  – Microcell: **4 ~ 13 dB**

# Shadowing (Cont.)

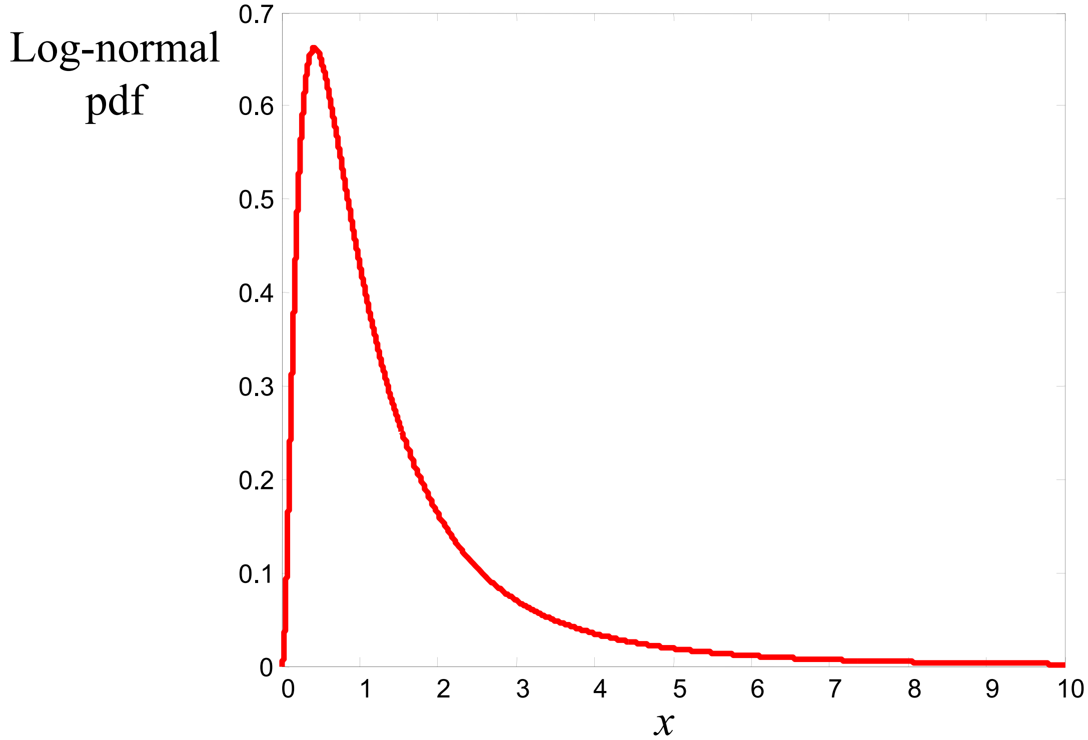




# Simulation of Shadowing

- A shadow simulator should account the spatial correlation
- One simple model: the log-normal shadowing is modeled as
  - A Gaussian white noise process
  - Filtered with a first-order low-pass filter

$$\Omega_{k+1(\mathrm{dBm})} = \zeta\, \Omega_{k(\mathrm{dBm})} + (1-\zeta)v_k$$

  - $k$: the location index
  - $\zeta$: control the spatial correlation of the shadowing
  - $v_k$: a zero-mean Gaussian random variable, $\phi_{vv}(n) = \tilde{\sigma}^2\delta(n)$
- The spatial autocorrelation function:

$$\phi_{\Omega_{(\mathrm{dBm})}\Omega_{(\mathrm{dBm})}}(n) = \frac{1-\zeta}{1+\zeta}\tilde{\sigma}^2\zeta^{|n|}$$

$$\sigma_\Omega^2 = \phi_{\Omega_{(\mathrm{dBm})}\Omega_{(\mathrm{dBm})}}(0) = \frac{1-\zeta}{1+\zeta}\tilde{\sigma}^2$$

# Simulation of Shadowing (Cont.)

$$\phi_{\Omega_{(\mathrm{dBm})}\Omega_{(\mathrm{dBm})}}(n) = \sigma_\Omega^2 \zeta^{|n|}$$

- This approach generates shadows that decorrelated **exponentially with distance**
- If an MS is traveling with velocity $v$, the envelope is sampled for every $T$ seconds, and $\zeta_D$ is the shadow correlation of spatial distance $D$ m
  – Time difference $kT \Rightarrow$ spatial distance $vkT$

$$\phi_{\Omega_{(\mathrm{dBm})}\Omega_{(\mathrm{dBm})}}(k) \equiv \phi_{\Omega_{(\mathrm{dBm})}\Omega_{(\mathrm{dBm})}}(kT) = \sigma_\Omega^2 \zeta_D^{(vT/D)|k|}$$

  – $\zeta = \zeta_D^{(vT/D)}$
- Suburban 900 MHz: $\sigma_\Omega \approx 7.5$ dB with corr. 0.82 (100m)
- Microcell 1700 MHz: $\sigma_\Omega \approx 4.3$ dB with corr. 0.3 (10m)



# Simulation of Shadowing (Cont.)

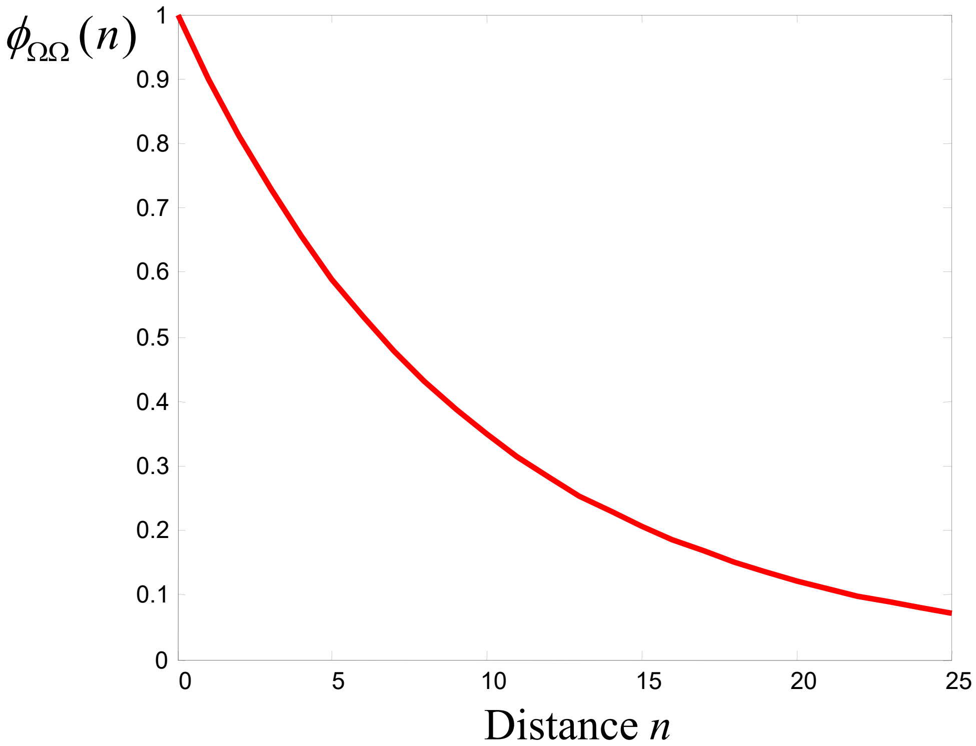

# Path Loss Models



# Free Space Path Loss Model

- Free space: the received signal power

$$\mu_{\Omega_p} = \Omega_t G_T G_R \left( \frac{\lambda_c}{4\pi d} \right)^2$$

$$\mu_{\Omega_p\,(\mathrm{dB})} = 10\log_{10}\left( \Omega_t G_T G_R \left( \frac{\lambda_c}{4\pi d} \right)^2 \right)$$

$$\mu_{\Omega_p\,(\mathrm{dB})} = 10\log_{10}(\Omega_t G_T G_R / 16\pi^2) + 20\log_{10}\lambda_c - 20\log_{10} d$$

  - $\Omega_t$: the transmission power
  - $G_T$ and $G_R$: the transmitter and receiver antenna gains
  - $\lambda_c$: the wavelength
  - $d$: the radio path length

# Mobile Radio Two-ray Path Loss Model

- Mobile radio environment (Two-ray model)

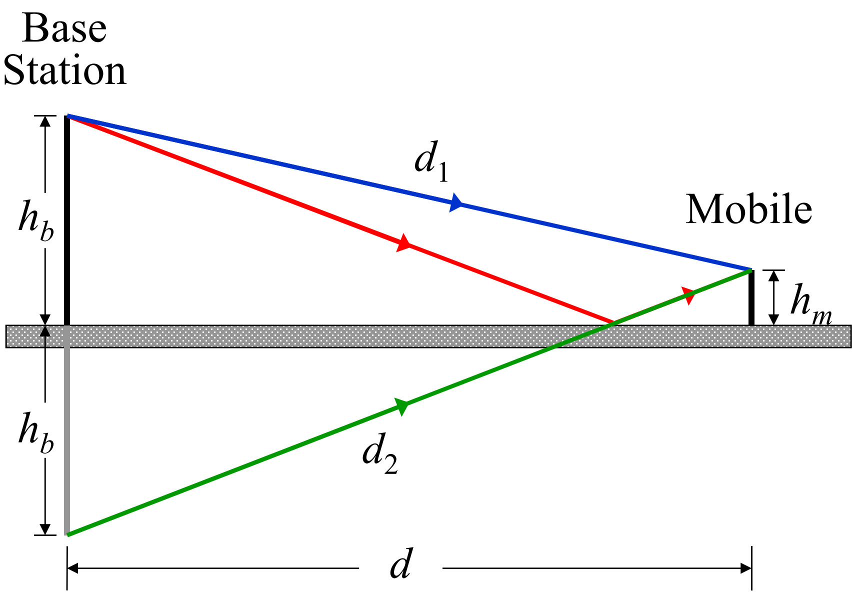




# Mobile Radio Two-ray Path Loss Model (Cont.)

$$P_r = P_t\left(\frac{\lambda_c}{4\pi d}\right)^2 \left|1+\alpha_v e^{j\Delta\phi}\right|^2$$

$$= P_t\left(\frac{\lambda_c}{4\pi d}\right)^2 \left|1-\cos\Delta\phi - j\sin\Delta\phi\right|^2$$

$$= P_t\left(\frac{\lambda_c}{4\pi d}\right)^2 \times 2(1-\cos\Delta\phi)$$

$$= P_t\left(\frac{\lambda_c}{4\pi d}\right)^2 \times 4\sin^2\frac{\Delta\phi}{2}$$

$\alpha_v$ : reflection coefficient
$\alpha_v = -1$, for mobile environment
$\Delta\phi$ : phase difference

$\Delta\phi = \frac{2\pi}{\lambda_c}\Delta d$, and $\Delta d = d_2 - d_1$

$d_1 = \sqrt{(h_b - h_m)^2 + d^2}$, and $d_2 = \sqrt{(h_b + h_m)^2 + d^2}$

$$d_2^2 - d_1^2 = 2d_1\Delta d + \Delta d^2 = 4h_b h_m$$

$$\Rightarrow \Delta d \approx 2h_b h_m / d, \quad \Delta\phi = \frac{4\pi h_b h_m}{\lambda_c d}$$

$$\left(\because \begin{cases} d_1 \approx d \\ \Delta d^2 \approx 0 \end{cases} \text{for } d >> 0\right)$$

$$\Rightarrow P_r = P_t\left(\frac{\lambda_c}{4\pi d}\right)^2 \times 4\sin^2\left(\frac{2\pi h_b h_m}{\lambda_c d}\right)$$

# Mobile Radio Two-ray Path Loss Model (Cont.)

- The received signal power is

$$\mu_{\Omega_p} = 4\Omega_t \left(\frac{\lambda_c}{4\pi d}\right)^2 G_T G_R \sin^2\left(\frac{2\pi h_b h_m}{\lambda_c d}\right)$$

- When $d >> h_b\, h_m$, $\sin x \approx x$

$$\mu_{\Omega_p} = \Omega_t G_T G_R \left(\frac{h_b h_m}{d^2}\right)^2$$

- The differences to the free space model are:
  - The path loss is not frequency dependent
  - The signal power decays with the 4th power of the distance
- The path loss is independent of $\Omega_t$, $G_T$, and $G_R$

$$L_{p(\mathrm{dB})} = 10\log_{10}\left\{\frac{\Omega_t G_T G_R}{\mu_{\Omega_p}}\right\} = -10\log_{10}\left\{4\left(\frac{\lambda_c}{4\pi d}\right)^2 \sin^2\left(\frac{2\pi h_b h_m}{\lambda_c d}\right)\right\} \text{ dB}$$



# Mobile Radio Two-ray Path Loss Model (Cont.)

- The last **local maximum** of the path loss occurs when $2\pi h_b h_m / \lambda_c d = \pi$
- The last **local minimum** of the path loss occurs when $2\pi h_b h_m / \lambda_c d = \pi/2$

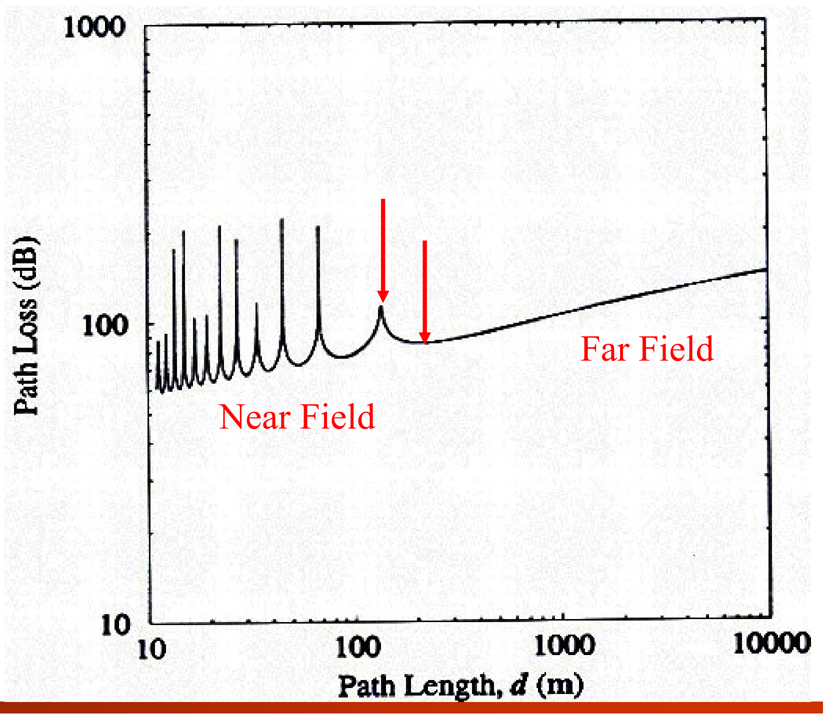

# Path Loss in Macrocells

- The path loss models used in macrocell applications are **empirical** models
  - The environment is **too complex** to obtained a completely theoretical-based model
  - Obtained by curve fitting based on the experimental data
- For 900 MHz cellular systems, the most common used path loss model is
  - **Okumura-Hata's model**
    - Empirical data was collected by Okumura (in Tokyo)
    - Modeled by Hata



# Okumura-Hata's Model

- $f_c$: 150~1500MHz, $d$: >1Km, $h_b$: 30~200m, $h_m$: 1~10m

$$L_{p(\mathrm{dB})} = \begin{cases} A + B\log_{10}(d) & \text{for urban area} \\ A + B\log_{10}(d) - C & \text{for suburban area} \\ A + B\log_{10}(d) - D & \text{for open area} \end{cases}$$

  - where

$$A = 69.55 + 26.16\log_{10}(f_c) - 13.82\log_{10}(h_b) - a(h_m)$$
$$B = 44.9 - 6.55\log_{10}(h_b)$$
$$C = 5.4 + 2[\log_{10}(f_c/28)]^2$$
$$D = 40.94 + 4.78[\log_{10}(f_c)]^2 - 18.33\log_{10}(f_c)$$

$$a(h_m) = \begin{cases} [1.1\log_{10}(f_c) - 0.7]h_m - [1.56\log_{10}(f_c) - 0.8], & \text{for medium or small city} \\ \begin{cases} 8.28[\log_{10}(1.54h_m)]^2 - 1.1, & \text{for } f_c \le 200 \text{ MHz} \\ 3.2[\log_{10}(11.75h_m)]^2 - 4.97, & \text{for } f_c \ge 400 \text{ MHz} \end{cases}, & \text{for large city} \end{cases}$$

# Okumura-Hata's Model (Cont.)

- Another empirical model published by the CCIR:

$$L_{p(\mathrm{dB})} = A + B\log_{10}(d) - E$$

  - where

$$A = 69.55 + 26.16\log_{10}(f_c) - 13.82\log_{10}(h_b) - a(h_m)$$

$$B = 44.9 - 6.55\log_{10}(h_b)$$

$$E = 30 - 25\log_{10}(\text{\% of area covered by buildings: } 1\sim100)$$

$$a(h_m) = \left[1.1\log_{10}(f_c) - 0.7\right]h_m - \left[1.56\log_{10}(f_c) - 0.8\right]$$

- The parameter $E$ accounts for the degree of urbanization
  - $E = 0$ when the area is covered by approximately 16 % of buildings



# Okumura-Hata's Model (Cont.)

- **Another expression**
- $f_c$: 150~1500MHz, $d$: >1Km, $h_b$: 30~200m, $h_m$: 1~10m
- $P_O = A + B \log(d)$
  $= [69.55 + 26.16 \log(f_c) - 13.82 \log(h_b)]$
  $+ [44.9 - 6.55\log(h_b)] \log(d)$
- $a(h_m)$:
  - Large city:
    - $f_c < 200$MHz: $a(h_m) = 8.28 [\log(1.54\, h_m)]^2 - 1.1$
    - $f_c > 400$MHz: $a(h_m) = 3.2 [\log(11.75\, h_m)]^2 - 4.97$
  - Medium or Small city:
    - $a(h_m) = [1.1 \log(f_c) - 0.7]h_m - [1.56\log(f_c) - 0.8]$

# Okumura-Hata's Model (Cont.)

- **Distance correction factor**:
  - $d < 20$Km: cr($d$) = 0
  - $d > 20$Km: cr($d$) = ($d$ – 20)[0.31081 + 0.1865log($h_b$/100)]
  - $d > 64.36$Km: cr($d$) = ($d$ – 20)[0.31081 + 0.1865 log($h_b$/100)] – 0.174($d$ – 64.36)
- Environment correction factor:
  - Urban area: ce($f_c$) = 0
  - Suburban area: ce($f_c$) = – 2[log($f_c$/28)]$^2$ – 5.4
  - Open area: ce($f_c$) = – 4.78[log($f_c$)]$^2$ + 18.33 log($f_c$) – 40.94
- $\mathbf{P_L = P_O - a(h_m) + cr(d) + ce(f_c)}$ **dB**



# Okumura-Hata's Model (Cont.)

- $f_c$ = 900 MHz, $h_b$ = 70 m, $h_m$ = 1.5 m

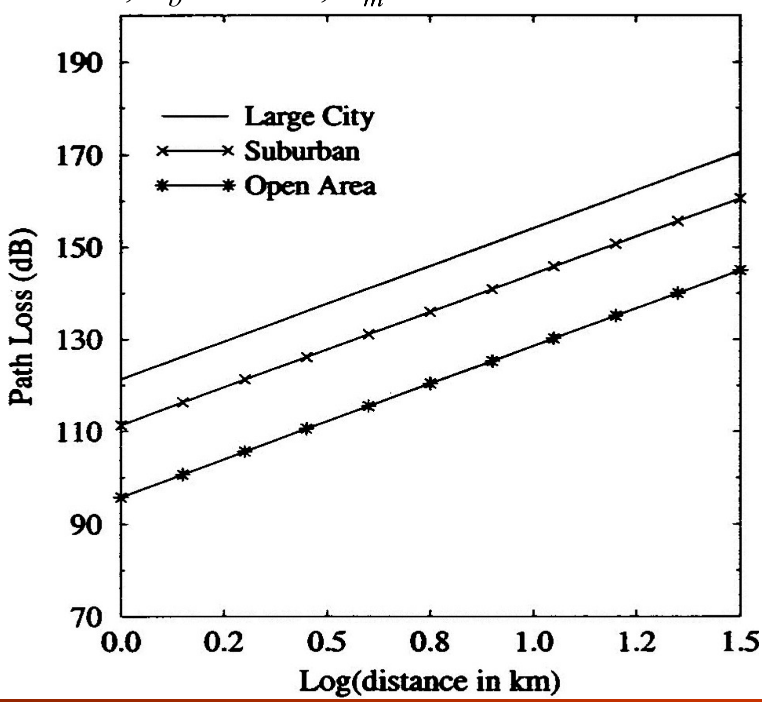

# Path Loss in Outdoor Macro-/Micro-cells

- For the PCS microcellular systems operating in 1800-2000 MHz frequency bands, the two common used path loss models are
  - COST231-Hata model (Macrocellular)
  - Two-slope model (Microcellular)



# COST231-Hata Model

- Extend Okumura-Hata model for 1500-2000 MHz range
- $f_c$: 1500~2000 MHz, $d$: 1~20 Km, $h_b$: 30~200m, $h_m$: 1~10m

$$L_{p(\text{dB})} = A + B\log_{10}(d) + C$$

Okumura-Hata's Model

$$A = 69.55 + 26.16\log_{10}(f_c) - 13.82\log_{10}(h_b) - a(h_m)$$
$$B = 44.9 - 6.55\log_{10}(h_b)$$

$$A = 46.3 + 33.9\log_{10}(f_c) - 13.82\log_{10}(h_b) - a(h_m)$$
$$B = 44.9 - 6.55\log_{10}(h_b)$$
$$C = \begin{cases} 0 & \text{medium city and suburban areas with moderate tree density} \\ 3 & \text{for metropolitan centers} \end{cases}$$

- Good accuracy for a path length larger than 1 km
- Should not be used for smaller ranges (near field)
  - The path loss becomes **highly dependent** upon the local topography

# Two-Slope Model (Street Microcells)

- For a range less than 500m and the antenna height less than 20m

$$\mu_{\Omega_p} = \frac{k\Omega_t}{d^a (1+d/g)^b}$$

$$\begin{aligned}
\mu_{\Omega_p} &= 10\log_{10}(k\Omega_t) - 10\log_{10}(d^a(1+d/g)^b) \quad \text{(dBm)} \\
&= 10\log_{10}(k\Omega_t) - 10\log_{10} g^a - 10\log_{10}(d/g)^a - 10\log_{10}(1+d/g)^b \\
&= 10\log_{10}(k\Omega_t) - 10a\log_{10} g - 10a\log_{10}(d/g) - 10b\log_{10}(1+d/g) \\
&\approx \begin{cases} 10\log_{10}(k\Omega_t) - 10a\log_{10} d, & \text{if } d \ll g \\ 10\log_{10}(k\Omega_t) - 10a\log_{10} g - 10(a+b)\log_{10}(d/g), & \text{if } d \gg g \end{cases}
\end{aligned}$$

- When close into the BS: free-space propagation $\Rightarrow a = 2$
- At larger distance: inverse-fourth power law $\Rightarrow b = 2$



# Two-Slope Model (Street Microcells) (Cont.)

- The last local minimum of the path loss occurs when $2\pi h_b h_m / \lambda_c d = \pi/2$

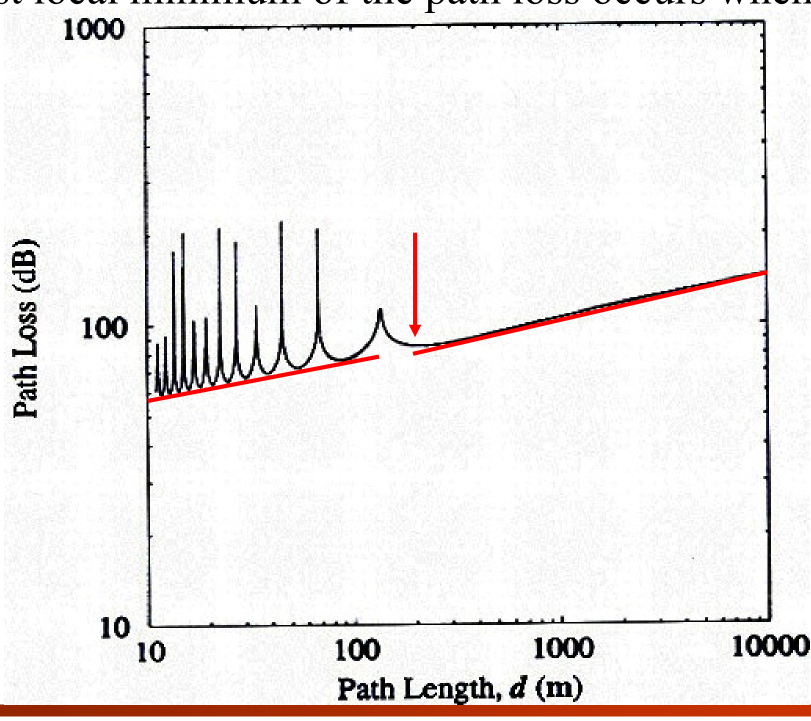

## Two-Slope Model (Street Microcells) (Cont.)

- The first Fresnel Zone

$$\Delta d = \sqrt{\Sigma^2 + g^2} - \sqrt{\Delta^2 + g^2} = \frac{\lambda_c}{2}$$

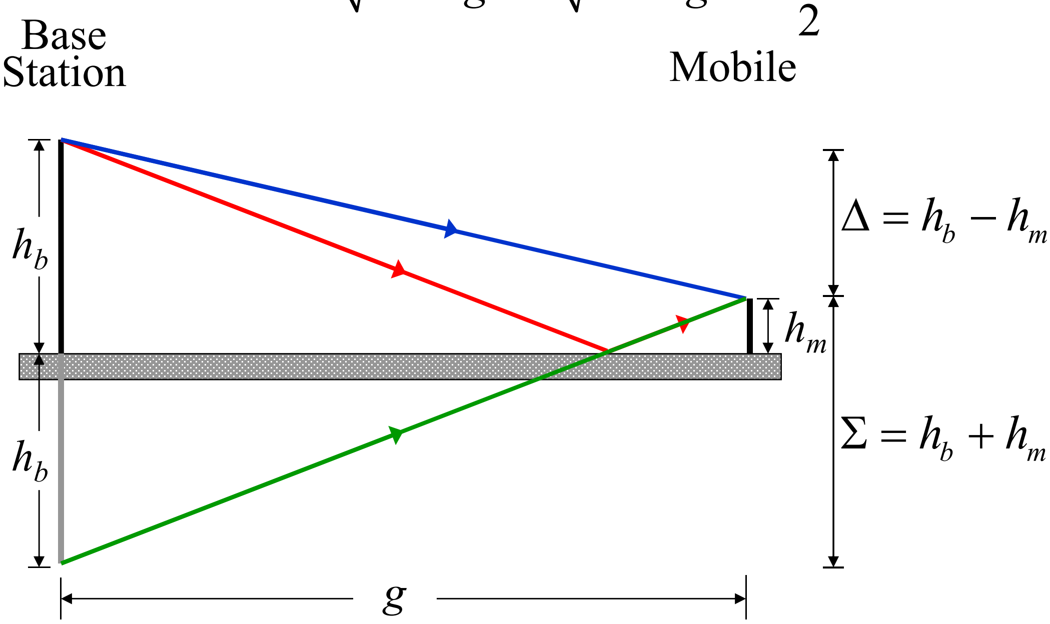




## Two-Slope Model (Street Microcells) (Cont.)

- We set $\Sigma = h_b + h_m$ and $\Delta = h_b - h_m$
- Find the break-point $g$

$$\sqrt{\Sigma^2 + g^2} - \sqrt{\Delta^2 + g^2} = \frac{\lambda_c}{2}$$

$$\sqrt{\Sigma^2 + g^2} = \sqrt{\Delta^2 + g^2} + \frac{\lambda_c}{2}$$

$$\Sigma^2 + g^2 = \Delta^2 + g^2 + \lambda_c\sqrt{\Delta^2 + g^2} + (\tfrac{\lambda_c}{2})^2$$

$$\left[\Sigma^2 - \Delta^2 - (\tfrac{\lambda_c}{2})^2\right]^2 = (\lambda_c)^2(\Delta^2 + g^2)$$

$$(\Sigma^2 - \Delta^2)^2 - 2(\Sigma^2 + \Delta^2)(\tfrac{\lambda_c}{2})^2 + (\tfrac{\lambda_c}{2})^4 = (\lambda_c)^2 g^2$$

$$g = \frac{1}{\lambda_c}\sqrt{(\Sigma^2 - \Delta^2)^2 - 2(\Sigma^2 + \Delta^2)(\tfrac{\lambda_c}{2})^2 + (\tfrac{\lambda_c}{2})^4}$$

# Two-Slope Model (Street Microcells) (Cont.)

- For conventional environments, break point $g$ = 150 ~ 300m

$$g = \frac{1}{\lambda_c}\sqrt{\left(\Sigma^2 - \Delta^2\right)^2 - 2(\Sigma^2 + \Delta^2)\left(\frac{\lambda_c}{2}\right)^2 + \left(\frac{\lambda_c}{2}\right)^4}$$

- For high frequency ($\lambda_c^2 \ll (\Sigma^2 - \Delta^2)^2$):

$$g \approx \frac{1}{\lambda_c}\sqrt{\left(\Sigma^2 - \Delta^2\right)^2} = \frac{\Sigma^2 - \Delta^2}{\lambda_c} = \frac{4h_b h_m}{\lambda_c}$$



# Two-Slope Model (Street Microcells) (Cont.)

- JTC model (microcell model)
  - $d_{bp} = (4\ h_b\ h_m)/\lambda_c$, (break point)

$$L_{P(\text{dB})} = \begin{cases} 38.1 + 25\log_{10}(d), & d < d_{bp} \\ 38.1 + 25\log_{10}(d_{bp}) + 45\log_{10}(d/d_{bp}), & d > d_{bp} \end{cases}$$

***a* = 2.5, *b* = 2**

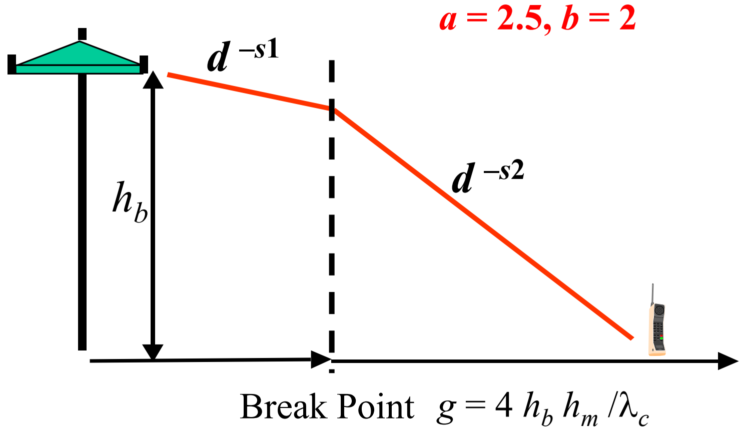

# Street Microcells Coverage

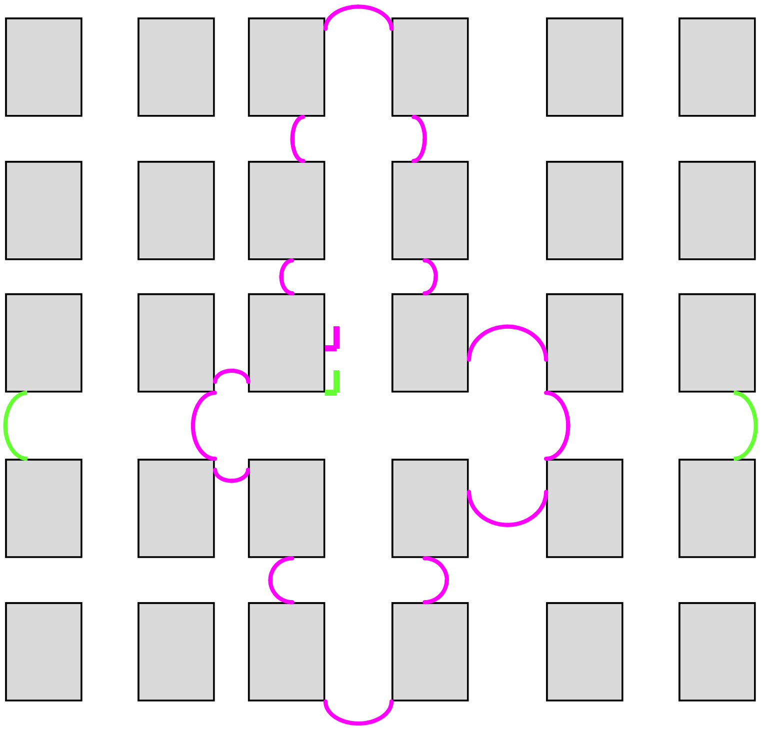



# Corner Effect (Street Microcells)

- Corner Effect: street microcells with NLOS propagation
  – The average received signal strength drops by **25~30 dB** over a distance as small as 10 m to 50 m
- The NLOS propagation is modeled as:
  – A LOS propagation from an **virtual transmitter** located at corner
  – The transmit power is equal to the received power at corner from BS

$$\mu_{\Omega_p} = \begin{cases} \dfrac{k\Omega_t}{d^a(1+d/g)^b}, & d \le d_c \\ \dfrac{k\Omega_t}{d_c^a(1+d_c/g)^b} \cdot \dfrac{1}{(d-d_c)^a(1+(d-d_c)/g)^b}, & d > d_c \end{cases}$$

# Corner Effect (Street Microcells) (Cont.)

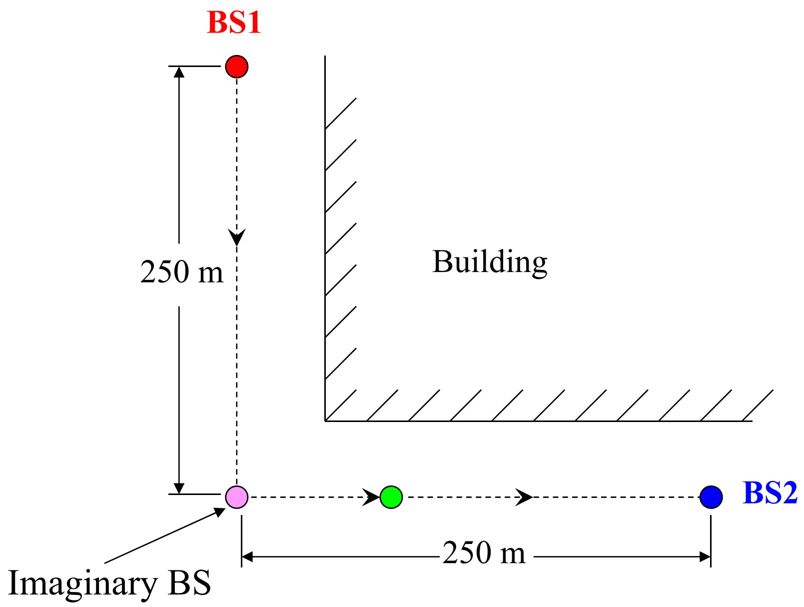




# Corner Effect (Street Microcells) (Cont.)

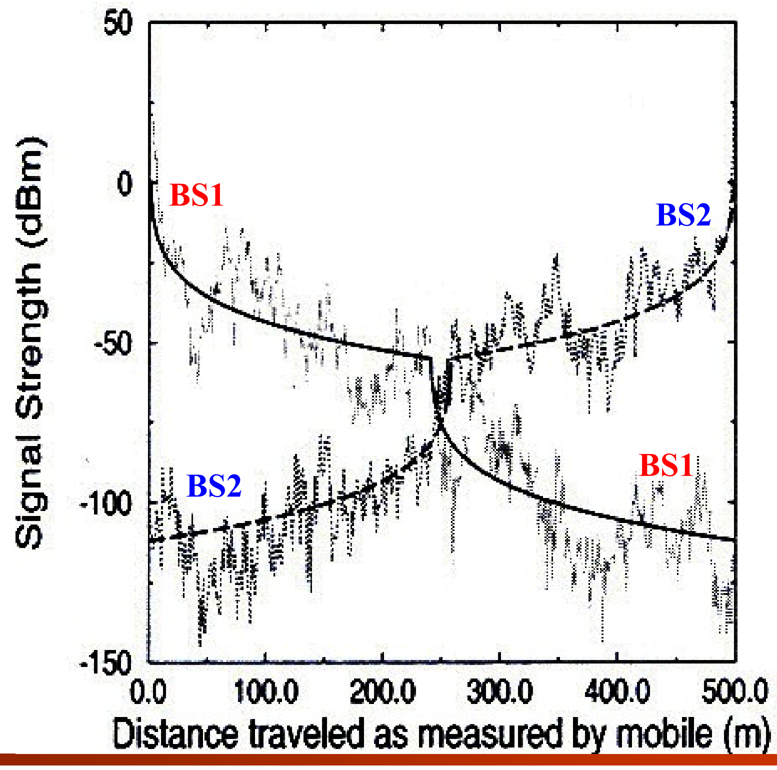

# Path Loss in Indoor Microcells

- The path loss and shadowing characteristics for indoor environments **vary greatly** from one building to another

| Building | Frequency (MHz) | $\beta$ | $\sigma_\Omega$ (dB) |
|---|---|---|---|
| Retail Stores | 914 | 2.2 | 8.7 |
| Grocery Stores | 914 | 1.8 | 5.2 |
| Office, hard partition | 1500 | 3.0 | 7.0 |
| Office, soft partition | 900 | 2.4 | 9.6 |
| Office, soft partition | 1900 | 2.6 | 14.1 |

- Floor loss:
  - One floor: 15 ~ 20 dB
  - Up to 4 floors: additional 6 ~ 10 dB/floor
  - 5 or more floors: increase only a few dB for each additional floor



# Path Loss in Indoor Microcells (Cont.)

- Building penetration loss:
  - Decreases with the increase in frequency
  - Typical values: 16.4, 11.6 and 7.6 dB at 441 MHz, 896.5 MHz and 1400 MHz
  - Decreases by about 2 dB/floor from ground level up to about 9~15 floors and then **increases again**

  $\Rightarrow$ It is due to the BS antenna heights and the antenna pattern

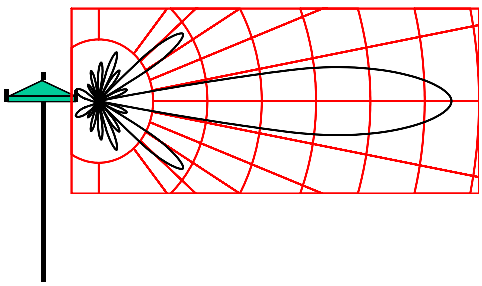

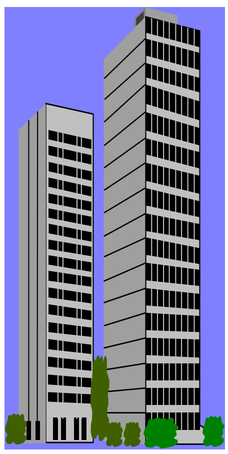

# Path Loss & Shadowing

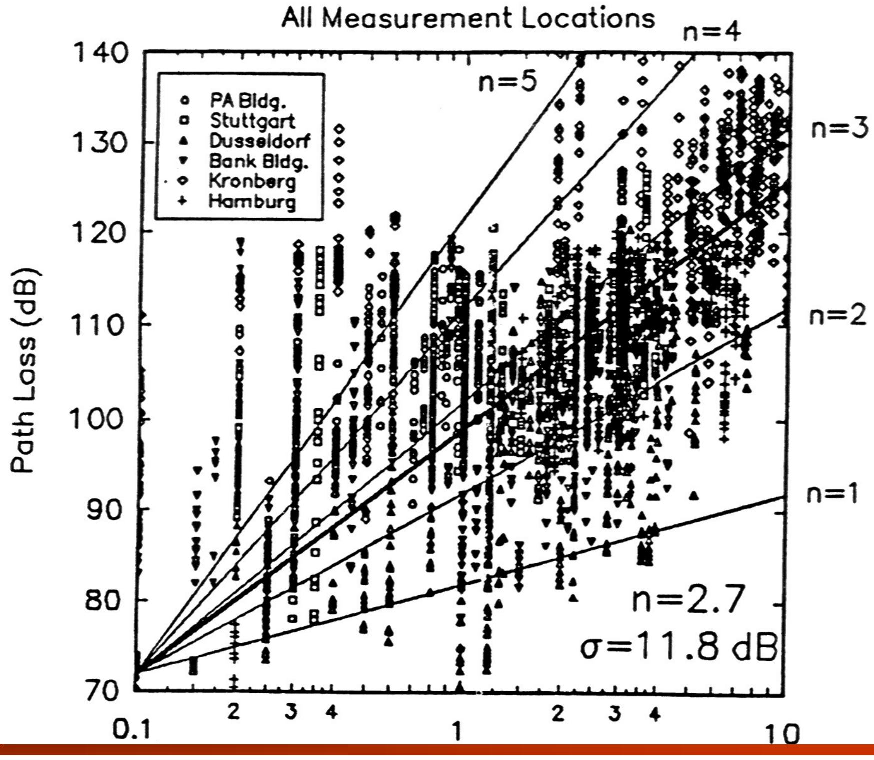




# Question

- **Question:**
  - What kind of path loss models should be applied?
  - Why the shadowing loss can be positive or negative?
- It depends on the applications (macro- or micro-cellular Sys.) and the requirements (Accuracy, Complexity, …)

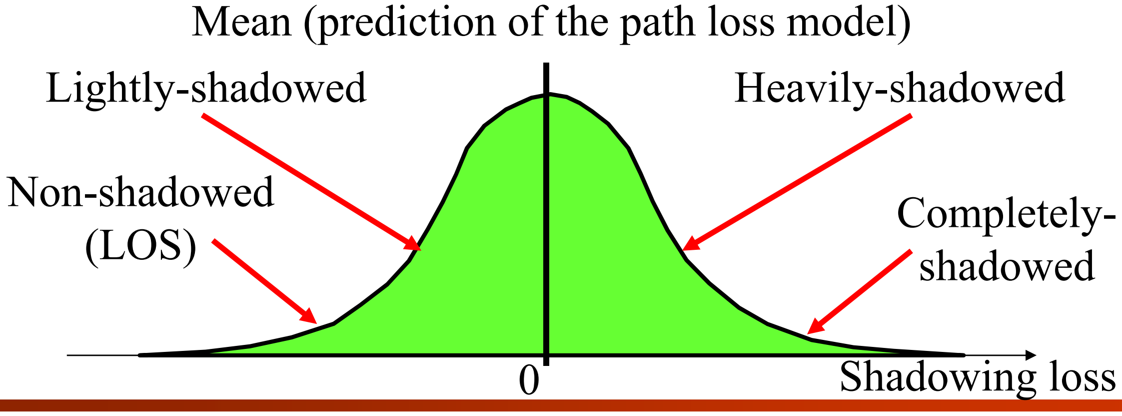

# MIMO Channel Models



# MIMO Channel Models

- A MIMO (Multiple-Input and Multiple-Output) system is one that consists of multiple transmit and receive antennas.
- For a system consisting of $N_t$ transmit and $N_r$ receive antennas, the channel can be described by the $N_r \times N_t$ matrix.

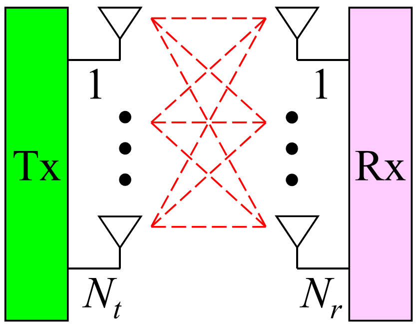


**Mutually Correlated!**

$$\mathbf{G}(t,\tau) = \begin{bmatrix} g_{1,1}(t,\tau) & g_{1,2}(t,\tau) & \cdots & g_{1,N_t}(t,\tau) \\ g_{2,1}(t,\tau) & g_{2,2}(t,\tau) & \cdots & g_{2,N_t}(t,\tau) \\ \vdots & \vdots & & \vdots \\ g_{N_r,1}(t,\tau) & g_{N_r,2}(t,\tau) & \cdots & g_{N_r,N_t}(t,\tau) \end{bmatrix}$$

– where $g_{q,p}(t,\tau)$ denotes the time-varying sub-channel impulse response between the $p$th transmit and $q$th receive antennas.

# Analytical MIMO Channel Models

- **Analytical MIMO channel models** are most often used under quasi-static flat fading conditions.
- The time-variant channel impulses $g_{q,p}(t,\tau)$ for flat fading channels can be treated as complex Gaussian random processes under conditions of **Rayleigh** and **Ricean** fading.
- The various analytical models generate the MIMO matrices as realizations of complex Gaussian random variables having specified **means** and **correlations**.
- For Ricean fading, the channel matrix can be expressed as

$$\mathbf{G} = \sqrt{\frac{K}{K+1}}\bar{\mathbf{G}} + \sqrt{\frac{1}{K+1}}\mathbf{G}_S$$

  - $\bar{\mathbf{G}}$: is the LOS or specular component (a deterministic part)
  - $\mathbf{G}_S$: is the scatter component having zero-mean (a random part)



# Analytical MIMO Channel Models (Cont.)

- The **simplest** MIMO model assumes that the entries of the matrix **G** are **independent and identically distributed (i.i.d.)** complex Gaussian random variables.
  - The **rich scattering** or **spatially white** environment.
  - It simplifies the performance analysis on MIMO channels.
  - However, **in reality** the sub-channels will be **correlated**, and the i.i.d. model will lead to optimistic results.
- Define $\mathbf{g} = \text{vec}\{\mathbf{G}\} = \left[\mathbf{g}_1^T, \mathbf{g}_2^T, \cdots, \mathbf{g}_{N_t}^T\right]^T$
  - where $\mathbf{G} = [\mathbf{g}_1, \mathbf{g}_2, \cdots, \mathbf{g}_{N_t}]$ is the channel matrix
  - $\mathbf{g}$ is a zero-mean complex Gaussian random column vector of length $n = N_t \times N_r$
  - Its statistics are fully specified by the $n \times n$ covariance matrix $\mathbf{R}_\mathbf{G}$ = ½ E[$\mathbf{g}\mathbf{g}^H$]

## Analytical MIMO Channel Models (Cont.)

- Hence, $\mathbf{g}$ is a multivariate complex Gaussian distributed vector
  - $\mathbf{g} \sim \mathcal{CN}(\mathbf{0}, \mathbf{R_G})$
- If $\mathbf{R_G}$ is invertible, the probability density function of $\mathbf{g}$ is

$$f(\mathbf{g}) = \frac{1}{(2\pi)^n \det(\mathbf{R_G})} \exp\left[-\tfrac{1}{2}\mathbf{g}^H \mathbf{R_G}^{-1}\mathbf{g}\right], \quad \mathbf{g} \in C^n$$

- The covariance matrix $\mathbf{R_G}$ depends on the **propagation environments** and the **antenna configuration**.
- Given a covariance matrix $\mathbf{R_G}$, realizations of an MIMO channel can be generated by

$$\mathbf{G} = \text{unvec}\{\mathbf{g}\}, \quad \text{with } \mathbf{g} = \mathbf{R_G}^{1/2}\mathbf{w}$$

  - $\mathbf{R_G}^{1/2}$ is any matrix square root of $\mathbf{R_G}$; that is, $\mathbf{R_G} = \mathbf{R_G}^{1/2}(\mathbf{R_G}^{1/2})^H$
  - $\mathbf{w}$ is a length $n$ vector where $\mathbf{w} \sim \mathcal{CN}(\mathbf{0}, \mathbf{I})$ (a white noise vector)



## Kronecker Model

- The Kronecker model constructs the MIMO channel matrix $\mathbf{G}$ under the assumption that the spatial correlation at the **transmitter and receiver** is **separable**.
- This is equivalent to restricting the correlation matrix $\mathbf{R_G}$ to have the Kronecker product form $\mathbf{R_G} = \mathbf{R}_t \otimes \mathbf{R}_r$
  - where $\otimes$ is the Kronecker product
  - The $N_t \times N_t$ and $N_r \times N_r$ transmit and receive correlation matrices are $\mathbf{R}_t = \frac{1}{\sqrt{2}} E\left[\mathbf{G}^H\mathbf{G}\right], \quad \mathbf{R}_r = \frac{1}{\sqrt{2}} E\left[\mathbf{G}\mathbf{G}^H\right]$
- The Kronecker product of an $n \times n$ matrix $\mathbf{A}$ and an $m \times m$ matrix $\mathbf{B}$:

$$\mathbf{A} \otimes \mathbf{B} = \begin{bmatrix} a_{1,1}\mathbf{B} & \cdots & a_{1,n}\mathbf{B} \\ \vdots & \ddots & \vdots \\ a_{n,1}\mathbf{B} & \cdots & a_{n,n}\mathbf{B} \end{bmatrix}$$

# Kronecker Model (Cont.)

- Given covariance matrices $\mathbf{R}_t$ and $\mathbf{R}_r$, realizations of an MIMO channel for the Kronecker model can be generated by

$$\mathbf{g} = \mathbf{R}_{\mathbf{G}}^{1/2}\mathbf{w} = (\mathbf{R}_t \otimes \mathbf{R}_r)^{1/2}\mathbf{w} \Rightarrow \mathbf{G} = \mathbf{R}_r^{1/2}\mathbf{W}\left(\mathbf{R}_t^{1/2}\right)^T$$

  – where $\mathbf{W}$ is an $N_r \times N_t$ matrix consisting of i.i.d. zero mean complex Gaussian random variables (a white noise matrix)

- In general, the elements of the matrix $\mathbf{R}_{\mathbf{G}}$ represent correlations between the faded envelopes of the MIMO sub-channels:

$$\frac{1}{2}E\left[g_{q,p}g^{*}_{\tilde{q},\tilde{p}}\right] = \phi\left(q,p,\tilde{q},\tilde{p}\right)$$

  – A function of **four** sub-channel index parameters

- One important implication of the Kronecker property is **spatial stationarity** $\frac{1}{2}E\left[g_{q,p}g^{*}_{\tilde{q},\tilde{p}}\right] = \phi\left(q-\tilde{q},p-\tilde{p}\right)$



# Kronecker Model (Cont.)

- The **spatial stationarity** property implies that the sub-channel correlations are determined not by their position in the matrix **G**, but by their **difference in position**.
- In addition to the stationary property, the Kronecker product form also implies that

$$\frac{1}{2}E\left[g_{q,p}g^{*}_{\tilde{q},\tilde{p}}\right] = \phi_T\left(p-\tilde{p}\right)\cdot\phi_R\left(q-\tilde{q}\right)$$

- This means that the correlation can be separated into two parts: **a transmitter part** and **a receiver part**, and both parts are **stationary**.

# Angular-domain Model

- We assume that $N_t$ transmit antennas and $N_r$ receive antennas are placed in **uniform linear arrays** with the normalized (to $\boldsymbol{\lambda_c}$) antenna separations $\Delta_t << d$ and $\Delta_r << d$, respectively.
- Considering a **SIMO** channel with the incidence angle $\phi_r$, the time impulse response between the signal source and the $i$-th receive antenna is

$$h_i(\tau) = a\delta(\tau - d_i/c)$$

  - where $a$ is the path attenuation, $c$ is the light speed, and

$$d_i = d + (i-1)\Delta_r\lambda_c \cos\phi_r$$

$$d_i = d + (i-1)\Delta_r\lambda_c \sin\phi_r'$$

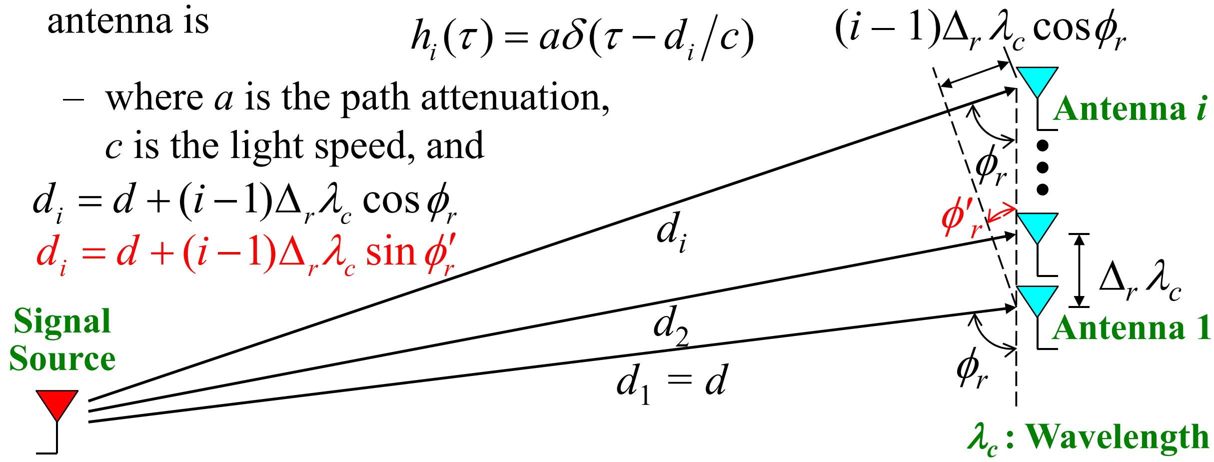




# Angular-domain Model (Cont.)

- Assume that the channel is a **frequency non-selective fading** channel $(d_i - d)/c << 1/W$, where $W$ is the channel bandwidth
- The channel gain at the $i$-th receive antenna is

$$g_i = a\exp(-j2\pi f_c d_i/c) = a\exp(-j2\pi d_i/\lambda_c)$$

  - where $\lambda_c$ is the carrier wavelength and $f_c$ is the carrier frequency
- For the considered **SIMO** channel, the received signal vector can be represented as $\mathbf{y} = \mathbf{g}x + \mathbf{w}$
  - where $x$ is the transmit signal, $\mathbf{w}$ is the channel noise vector, and

$$\mathbf{g} = a\exp\left(-j2\pi d/\lambda_c\right)\begin{bmatrix} 1 \\ \exp[-j2\pi\Delta_r\Omega_r] \\ \exp[-j2\pi 2\Delta_r\Omega_r] \\ \vdots \\ \exp[-j2\pi(N_r-1)\Delta_r\Omega_r] \end{bmatrix}$$

$$\boxed{\boldsymbol{\Omega_r = \cos\phi_r}}$$

# Angular-domain Model (Cont.)

- Assume that $d_i/c << 1/W$, where $W$ is the channel bandwidth
  - A **frequency non-selective fading** channel ($(d_i - d)/c << 1/W$)
- The channel gain at the $i$-th receive antenna is

$$g_i = a\exp(-j2\pi f_c d_i/c) = a\exp(-j2\pi d_i/\lambda_c)$$

  - where $\lambda_c$ is the carrier wavelength and $f_c$ is the carrier frequency
- For the considered **SIMO** channel, the received signal vector can be represented as $\mathbf{y} = \mathbf{g}x + \mathbf{w}$
  - where $x$ is the transmit signal, $\mathbf{w}$ is the channel noise vector, and

$$\mathbf{g} = a\exp\left(-j2\pi d/\lambda_c\right)\begin{bmatrix} 1 \\ \exp\left[-j2\pi\Delta_r\Omega_r\right] \\ \exp\left[-j2\pi 2\Delta_r\Omega_r\right] \\ \vdots \\ \exp\left[-j2\pi(N_r-1)\Delta_r\Omega_r\right] \end{bmatrix}$$

$$\boxed{\boldsymbol{\Omega_r = \cos\phi_r}}$$



# Angular-domain Model (Cont.)

- Similarly, for a **MISO** channel with the radiation angle $\phi_t$, , the received signal can be represented as

$$y = \tilde{\mathbf{g}}^T\mathbf{x} + w$$

  - where $\mathbf{x}$ is the transmitted signal vector, $w$ is the channel noise, and

$$\tilde{\mathbf{g}} = a\exp(-j2\pi d/\lambda_c)\begin{bmatrix} 1 \\ \exp\left[-j2\pi\Delta_t\Omega_t\right] \\ \exp\left[-j2\pi 2\Delta_t\Omega_t\right] \\ \vdots \\ \exp\left[-j2\pi(N_t-1)\Delta_t\Omega_t\right] \end{bmatrix}$$

$$\boxed{\boldsymbol{\Omega_t = \cos\phi_t}}$$

# Angular-domain Model (Cont.)

- Consider a narrowband **MIMO** channel ($N_r \times N_t$ channel matrix)

$$\mathbf{y} = \mathbf{G}\mathbf{x} + \mathbf{w}$$

  - where **G** is the **spatial-domain** MIMO channel model
- Suppose there be an arbitrary number of physical paths between the transmitter and the receiver.

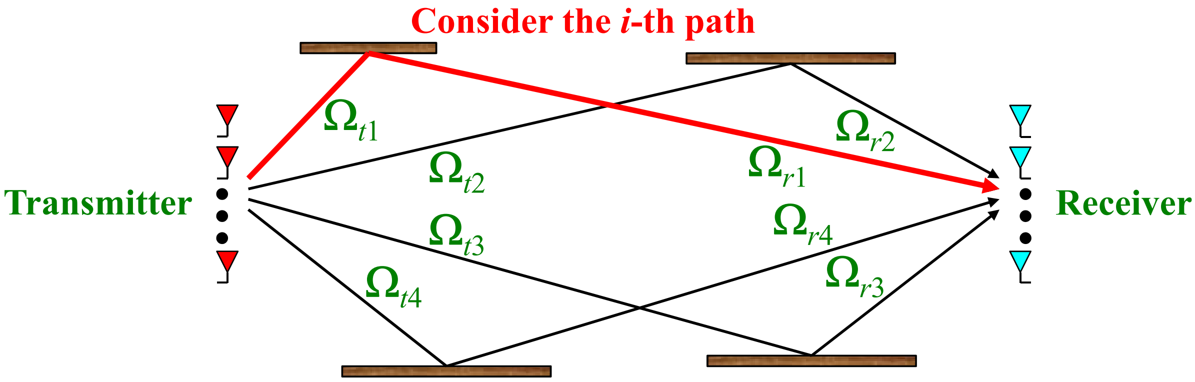




# Angular-domain Model (Cont.)

- The $i$-th path has an overall attenuation of $a_i$, making an angle of $\phi_{ti}$ ($\Omega_{ti} = \cos\phi_{ti}$) with the transmit antenna array and an angle of $\phi_{ri}$ ($\Omega_{ri} = \cos\phi_{ri}$) with the receive antenna array.
- The **channel matrix G** can be represented as (sum of all paths)

$$\mathbf{G} = \sum_i a_i \sqrt{N_t N_r} \exp(-j2\pi d^{(i)} / \lambda_c) \mathbf{e}_r(\Omega_{ri}) \mathbf{e}_t(\Omega_{ti})$$

  - where $d^{(i)}$ is the distance between transmit antenna 1 and receive antenna 1 along **the *i*-th path**, and

$$\mathbf{e}_t(\Omega) \triangleq \frac{1}{\sqrt{N_t}} \begin{bmatrix} 1 \\ \exp[-j2\pi\Delta_t\Omega] \\ \exp[-j2\pi 2\Delta_t\Omega] \\ \vdots \\ \exp[-j2\pi(N_t-1)\Delta_t\Omega] \end{bmatrix}; \mathbf{e}_r(\Omega) \triangleq \frac{1}{\sqrt{N_r}} \begin{bmatrix} 1 \\ \exp[-j2\pi\Delta_r\Omega] \\ \exp[-j2\pi 2\Delta_r\Omega] \\ \vdots \\ \exp[-j2\pi(N_r-1)\Delta_r\Omega] \end{bmatrix}$$

# Angular-domain Model (Cont.)

- How to represent the channel by using the **path directions**?
- Define the normalized total antenna length: $L_t = \Delta_t N_t$; $L_r = \Delta_r N_r$
- Let $\mathbf{U}_t$ and $\mathbf{U}_r$ be the $N_t \times N_t$ and $N_r \times N_r$ unitary matrices

$$\mathbf{U}_t \triangleq \left[ \mathbf{e}_t(0) \quad \mathbf{e}_t(1/L_t) \quad \cdots \quad \mathbf{e}_t((N_t-1)/L_t) \right]$$
$$\mathbf{U}_r \triangleq \left[ \mathbf{e}_r(0) \quad \mathbf{e}_r(1/L_r) \quad \cdots \quad \mathbf{e}_r((N_r-1)/L_r) \right]$$

  – where the columns of the matrices are

$$\mathbf{e}_t(\Omega) \triangleq \frac{1}{\sqrt{N_t}} \begin{bmatrix} 1 \\ \exp[-j2\pi\Delta_t\Omega] \\ \exp[-j2\pi 2\Delta_t\Omega] \\ \vdots \\ \exp[-j2\pi(N_t-1)\Delta_t\Omega] \end{bmatrix}; \mathbf{e}_r(\Omega) \triangleq \frac{1}{\sqrt{N_r}} \begin{bmatrix} 1 \\ \exp[-j2\pi\Delta_r\Omega] \\ \exp[-j2\pi 2\Delta_r\Omega] \\ \vdots \\ \exp[-j2\pi(N_r-1)\Delta_r\Omega] \end{bmatrix}$$

- The column vectors form a set of **orthonormal** bases
  – Both $\mathbf{U}_t$ and $\mathbf{U}_r$ are **DFT matrices**



# Angular-domain Model (Cont.)

- If the antenna separation is $\Delta_r = \Delta_t = 1/2$, each basis vector, $\mathbf{e}_t(k/L_t)$ or $\mathbf{e}_r(k/L_r)$, corresponds to **a single pair of main lobes** around the angles $\pm\cos^{-1}(k/L_t)$ or $\pm\cos^{-1}(k/L_r)$.
  – Provide the best angle-domain resolution
- If $\Delta_r = \Delta_t > 1/2$, some of the basis vectors have more than one pair of main lobes.
- If $\Delta_r = \Delta_t < 1/2$, some of the basis vectors have no main lobes.

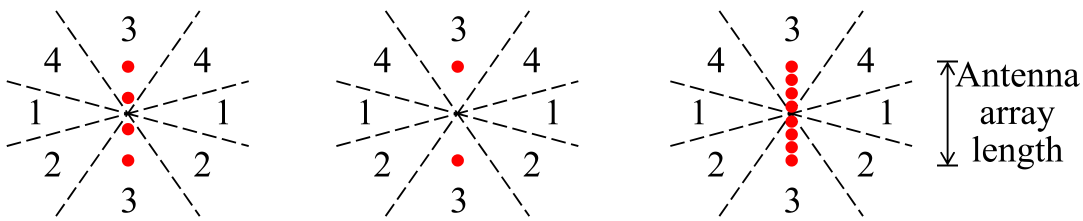


$\Delta_r = \Delta_t = 1/2$ $\Delta_r = \Delta_t > 1/2$ $\Delta_r = \Delta_t < 1/2$

## Angular-domain Model (Cont.)

- Assume that the antenna separation is $\Delta_t = \Delta_r = 1/2$, each basis vector corresponds to a **radiation** angle or an **incidence** angle.
- The transformations $\mathbf{x}^{(a)} \triangleq \mathbf{U}_t^H \mathbf{x}$ and $\mathbf{y}^{(a)} \triangleq \mathbf{U}_r^H \mathbf{y}$ correspond to transferring the coordinates of the transmitted and received signals into **the angular-domain**. ($(\cdot)^H$: Hermitian operator)
- The received signal in the angular-domain is represented as

$$\begin{aligned}\mathbf{y}^{(a)} &= \mathbf{U}_r^H \mathbf{y} = \mathbf{U}_r^H \mathbf{G}\mathbf{x} + \mathbf{U}_r^H \mathbf{w} \\ &= \mathbf{U}_r^H \mathbf{G}\mathbf{U}_t \mathbf{x}^{(a)} + \mathbf{U}_r^H \mathbf{w} \\ &\triangleq \mathbf{G}^{(a)}\mathbf{x}^{(a)} + \mathbf{w}^{(a)}\end{aligned}$$

  – where the **angular-domain channel matrix** is

$$\mathbf{G}^{(a)} = \mathbf{U}_r^H \mathbf{G}\mathbf{U}_t$$

  – The angular-domain noise vector is

$$\mathbf{w}^{(a)} = \mathbf{U}_r^H \mathbf{w}$$

**The noise power remains the same**



## Angular-domain Model (Cont.)

- Hence, different physical paths (different radiation angles and/or different incidence angles) approximately contribute to different entries in the angular-domain channel matrix $\mathbf{G}^{(a)}$.
  – The angular resolution depends on $L_t$ ($L_r$), and $\Delta_t$ ($\Delta_r$)
- Based on $\mathbf{G}^{(a)} = \mathbf{U}_r^H \mathbf{G}\mathbf{U}_t$, the $(i, j)$-th element is

$$g_{i,j}^{(a)} = \mathbf{e}_r^H\left(\left(i-1\right)/L_r\right)\mathbf{G}\mathbf{e}_t\left(\left(j-1\right)/L_t\right)$$

  – which is an element contributed by the path corresponding to the $j$-th radiation angle and the $i$-th incidence angle

$$\mathbf{G}^{(a)} = \begin{bmatrix} g_{1,1}^{(a)} & g_{1,2}^{(a)} & \cdots & g_{1,N_t}^{(a)} \\ g_{2,1}^{(a)} & g_{2,2}^{(a)} & \cdots & g_{2,N_t}^{(a)} \\ \vdots & \vdots & & \vdots \\ g_{N_r,1}^{(a)} & g_{N_r,2}^{(a)} & \cdots & g_{N_r,N_t}^{(a)} \end{bmatrix}$$

# Angular-domain Model (Cont.)

- For an environment with limited angular spread at the receiver and/or the transmitter, many entries of $\mathbf{G}^{(a)}$ may be zero.
  - Significantly reduce the estimation and computation complexity

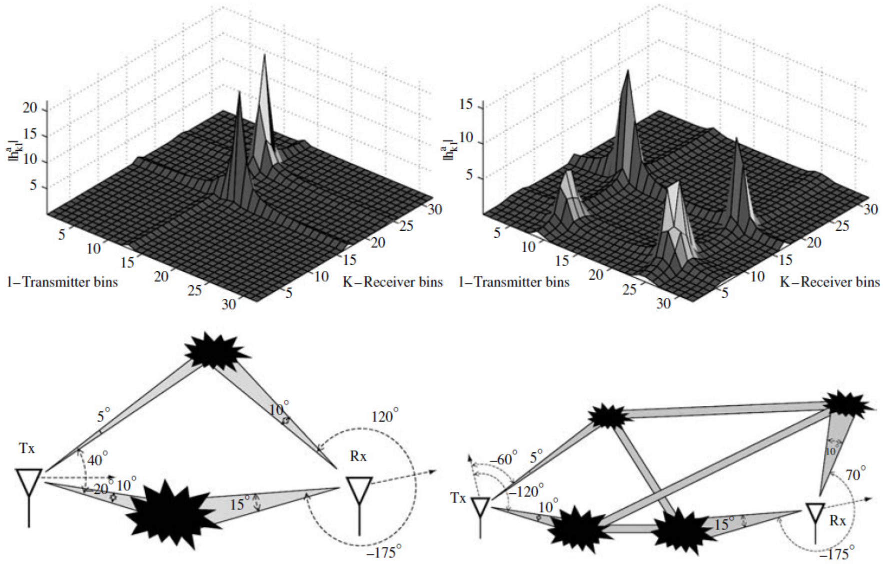




# Some Stochastic Channel Models

# Stochastic Channel Model (SCM)

- **SCM** is a **parametric model** for the **delay spread functions**
- **Requirements for SCMs:**
  - **Completeness**: SCMs must reproduce all effects that impact on the performance of communication systems
  - **Accuracy**: SCMs must accurately describe these effects.
  - **Simplicity/low complexity**: Each effect must be described by a simple model.
- Good **SCMs** can
  - Guarantee simulation scenarios close to reality
  - Enable theoretical study of some particular system aspects and performance
  - Be used to simulate the channel in Monte Carlo simulations with acceptable computational effort



# COST 207 Channel Models

# Channel Models Proposed by COST

- **COST**: European COoperation in Science and Technology
- **COST-207**: Digital Land Mobile Radiocommunications (1988)
  - Channel models for GSM 900 systems
- **COST-231**: Evolution of Land Mobile Radio (including personal) Communication (1996)
  - Channel models for GSM 1800 systems
- **COST-259**: Wireless Flexible Personalized Communications (2000)
  - Channel models for DECT, UMTS and HIPERLAN 2
- **COST-273**: Towards Mobile Broadband Multimedia Networks (2005)
  - Channel models for UMTS and WLAN
  - **MIMO** channel models



# COST 207 Channel Models

- Normalized delay-Doppler scattering (power) function:

$$S_n^{(\mathrm{P})}(\tau,\nu) \triangleq S^{(\mathrm{P})}(\tau,\nu)/P \Rightarrow \int S_n^{(\mathrm{P})}(\tau,\nu)\, d\tau\, d\nu = 1$$

  - where $P$ is the total received power
- We can decompose $S_n^{(\mathrm{P})}(\tau,\nu)$ as

$$S_n^{(\mathrm{P})}(\tau,\nu) = \underbrace{S_n^{(\mathrm{P})}(\tau)}_{\text{Normalized delay scattering function}} \times \underbrace{S_n^{(\mathrm{P})}(\nu|\tau)}_{\text{Delay-dependent normalized Doppler scattering function}}$$

- The COST 207 models are specified by the two functions:
  - $S_n^{(\mathrm{P})}(\tau)$: scattering power of the channel in terms of the time delay $\tau$
  - $S_n^{(\mathrm{P})}(\nu|\tau)$: scattering power of the channel in terms of Doppler frequency $\nu$, given the time delay $\tau$

# COST 207 – Normalized Delay Scattering Fun.

- **Typical urban non-hilly area (TU)**:

$$S_n^{(\mathrm{P})}(\tau) \propto \begin{cases} \exp(-\tau); & 0 \le \tau \le 7\mu\mathrm{s} \\ 0; & \text{elsewhere} \end{cases}$$

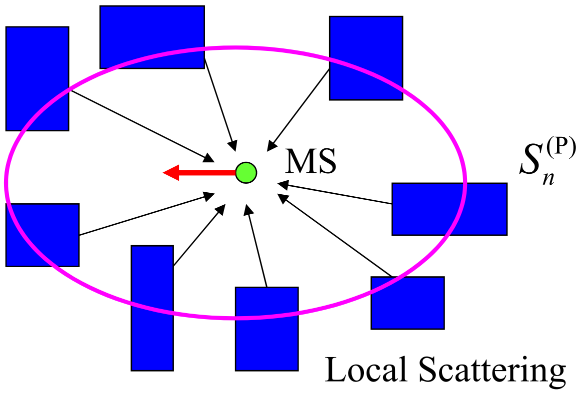


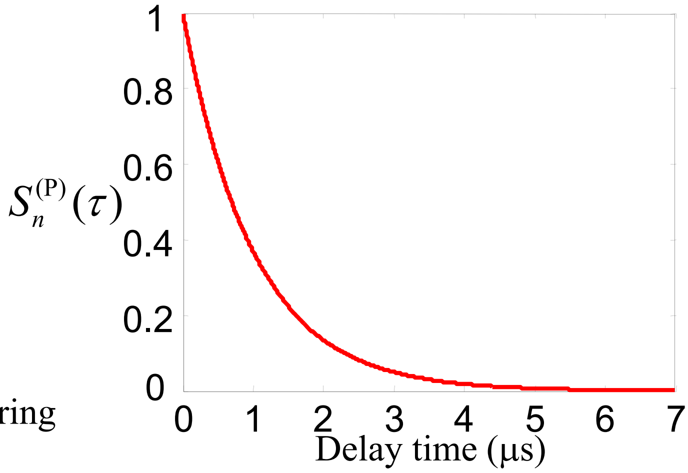




# COST 207 – Normalized DS Fun. (Cont.)

- **Typical bad urban hilly area (BU)**:

$$S_n^{(\mathrm{P})}(\tau) \propto \begin{cases} \exp(-\tau); & 0 \le \tau \le 5\mu\mathrm{s} \\ 0.5\exp(5-\tau); & 5\mu\mathrm{s} \le \tau \le 10\mu\mathrm{s} \\ 0; & \text{elsewhere} \end{cases}$$

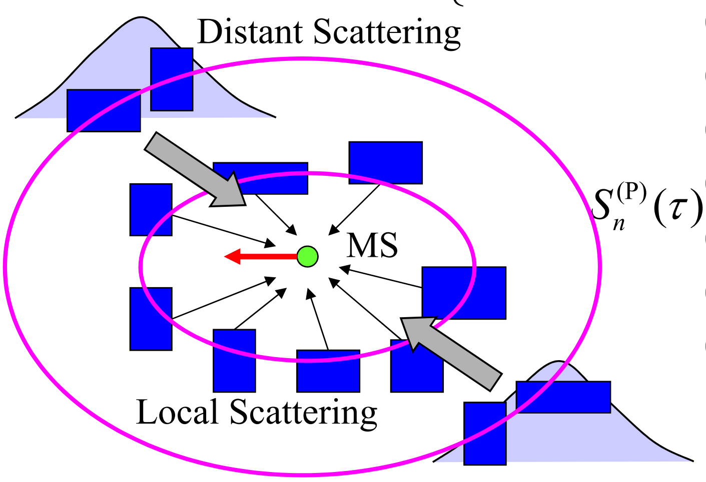


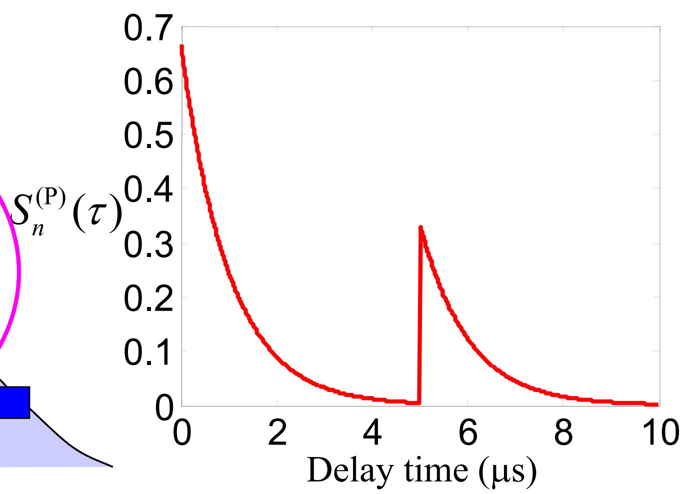

# COST 207 – Normalized DS Fun. (Cont.)

- **Typical rural non-hilly area (RA)**:

$$S_n^{(\mathrm{P})}(\tau) \propto \begin{cases} \exp(-9.2\tau); & 0 \le \tau \le 0.7\mu\mathrm{s} \\ 0; & \text{elsewhere} \end{cases}$$

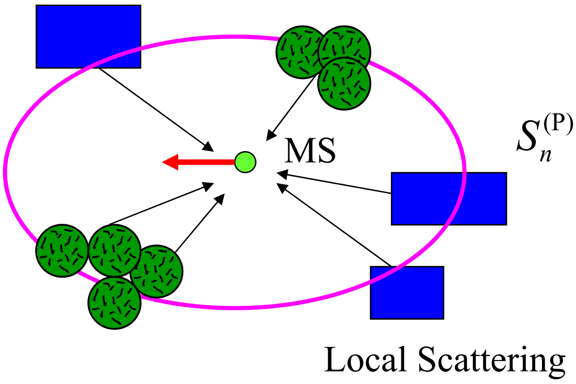


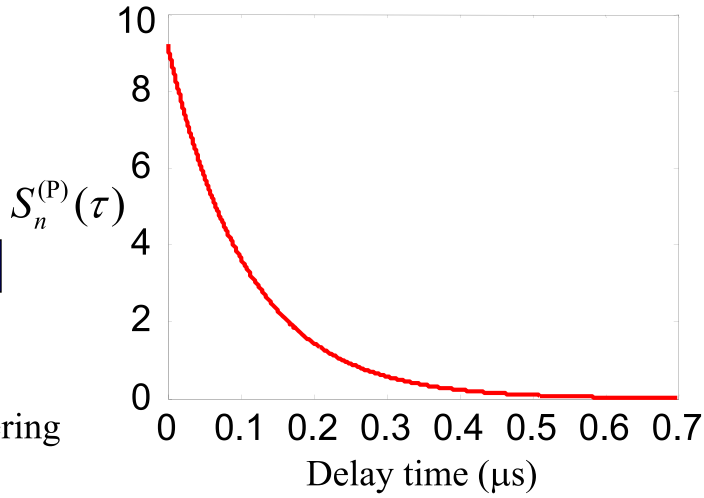




# COST 207 – Normalized DS Fun. (Cont.)

- **Typical hilly terrain (HT)**:

$$S_n^{(\mathrm{P})}(\tau) \propto \begin{cases} \exp(-3.5\tau); & 0 \le \tau \le 2\mu\mathrm{s} \\ 0.1\exp(15-\tau); & 15\mu\mathrm{s} \le \tau \le 20\mu\mathrm{s} \\ 0; & \text{elsewhere} \end{cases}$$

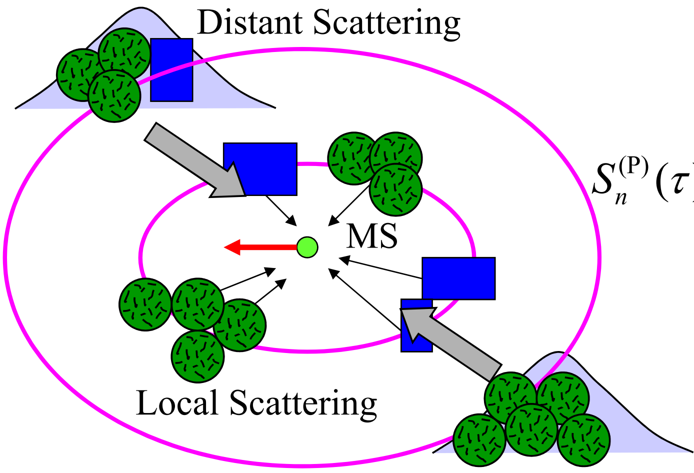


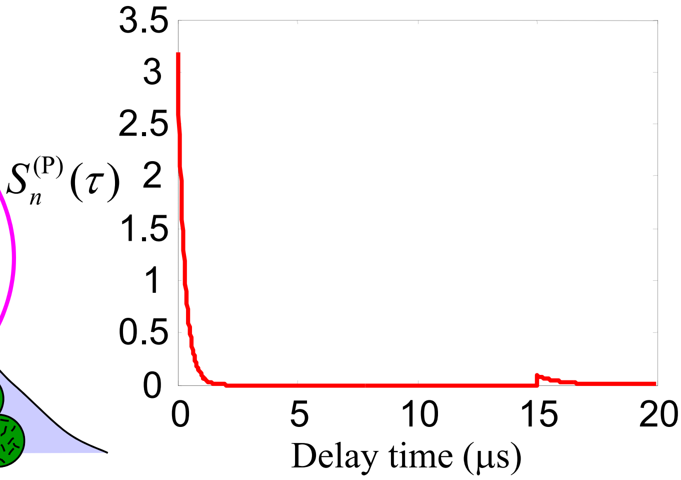

# COST 207 – Normalized DS Fun. (Cont.)

- **Classical Doppler spectrum (CLASS)**: isotropic scattering ($\tau \le 0.5\mu s$)

$$S_n^{(P)}(\nu|\tau) \propto \begin{cases} \dfrac{1}{\pi f_m} \times \dfrac{1}{\sqrt{1-(\nu/f_m)^2}}; & |\nu| \le f_m \\ 0; & \text{elsewhere} \end{cases}$$

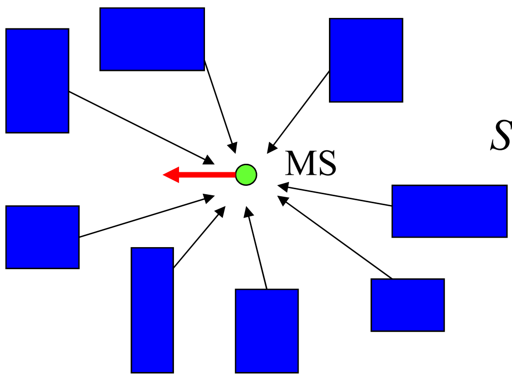


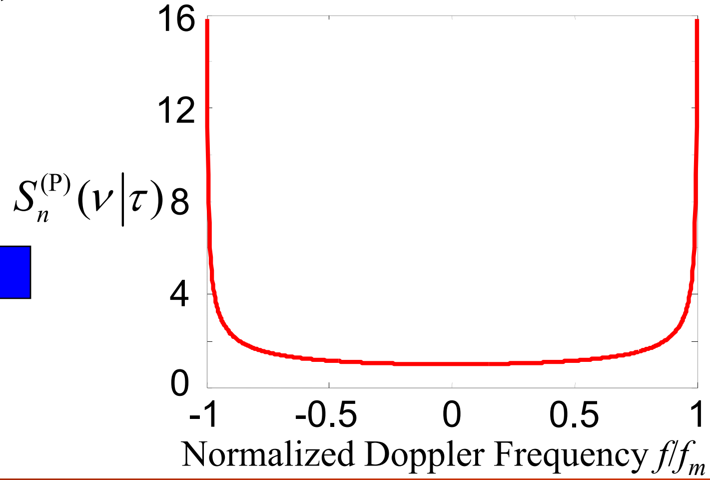




# COST 207 – Normalized DS Fun. (Cont.)

- **Gaussian 1 Doppler spectrum (GAUS1)**: non-isotropic scattering ($0.5\mu s \le \tau \le 2\mu s$)

$$S_n^{(P)}(\nu|\tau) \propto G(\nu; a_1, -0.8 f_m, 0.05 f_m) + G(\nu; a_2, 0.4 f_m, 0.1 f_m)$$

$$G(\nu; a, \nu_1, \nu_2) = a \times \exp(-(\nu-\nu_1)^2 / 2\nu_2^2), \quad a_2/a_1 = -10 \text{ dB}$$

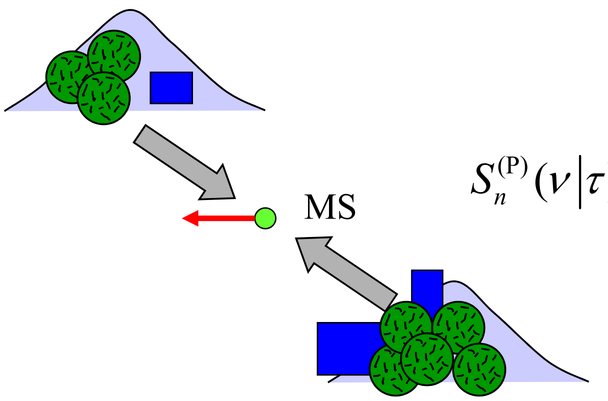


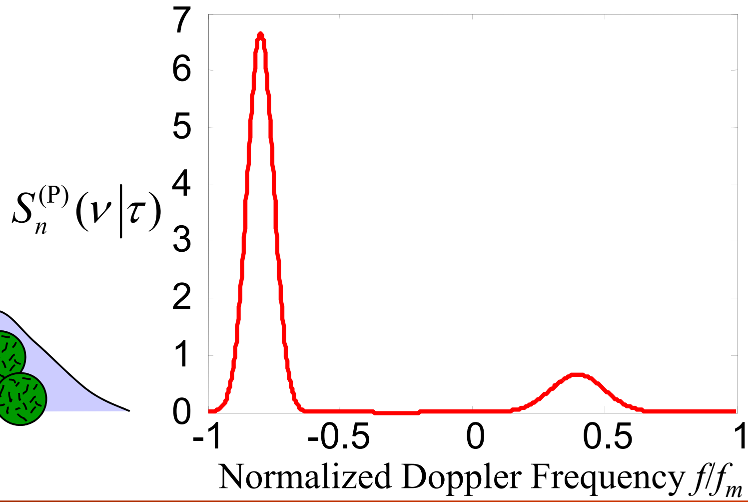

# COST 207 – Normalized DS Fun. (Cont.)

- **Gaussian 2 Doppler spectrum (GAUS2)**: non-isotropic scattering ($2\mu s \le \tau$)

$$S_n^{(\mathrm{P})}(\nu|\tau) \propto G(\nu; a_1, 0.7 f_m, 0.1 f_m) + G(\nu; a_2, -0.4 f_m, 0.15 f_m)$$

$$G(\nu; a, \nu_1, \nu_2) = a \times \exp(-(\nu - \nu_1)^2 / 2\nu_2^2), \quad a_2 / a_1 = -15 \text{ dB}$$

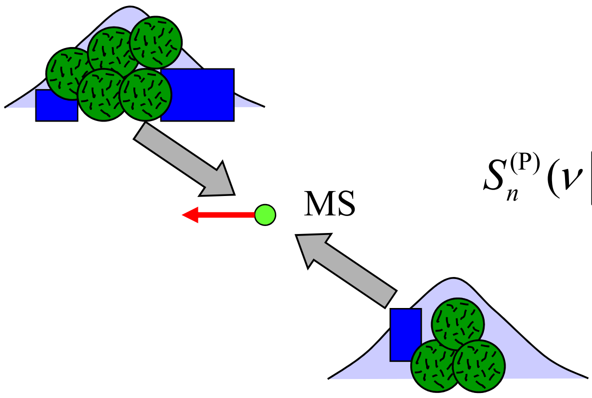


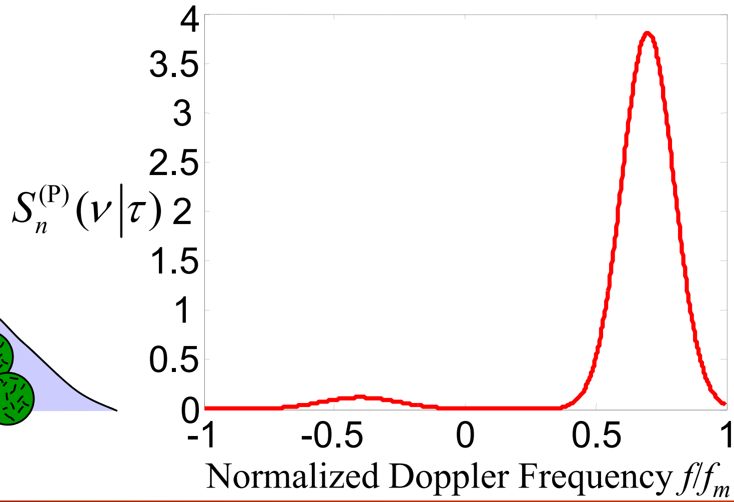




# COST 207 – Normalized DS Fun. (Cont.)

- **RICE Doppler spectrum (RICE)**: isotropic scattering with LOS

$$S_n^{(\mathrm{P})}(\nu|\tau) \propto \begin{cases} \dfrac{0.41}{2\pi f_m} \times \dfrac{1}{\sqrt{1-(\nu/f_m)^2}} + 0.91\delta(\nu - 0.7 f_m); & |\nu| \le f_m \\ 0; & \text{elsewhere} \end{cases}$$

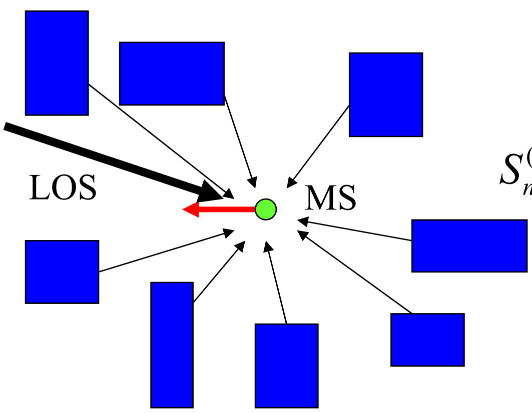


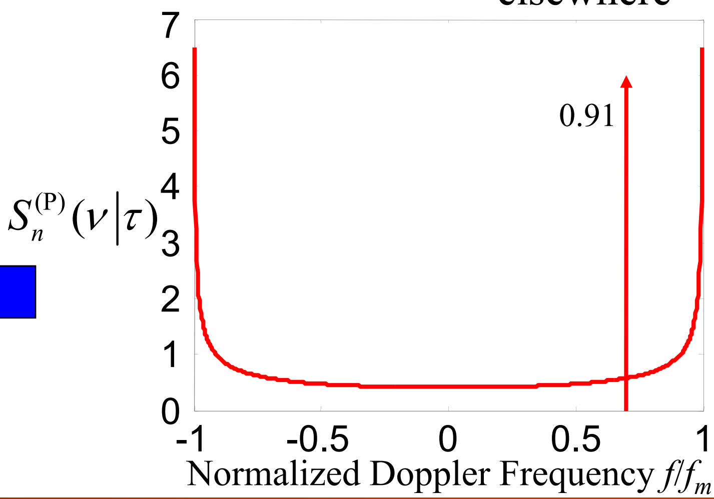

# COST 207 Channel Models – TU/BU

- **Typical urban (TU)** ($\sigma_\tau = 1.0$ μs) and **bad urban (BU)** ($\sigma_\tau = 2.5$ μs) power delay profiles

| Typical Urban (TU) | | | Bad Urban (BU) | | |
|---|---|---|---|---|---|
| Delay (μs) | Fractional Power | Doppler | Delay (μs) | Fractional Power | Doppler |
| 0.0 | 0.092 | CLASS | 0.0 | 0.033 | CLASS |
| 0.1 | 0.115 | CLASS | 0.1 | 0.089 | CLASS |
| 0.3 | 0.231 | CLASS | 0.3 | 0.141 | CLASS |
| 0.5 | 0.127 | CLASS | 0.7 | 0.194 | GAUS1 |
| 0.8 | 0.115 | GAUS1 | 1.6 | 0.114 | GAUS1 |
| 1.1 | 0.074 | GAUS1 | 2.2 | 0.052 | GAUS2 |
| 1.3 | 0.046 | GAUS1 | 3.1 | 0.035 | GAUS2 |
| 1.7 | 0.074 | GAUS1 | 5.0 | 0.140 | GAUS2 |
| 2.3 | 0.051 | GAUS2 | 6.0 | 0.136 | GAUS2 |
| 3.1 | 0.032 | GAUS2 | 7.2 | 0.041 | GAUS2 |
| 3.2 | 0.018 | GAUS2 | 8.1 | 0.019 | GAUS2 |
| 5.0 | 0.025 | GAUS2 | 10.0 | 0.006 | GAUS2 |



# Time-domain Fading Gain – CLASS

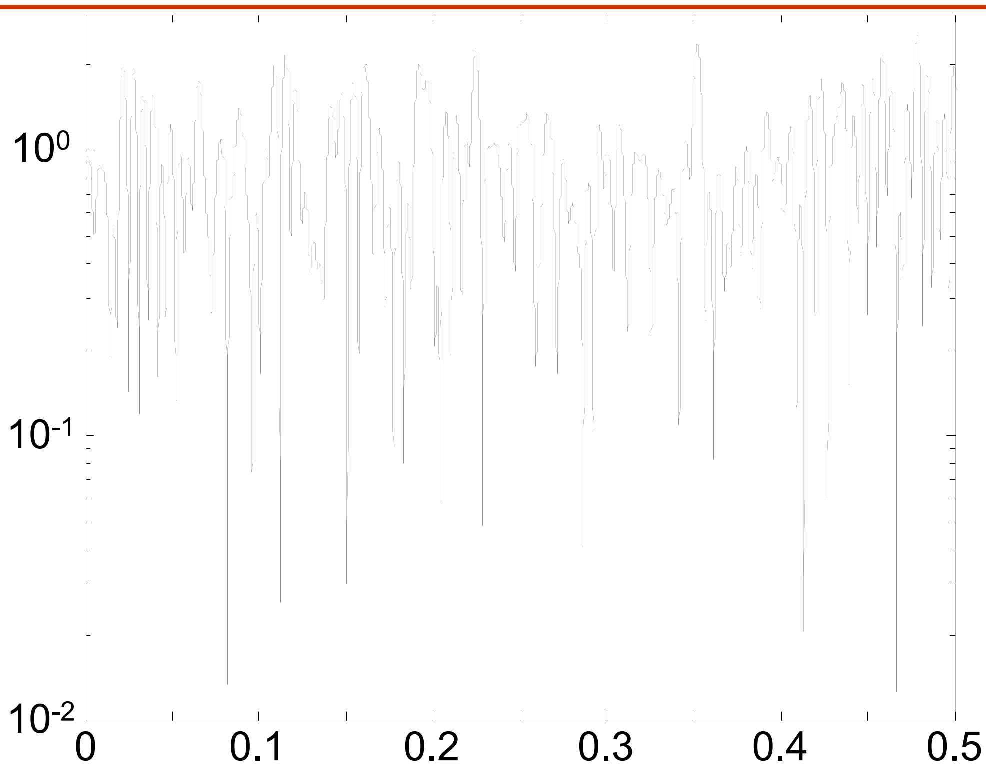

# Time-domain Fading Gain – GAUS1

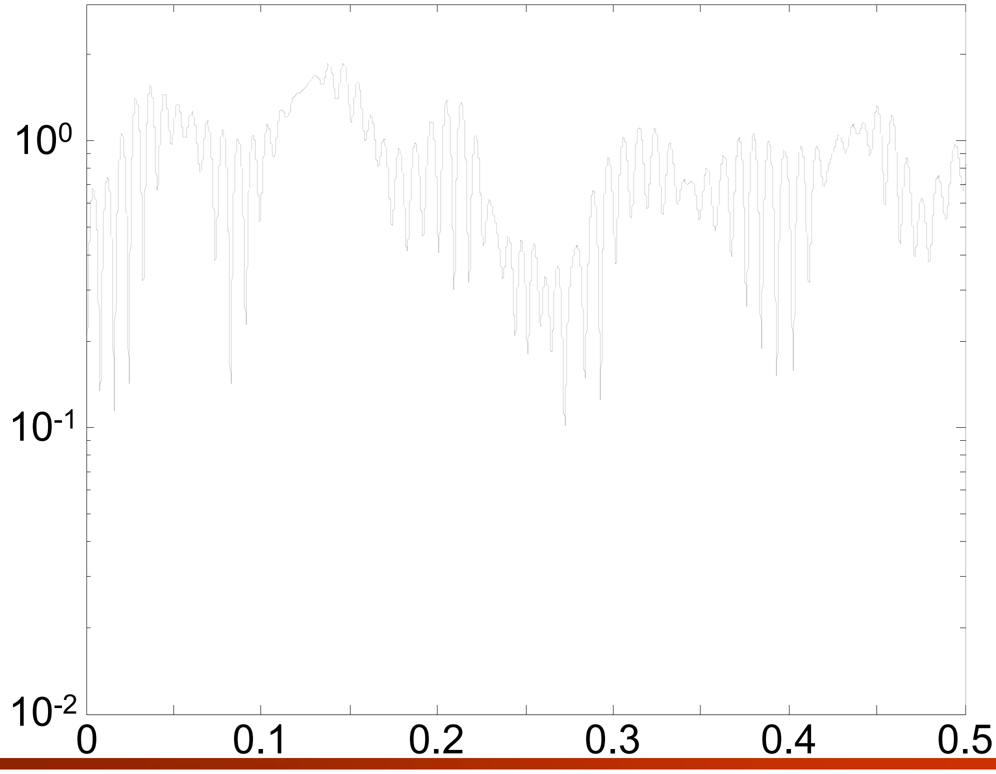




# Time-domain Fading Gain – GAUS2

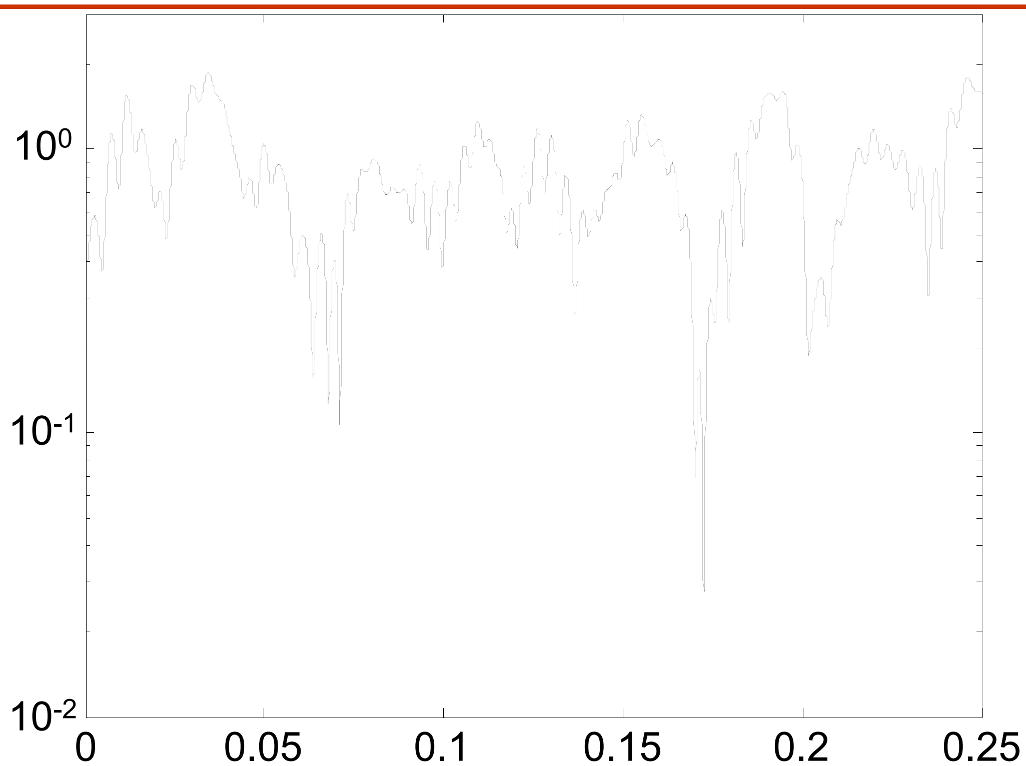

## Comparison in Auto-Correlation

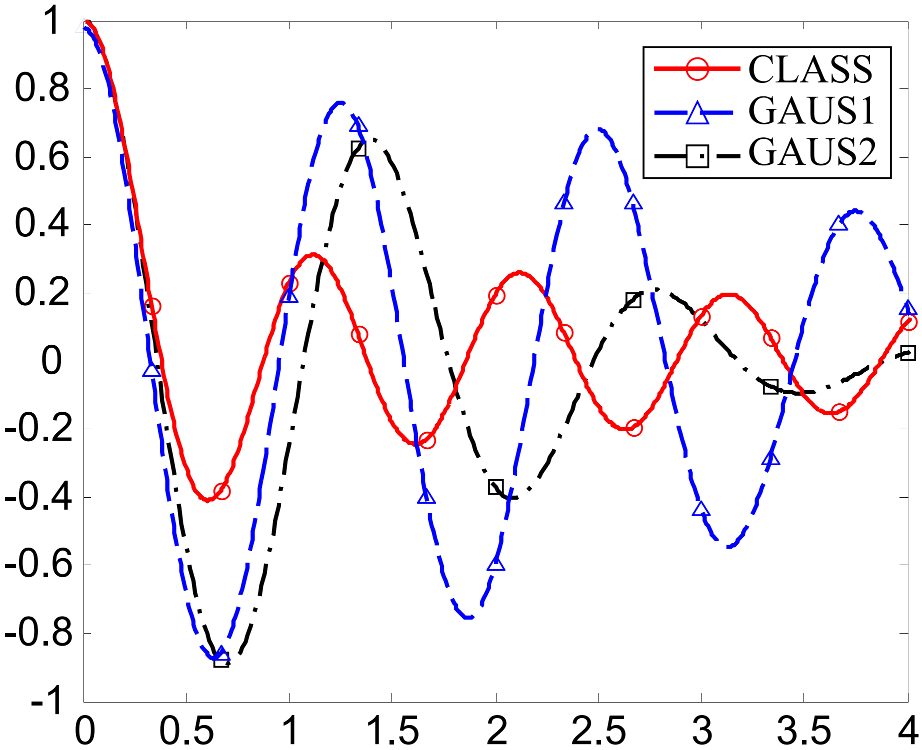




# IEEE 802.16 Broadband Wireless Access Working Group

(Channel Models for Fixed Wireless Applications)

# IEEE 802.16 Broadband Wireless Access

- **Channel Models for Fixed Wireless Applications** (2003)
  - A set of propagation models applicable to the multi-cell architecture with non-line-of-sight (NLOS) conditions is presented.
- Typically, the scenario is as follows:
  - Cells are < 10 km in radius
  - Under-the-eave/window or rooftop installed **directional** antennas (2 – 10 m) at the receiver
  - 15 – 40 m BTS antennas
  - High cell coverage requirement (80-90%)
- The wireless channel is characterized by:
  - Path loss (including shadowing), Multipath delay spread, Fading characteristics, Doppler spread, Co-channel and adjacent channel interference



# IEEE 802.16 CMs – Path Loss

- For a given close-in reference distance $d_0$, the path loss is

$$PL_{(\mathrm{dB})} = A + 10\gamma \log_{10}(d/d_0) + s, \quad \text{for } d > d_0$$

$$A = 20\log_{10}(4\pi d_0/\lambda), \quad \gamma = a - bh_b + c/h_b, \quad d_0 = 100m$$

  - **Category A:** hilly terrain with moderate-to-heavy tree densities
  - **Category B:** Intermediate path loss condition
  - **Category C:** mostly flat terrain with light tree densities
  - $s$: the shadowing effect, which follows lognormal distribution with the std. ranged between **8.2** and **10.6 dB**.

| Model parameter | Terrain Type A | Terrain Type B | Terrain Type C |
|---|---|---|---|
| $a$ | 4.6 | 4 | 3.6 |
| $b$ | 0.0075 | 0.0065 | 0.005 |
| $c$ | 12.6 | 17.1 | 20 |

# IEEE 802.16 CMs – Path Loss (Cont.)

- The above path loss model is based on published literature for frequencies close to **2 GHz** and for receive antenna heights close to **2 m**.
- In order to use the model for other frequencies and for **receive antenna heights** between **2 m and 10 m**, correction terms have to be included.

$$PL_{\text{modified}} = PL + \Delta PL_f + \Delta PL_h$$

  - The frequency (MHz) correction term: $\Delta PL_f = 6\log_{10}(f/2000)$
  - The receive antenna height correction term:
    - Categories A and B: $\Delta PL_h = -10.8\log_{10}(h_b/2)$
    - Category C: $\Delta PL_h = -20\log_{10}(h_b/2)$



# IEEE 802.16 CMs – Multipath Delay Profile

- For directional antennas, the delay profile can be represented by **a spike-plus-exponential shape**. It is characterized by $\tau_{\text{rms}}$ (RMS delay spread) which is defined as

$$\tau_{\text{rms}} = \sqrt{\sum_j P_j \tau_j^2 - (\tau_{\text{avg}})^2}$$

- The delay profile is given by

$$P(\tau) = A\delta(\tau) + B\sum_{i=0}^{\infty} \exp(-i\Delta\tau/\tau_0)\delta(\tau - i\Delta\tau)$$

  - where $A$, $B$ and $\Delta\tau$ are experimentally determined
- The delay spread model is of the following form $\boxed{\tau_{\text{rms}} = T_1 d^{\varepsilon} y}$
  - where $d$ is the distance in km, $T_1$ is the median value of $\tau_{\text{rms}}$ at $d$ = 1 km, $\varepsilon$ is an exponent that lies between 0.5-1.0, and $y$ is a lognormal variate.
  - 32° and 10° **directive antennas** reduce the median $\tau_{\text{rms}}$ values for omni-directional antennas by factors of 2.3 and 2.6, respectively.

# IEEE 802.16 CMs – Fading Characteristics

- The narrow band received signal fading can be characterized by a **Ricean** distribution.
- A model for estimating the K-factor (in linear scale) is

$$K = F_s F_h F_b K_o d^{\gamma} u$$

  - $F_s$ is a **seasonal factor**, $F_s$ = 1.0 in summer (leaves); 2.5 in winter (no leaves)
  - $F_h$ is the receive antenna height factor, $F_h = (h/3)^{0.46}$ ($h$ is the receive antenna height in meters)
  - $F_b$ is the beam-width factor, $F_b = (b/17)^{-0.62}$ ($b$ in degrees)
  - $K_o$ and $\gamma$ are regression coefficients, $K_o = 10$; $\gamma = -0.5$
  - $u$ is a lognormal variable which has zero dB mean and a std. 8 dB



# IEEE 802.16 CMs – Doppler Spectrum

- In fixed wireless channels the Doppler PSD of the scattering component is mainly distributed around $f = 0$ Hz.
  - A rounded shape is used as a rough approximation

$$S(f) = \begin{cases} 1 - 1.72 f_0^2 + 0.785 f_0^4, & |f_0| \le 1 \\ 0, & |f_0| > 1 \end{cases}, \quad f_0 = \frac{f}{f_m}$$

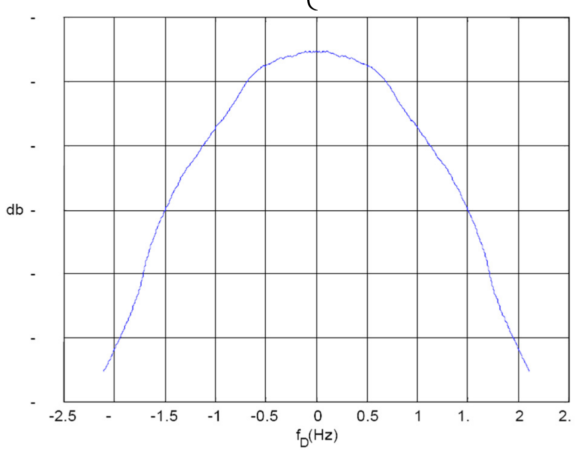


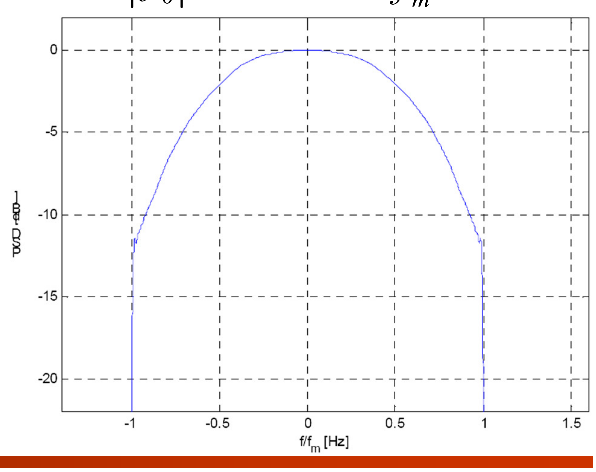

# IEEE 802.16 CMs – Antenna Gain Reduction

- The gain due to the **directivity** can be reduced because of the **scattering**.
  - The effective gain is less than the actual gain.
- Denote $\Delta G_{\mathrm{BW}}$ as the Antenna Gain Reduction Factor.
  - **Gaussian distributed** random variable (truncated at 0 dB, i.e., $\Delta G_{\mathrm{BW}} \geq 0$) with a mean ($\mu_{\mathrm{grf}}$) and std. ($\sigma_{\mathrm{grf}}$) given by

$$\mu_{\mathrm{grf}} = -(0.53 + 0.1I)\ln(\beta/360) + (0.5 + 0.04I)(\ln(\beta/360))^2$$
$$\sigma_{\mathrm{grf}} = -(0.93 + 0.02I)\ln(\beta/360)$$

  - $\beta$: the beam-width (in degrees); $I = 1$ (winter) or $I = -1$ (summer)
- In the link budget calculation, if $G$ is the gain of the antenna (dB), the effective gain of the antenna equals $G - \Delta G_{\mathrm{BW}}$.
  - If a 20-degree antenna is used, the mean of $\Delta G_{\mathrm{BW}} \approx 7$ dB.



# IEEE 802.16 CMs – Modified SUI CMs

- **Stanford University Interim (SUI)** channel models
- The parametric view of the SUI channels is summarized in the following tables.

| SUI Channels | Terrain Type | Delay Spread | Doppler Spread | K-Factor |
|---|---|---|---|---|
| **SUI-1** | C | Low | Low | High |
| **SUI-2** | C | Low | Low | High |
| **SUI-3** | B | Low | Low | Low |
| **SUI-4** | B | Moderate | High | Low |
| **SUI-5** | A | High | Low | Low |
| **SUI-6** | A | High | High | Low |

# IEEE 802.16 CMs – SUI - 1 Channel Model

| SUI - 1 | Tap 1 | Tap 2 | Tap 3 | Units |
|---|---|---|---|---|
| Delay | 0 | 0.4 | 0.9 | μs |
| Power (omni ant.)<br>90 % K-fact.<br>75 % K-fact. | 0<br>4<br>20 | -15<br>0<br>0 | -20<br>0<br>0 | dB |
| Power (30° ant.)<br>90 % K-fact.<br>75 % K-fact. | 0<br>16<br>72 | -21<br>0<br>0 | -32<br>0<br>0 | dB |
| Doppler | 0.4 | 0.3 | 0.5 | Hz |

**Antenna Correlation:** $\rho_{ENV} = 0.7$
**Gain Reduction Factor:** $\Delta G_{BW} = 0$ dB
**Normalization Factor:**
$F_{omni} = -0.1771$ dB, $F_{30°} = -0.0371$ dB

**Terrain Type:** C
**Omni antenna:** $\tau_{RMS} = 0.111$ μs,
overall $K$: $K = 3.3$ (90%); $K = 10.4$ (75%)
**30° antenna:** $\tau_{RMS} = 0.042$ μs,
overall $K$: $K = 14.0$ (90%); $K = 44.2$ (75%)



# 3GPP 5G Channel Models

# 3GPP 5G Channel Models

- Study on channel model for frequencies from **0.5 to 100 GHz**
  – 3GPP TR 38.901 V16.0.0 (2019-10)
- The channel model is applicable for **link-level** and **system-level** simulations in the following conditions:
- For system level simulations, supported scenarios are
  – Urban microcell street canyon (UMi)
  – Urban macrocell (UMa)
  – Rural macrocell (RMa)
  – Indoor hotspot office (InH)
  – Indoor factory (InF)
- Bandwidth is supported up to **10%** of the center frequency but no larger than **2GHz**.



# Path Loss

- The distance definitions includes 3D distance and 2D distance
  – Outdoor UEs: $d_{2D}$, $d_{3D}$
  – Indoor UEs: $d_{2D\text{-out}}$, $d_{2D\text{-in}}$, $d_{3D\text{-out}}$, $d_{3D\text{-in}}$

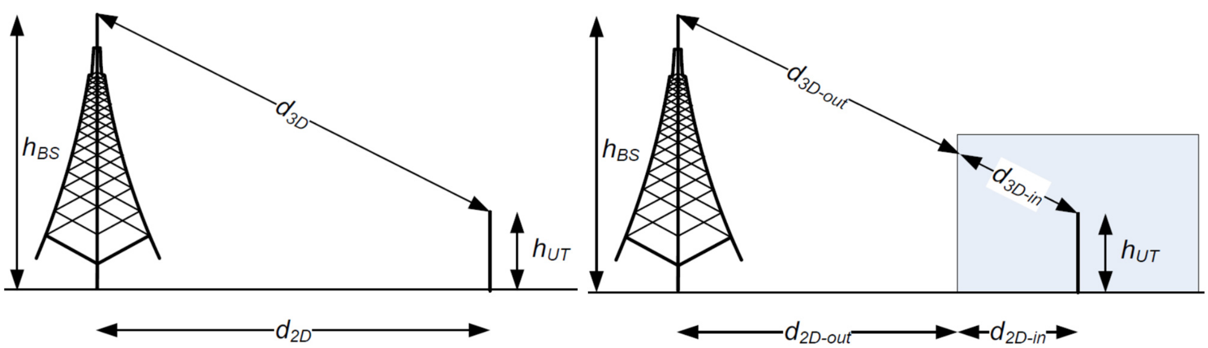


**$d_{2D}$ and $d_{3D}$ for outdoor UTs** **$d_{2D\text{-out}}$, $d_{2D\text{-in}}$ and $d_{3D\text{-out}}$, $d_{3D\text{-in}}$ for indoor UTs**

# Path Loss (Cont.)

- RMa

| | | Path loss | Shadow fading | Parameters |
|---|---|---|---|---|
| RMa | LOS | $PL_{\text{RMa-LOS}} = \begin{cases} PL_1 & 10\text{m} \le d_{2D} \le d_{BP} \\ PL_2 & d_{BP} \le d_{2D} \le 10\text{km} \end{cases}$, see note 5<br>$PL_1 = 20\log_{10}(40\pi d_{3D} f_c / 3) + \min(0.03h^{1.72}, 10)\log_{10}(d_{3D}) - \min(0.044h^{1.72}, 14.77) + 0.002\log_{10}(h) d_{3D}$<br>$PL_2 = PL_1(d_{BP}) + 40\log_{10}(d_{3D}/d_{BP})$ | $\sigma_{SF} = 4$<br>$\sigma_{SF} = 6$ | $h_{BS} = 35\text{m}$<br>$h_{UT} = 1.5\text{m}$<br>$W = 20\text{m}$<br>$h = 5\text{m}$<br>h = avg. building height<br>W = avg. street width<br>The applicability ranges:<br>$5\text{m} \le h \le 50\text{m}$<br>$5\text{m} \le W \le 50\text{m}$<br>$10\text{m} \le h_{BS} \le 150\text{m}$<br>$1\text{m} \le h_{UT} \le 10\text{m}$ |
| | NLOS | $PL_{\text{RMa-NLOS}} = \max(PL_{\text{RMa-LOS}}, PL'_{\text{RMa-NLOS}})$<br>for $10\text{m} \le d_{2D} \le 5\text{km}$<br>$PL'_{\text{RMa-NLOS}} = 161.04 - 7.1\log_{10}(W) + 7.5\log_{10}(h) - (24.37 - 3.7(h/h_{BS})^2)\log_{10}(h_{BS}) + (43.42 - 3.1\log_{10}(h_{BS}))(\log_{10}(d_{3D}) - 3) + 20\log_{10}(f_c) - (3.2(\log_{10}(11.75h_{UT}))^2 - 4.97)$ | $\sigma_{SF} = 8$ | |



# Path Loss (Cont.)

- UMa

| | | Path loss | Shadow fading | Parameters |
|---|---|---|---|---|
| UMa | LOS | $PL_{\text{UMa-LOS}} = \begin{cases} PL_1 & 10\text{m} \le d_{2D} \le d'_{BP} \\ PL_2 & d'_{BP} \le d_{2D} \le 5\text{km} \end{cases}$, see note 1<br>$PL_1 = 28.0 + 22\log_{10}(d_{3D}) + 20\log_{10}(f_c)$<br>$PL_2 = 28.0 + 40\log_{10}(d_{3D}) + 20\log_{10}(f_c) - 9\log_{10}((d'_{BP})^2 + (h_{BS} - h_{UT})^2)$ | $\sigma_{SF} = 4$ | $1.5\text{m} \le h_{UT} \le 22.5\text{m}$<br>$h_{BS} = 25\text{m}$ |
| | NLOS | $PL_{\text{UMa-NLOS}} = \max(PL_{\text{UMa-LOS}}, PL'_{\text{UMa-NLOS}})$<br>for $10\text{m} \le d_{2D} \le 5\text{km}$<br>$PL'_{\text{UMa-NLOS}} = 13.54 + 39.08\log_{10}(d_{3D}) + 20\log_{10}(f_c) - 0.6(h_{UT} - 1.5)$ | $\sigma_{SF} = 6$ | $1.5\text{m} \le h_{UT} \le 22.5\text{m}$<br>$h_{BS} = 25\text{m}$<br>Explanations: see note 3 |
| | | Optional $\text{PL} = 32.4 + 20\log_{10}(f_c) + 30\log_{10}(d_{3D})$ | $\sigma_{SF} = 7.8$ | |

# Path Loss (Cont.)

- UMi

| | | | | |
|---|---|---|---|---|
| UMi - Street Canyon | LOS | $PL_{\text{UMi-LOS}} = \begin{cases} PL_1 & 10\text{m} \le d_{2D} \le d'_{BP} \\ PL_2 & d'_{BP} \le d_{2D} \le 5\text{km} \end{cases}$, see note 1<br>$PL_1 = 32.4 + 21\log_{10}(d_{3D}) + 20\log_{10}(f_c)$<br>$PL_2 = 32.4 + 40\log_{10}(d_{3D}) + 20\log_{10}(f_c) - 9.5\log_{10}((d'_{BP})^2 + (h_{BS} - h_{UT})^2)$ | $\sigma_{SF} = 4$ | $1.5\text{m} \le h_{UT} \le 22.5\text{m}$<br>$h_{BS} = 10\text{m}$ |
| | NLOS | $PL_{\text{UMi-NLOS}} = \max(PL_{\text{UMi-LOS}}, PL'_{\text{UMi-NLOS}})$ for $10\text{m} \le d_{2D} \le 5\text{km}$<br>$PL'_{\text{UMi-NLOS}} = 35.3\log_{10}(d_{3D}) + 22.4 + 21.3\log_{10}(f_c) - 0.3(h_{UT} - 1.5)$ | $\sigma_{SF} = 7.82$ | $1.5\text{m} \le h_{UT} \le 22.5\text{m}$<br>$h_{BS} = 10\text{m}$<br>Explanations: see note 4 |



# LOS/NLOS Scenarios

- The LOS/NLOS scenarios are probabilistic with probabilities

| Scenario | LOS probability (distance is in meters) |
|---|---|
| RMa | $\Pr_{LOS} = \begin{cases} 1 & , d_{\text{2D-out}} \le 10\text{m} \\ \exp\left(-\frac{d_{\text{2D-out}} - 10}{1000}\right) & , 10\text{m} < d_{\text{2D-out}} \end{cases}$ |
| UMi - Street canyon | $\Pr_{LOS} = \begin{cases} 1 & , d_{\text{2D-out}} \le 18\text{m} \\ \frac{18}{d_{\text{2D-out}}} + \exp\left(-\frac{d_{\text{2D-out}}}{36}\right)\left(1 - \frac{18}{d_{\text{2D-out}}}\right) & , 18\text{m} < d_{\text{2D-out}} \end{cases}$ |
| UMa | $\Pr_{LOS} = \begin{cases} 1 & , d_{\text{2D-out}} \le 18\text{m} \\ \left[\frac{18}{d_{\text{2D-out}}} + \exp\left(-\frac{d_{\text{2D-out}}}{63}\right)\left(1 - \frac{18}{d_{\text{2D-out}}}\right)\right]\left(1 + C'(h_{UT})\frac{5}{4}\left(\frac{d_{\text{2D-out}}}{100}\right)^3 \exp\left(-\frac{d_{\text{2D-out}}}{150}\right)\right) & , 18\text{m} < d_{\text{2D-out}} \end{cases}$<br>where<br>$C'(h_{UT}) = \begin{cases} 0 & , h_{UT} \le 13\text{m} \\ \left(\frac{h_{UT} - 13}{10}\right)^{1.5} & , 13\text{m} < h_{UT} \le 23\text{m} \end{cases}$ |

## Shadowing

- The log-normal shadowing fading (in dB) is characterized by a Gaussian distributed random variable with zero mean and standard deviation $\sigma$.
- Due to the slow fading process versus distance $\Delta x$, adjacent fading values are correlated.
- Its normalized autocorrelation function $R(\Delta x)$ can be described by an exponential function

$$R(\Delta x) = \exp\left(-|\Delta x| / d_{cor}\right)$$

  - $d_{cor}$: the decorrelation length, which depends on the environment



## System-level Model/Link-level Model

- The **system-level model** is a **multi-link** physical model intended for **performance evaluation**
  - Each link represents **a cell** or **a sector within a cell**.
  - An MS receives **interference** from adjacent sectors of adjacent cells.
- Each link comprises an MS and BS **MIMO antenna array**
- Propagation is via **multipaths** and **sub-paths**.
  - The excess delays of **sub-paths** are closely clustered **around the delay of their (parent) multipath**.
  - This is assumed to originate from an environment with **closely spaced clusters of scatterers**.

# Link-level Model

- The clustered scatterers and resulting multipaths and sub-paths

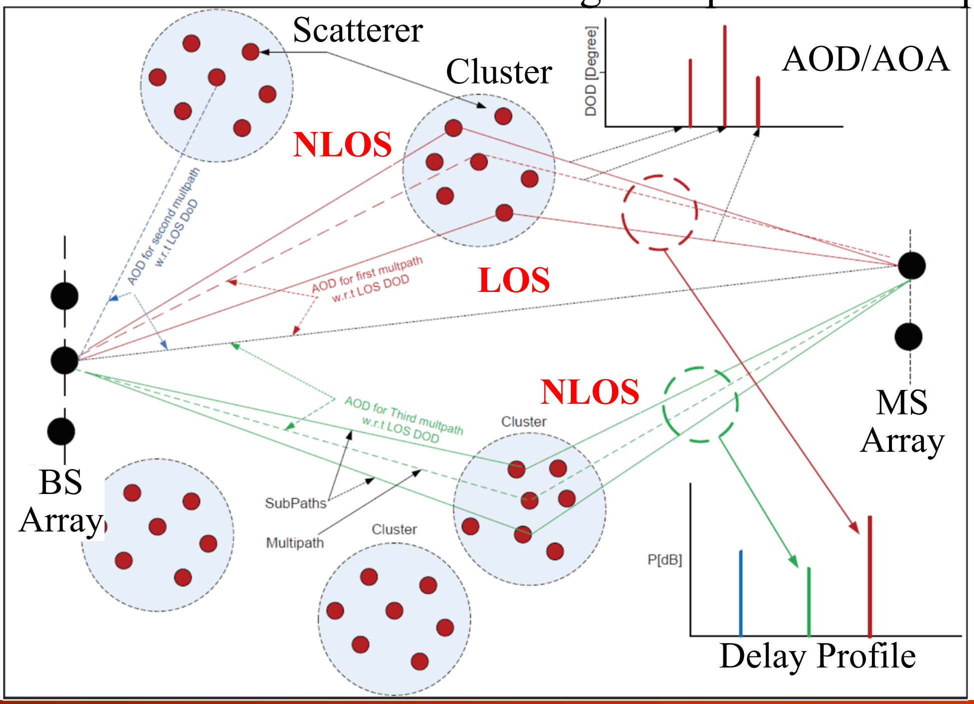




# Coordinate System

- The space is defined by the **zenith** angle $\theta$ (0° – 180°) and the **azimuth** angle $\phi$ (0° – 360°) in a Cartesian coordinate system
  - $\theta = 0°$ points to the **zenith** and $\theta = 90°$ points to the **horizon**.

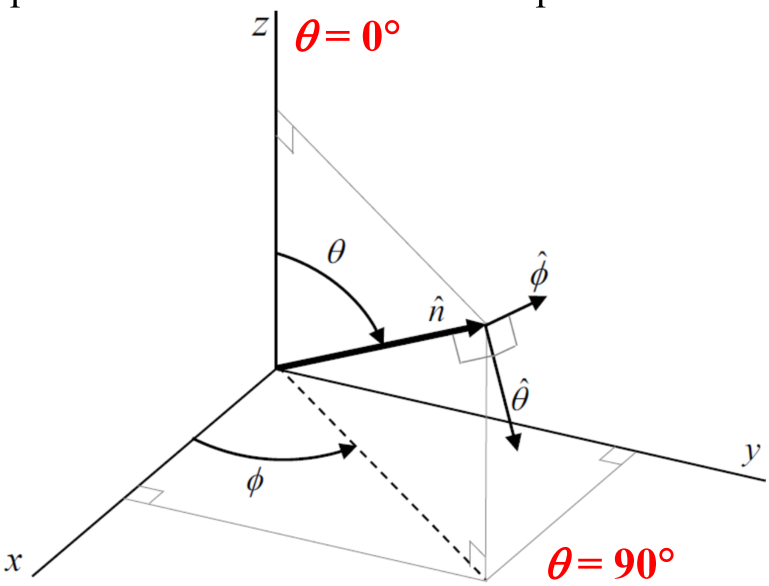

# Generate Cluster Delays

- Delays are drawn randomly from the exponential delay distribution $\tau'_n = -r_\tau \mathrm{DS} \ln(X_n)$
  - $r_\tau$ is the delay distribution proportionality factor
  - DS: rms delay spread
  - $X_n$: **uniformly** distributed within (0,1)
- For $X$ follows the uniform distribution within (0,1), $Y = -\ln X$ is exponentially distributed with the pdf $f(y) = e^{-y}$ and $E[Y] = 1$
  - $\tau'_n$ follows the **exponential distribution** with mean $r_\tau \mathrm{DS}$
- Normalize the delays by subtracting the **minimum delay** (only the relative delays are important) and sort the normalized delays in an ascending order

$$\tau_n = \mathrm{sort}\left(\tau'_n - \min\left(\tau'_n\right)\right)$$



# Generate Cluster Powers

- Cluster powers are calculated assuming a single slope **exponential** power delay profile.
- With exponential delay distribution the cluster powers are determined by

$$P'_n = \exp\left(-\tau_n \frac{r_\tau - 1}{r_\tau \mathrm{DS}}\right) \times \underline{10^{-Z_n/10}}$$

**Log-normal shadowing**

  - where $Z_n \sim N(0, \zeta^2)$ is the per cluster **shadowing** term in dB
- Normalize the cluster powers so that the sum of all cluster powers is equal to one, i.e., $P_n = P'_n \Big/ \sum_{n=1}^{N} P'_n$
- In the case of **LOS** condition:
  - Power of the single LOS ray is: $P_{1,\mathrm{LOS}} = K_\mathrm{R} \big/ \left(K_\mathrm{R} + 1\right)$
  - The cluster powers are $P_n = \dfrac{1}{K_\mathrm{R} + 1} \times \left(P'_n \Big/ \sum_{n=1}^{N} P'_n\right)$
  - $K_\mathrm{R}$ is the Ricean $K$-factor

# Generate Departure and Arrival Angles

- For **the *n*-th NLOS cluster**, the AOA of the cluster $\phi_{n,\mathrm{AOA}}$ is randomly generated **centering on the AOA of LOS**
  - Depending on the **Azimuth angle Spread of Arrival** (ASA)
- The AOAs are determined by applying the inverse Gaussian function with input parameters $P_n$ and RMS angle spread ASA

$$\phi'_{n,\mathrm{AOA}} = \frac{2(\mathrm{ASA}/1.4)\sqrt{-\ln\left[P_n/\max(P_n)\right]}}{C_\phi}$$

  - $P_n$ is the power of the $n$-th NLOS cluster
  - $C_\phi$ is a scaling factor related to the total number of clusters

$$\phi_{n,\mathrm{AOA}} = X_n\phi'_{n,\mathrm{AOA}} + Y_n + \phi_{\mathrm{LOS,AOA}}$$

  - $X_n$: a random variable equiprobable within the set $\{1, -1\}$
  - $Y_n \sim N\left(0,(\mathrm{ASA}/7)^2\right)$ and $\phi_{\mathrm{LOS,AOA}}$ is the LOS direction



# Generate Departure and Arrival Angles (Cont.)

- Generate the azimuth angle of arrival (AOA) for **the *m*-th ray in the *n*-th cluster**: $\phi_{n,m,\mathrm{AOA}} = \phi_{n,\mathrm{AOA}} + c_{\mathrm{ASA}}\alpha_m$
  - $c_{\mathrm{ASA}}$ is the **cluster-wise** rms azimuth spread of arrival angles
- The generation of AOD ($\phi_{n,m,\mathrm{AOD}}$), ZOA ($\theta_{n,m,\mathrm{AOA}}$), and ZOD ($\theta_{n,m,\mathrm{AOD}}$) follows a procedure similar to that for AOA.

| **Ray number *m*** | **Basis vector of offset angles $\alpha_m$** |
|---|---|
| 1, 2 | ± 0.0447 |
| 3, 4 | ± 0.1413 |
| 5, 6 | ± 0.2492 |
| 7, 8 | ± 0.3715 |
| 9, 10 | ± 0.5129 |
| 11, 12 | ± 0.6797 |
| 13, 14 | ± 0.8844 |
| 15, 16 | ± 1.1481 |
| 17, 18 | ± 1.5195 |
| 19, 20 | ± 2.1551 |

# Coupling of Rays within a Cluster

- Couple **randomly AOD** angles $\phi_{n,m,\mathrm{AOD}}$ with **AOA** angles $\phi_{n,m,\mathrm{AOA}}$ within a cluster $n$.
- Couple **randomly ZOD** angles $\theta_{n,m,\mathrm{AOD}}$ with **ZOA** angles $\theta_{n,m,\mathrm{AOA}}$ within a cluster $n$.
- Couple **randomly AOD** angles $\phi_{n,m,\mathrm{AOD}}$ with **ZOD** angles $\theta_{n,m,\mathrm{AOD}}$ within a cluster $n$.



# Cross Polarization Power Ratios

- Generate the **cross polarization power ratios** (XPR) $\kappa$ for each ray $m$ of each cluster $n$.
  - XPR is **log-Normal distributed**

$$\kappa_{n,m} = 10^{X_{n,m}/10}$$

  - where $X_{n,m} \sim N\left(\mu_{\mathrm{XPR}}, \sigma^2_{\mathrm{XPR}}\right)$ is **Gaussian** distributed
- In general, **co-polarization** represents the polarization the antenna is intended to radiate (or receive) and **cross-polarization** represents the polarization **orthogonal to** the co-polarization
- When **cross-polarized panel array antenna** is used, different polarization antennas have different but correlated received powers

# Initial Random Phases

- Draw random initial phases $\left\{\Phi_{n,m}^{\theta\theta}, \Phi_{n,m}^{\theta\phi}, \Phi_{n,m}^{\phi\theta}, \Phi_{n,m}^{\phi\phi}\right\}$ for each ray $m$ of each cluster $n$
  – Four polarization combinations ($\theta\theta$, $\theta\phi$, $\phi\theta$, $\phi\phi$) (AOD/AOA pair)
  – Uniformly distributed within ($-\pi$, $\pi$)



# Generate Channel Coefficients

- The method can be used for **drop-based evaluations**
  – Irrespective of user speed
- For the ***N* – 2 weakest** (**NLOS**) (i.e., 3, 4, …, $N$) **clusters**, the channel coefficients, for each receiver (UE) and transmitter (BS) element pair ($u$, $s$), are given by

$$H_{u,s,n}^{\text{NLOS}}(t) = \sqrt{\frac{P_n}{M}} \underbrace{\sum_{m=1}^{M}}_{\text{Sum of } M \text{ rays}} \overbrace{\begin{bmatrix} F_{rx,u,\theta}\left(\theta_{n,m,\text{ZOA}}, \phi_{n,m,\text{AOA}}\right) \\ F_{rx,u,\phi}\left(\theta_{n,m,\text{ZOA}}, \phi_{n,m,\text{AOA}}\right) \end{bmatrix}}^{\text{UE antenna pattern}}{}^{\mathrm{T}} \overbrace{\begin{bmatrix} \exp\left(j\Phi_{n,m}^{\theta\theta}\right) & \sqrt{\kappa_{n,m}^{-1}} \exp\left(j\Phi_{n,m}^{\theta\phi}\right) \\ \sqrt{\kappa_{n,m}^{-1}} \exp\left(j\Phi_{n,m}^{\phi\theta}\right) & \exp\left(j\Phi_{n,m}^{\phi\phi}\right) \end{bmatrix}}^{\text{Coupling between polarization components with random phases}}$$

$$\underbrace{\begin{bmatrix} F_{tx,s,\theta}\left(\theta_{n,m,\text{ZOD}}, \phi_{n,m,\text{AOD}}\right) \\ F_{tx,s,\phi}\left(\theta_{n,m,\text{ZOD}}, \phi_{n,m,\text{AOD}}\right) \end{bmatrix}}_{\text{BS antenna pattern}} \underbrace{\exp\left(\frac{j2\pi \mathbf{r}_{rx,n,m}^{\mathrm{T}} \cdot \mathbf{d}_{rx,u}}{\lambda_0}\right)}_{\text{Phase offset of UE antenna } u} \underbrace{\exp\left(\frac{j2\pi \mathbf{r}_{tx,n,m}^{\mathrm{T}} \cdot \mathbf{d}_{tx,s}}{\lambda_0}\right)}_{\text{Phase offset of BS antenna } s} \underbrace{\exp\left(\frac{j2\pi \mathbf{r}_{rx,n,m}^{\mathrm{T}} \cdot \mathbf{v}t}{\lambda_0}\right)}_{\text{Doppler phase shift}}$$

# Generate Channel Coefficients (Cont.)

- $rx$: receiver (UE); $tx$: transmitter (BS)
- $F_{rx,u,\theta}$ and $F_{rx,u,\phi}$ are the **field patterns** of receive antenna element $u$, corresponding to $\theta$ and $\phi$, respectively.
- $F_{tx,s,\theta}$ and $F_{tx,s,\phi}$ are the **field patterns** of transmit antenna element $s$, corresponding to $\theta$ and $\phi$, respectively.
- $\mathbf{r}_{rx,n,m}$ is the **spherical unit vector** with azimuth arrival angle $\phi_{n,m,\mathrm{AOA}}$ and elevation arrival angle $\theta_{n,m,\mathrm{ZOA}}$
- $\mathbf{r}_{tx,n,m}$ is the **spherical unit vector** with azimuth arrival angle $\phi_{n,m,\mathrm{AOD}}$ and elevation arrival angle $\theta_{n,m,\mathrm{ZOD}}$
- $\mathbf{d}_{rx,u}$ is the **location vector** of receive antenna element $u$
- $\mathbf{d}_{tx,s}$ is the **location vector** of transmit antenna element $s$
- $\mathbf{v}$ is the UE **velocity vector** with speed $v$
- $\lambda_0$ is the **wavelength** of the carrier frequency



# Generate Channel Coefficients (Cont.) – NLOS

- For the **two strongest clusters** (i.e., $n$ = 1 and 2) with **NLOS**, rays are spread in delay to three sub-clusters (per cluster)
  - $\tau_{n,1} = \tau_n$ ; $\tau_{n,2} = \tau_n + 1.28\, c_{DS}$ ; $\tau_{n,3} = \tau_n + 2.56\, c_{DS}$
  - $c_{\mathrm{DS}}$ is the **cluster delay spread**
- Twenty rays of a cluster are mapped to sub-clusters

| **Sub-cluster # $i$** | **Mapping to rays $R_i$** | **Delay offset $\tau_{n,1} - \tau_n$** |
|---|---|---|
| $i = 1$ | $R_1$ = {1, 2, 3, 4, 5, 6, 7, 8, 19, 20} | 0 |
| $i = 2$ | $R_2$ = {9, 10, 11, 12, 17, 18} | 1.28 $c_{\mathrm{DS}}$ |
| $i = 3$ | $R_3$ = {13, 14, 15, 16} | 2.56 $c_{\mathrm{DS}}$ |

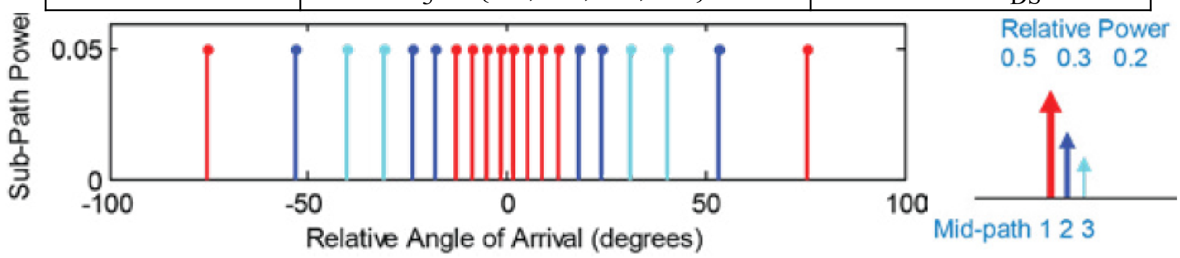

## Generate Channel Coefficients (Cont.) – NLOS

- Then, the channel impulse response is given by:

$$H_{u,s}^{\text{NLOS}}(\tau,t)=\sum_{n=1}^{2}\underbrace{\sum_{i=1}^{3}}_{\text{Sub-cluster}}\underbrace{\sum_{m\in R_i}}_{\text{Ray}} H_{u,s,n,m}^{\text{NLOS}}(t)\delta(\tau-\tau_{n,i})+\sum_{n=3}^{N}H_{u,s,n}^{\text{NLOS}}(t)\delta(\tau-\tau_n)$$

- The channel coefficients for the two strongest clusters are

$$H_{u,s,n,m}^{\text{NLOS}}(t)=\sqrt{\frac{P_n}{M}}\begin{bmatrix}F_{rx,u,\theta}\left(\theta_{n,m,\text{ZOA}},\phi_{n,m,\text{AOA}}\right)\\ F_{rx,u,\phi}\left(\theta_{n,m,\text{ZOA}},\phi_{n,m,\text{AOA}}\right)\end{bmatrix}^{\text{T}}\begin{bmatrix}\exp\left(j\Phi_{n,m}^{\theta\theta}\right) & \sqrt{\kappa_{n,m}^{-1}}\exp\left(j\Phi_{n,m}^{\theta\phi}\right)\\ \sqrt{\kappa_{n,m}^{-1}}\exp\left(j\Phi_{n,m}^{\phi\theta}\right) & \exp\left(j\Phi_{n,m}^{\phi\phi}\right)\end{bmatrix}$$
$$\begin{bmatrix}F_{tx,s,\theta}\left(\theta_{n,m,\text{ZOD}},\phi_{n,m,\text{AOD}}\right)\\ F_{tx,s,\phi}\left(\theta_{n,m,\text{ZOD}},\phi_{n,m,\text{AOD}}\right)\end{bmatrix}\exp\left(\frac{j2\pi\mathbf{r}_{rx,n,m}^{\text{T}}\cdot\mathbf{d}_{rx,u}}{\lambda_0}\right)\exp\left(\frac{j2\pi\mathbf{r}_{tx,n,m}^{\text{T}}\cdot\mathbf{d}_{tx,s}}{\lambda_0}\right)\exp\left(\frac{j2\pi\mathbf{r}_{rx,n,m}^{\text{T}}\cdot\mathbf{v}t}{\lambda_0}\right)$$



## Generate Channel Coefficients (Cont.) – LOS

- For the **LOS case**, the LOS channel coefficient is given as:

$$H_{u,s,1}^{\text{LOS}}(t)=\sqrt{\frac{P_n}{M}}\begin{bmatrix}F_{rx,u,\theta}\left(\theta_{\text{LOS,ZOA}},\phi_{\text{LOS,AOA}}\right)\\ F_{rx,u,\phi}\left(\theta_{\text{LOS,ZOA}},\phi_{\text{LOS,AOA}}\right)\end{bmatrix}^{\text{T}}\begin{bmatrix}1 & 0\\ 0 & -1\end{bmatrix}\begin{bmatrix}F_{tx,s,\theta}\left(\theta_{\text{LOS,ZOD}},\phi_{\text{LOS,AOD}}\right)\\ F_{tx,s,\phi}\left(\theta_{\text{LOS,ZOD}},\phi_{\text{LOS,AOD}}\right)\end{bmatrix}$$
$$\underbrace{\exp\left(\frac{-j2\pi d_{3\text{D}}}{\lambda_0}\right)}_{\text{Phase offset due to propagation}}\exp\left(\frac{j2\pi\mathbf{r}_{rx,\text{LOS}}^{\text{T}}\cdot\mathbf{d}_{rx,u}}{\lambda_0}\right)\exp\left(\frac{j2\pi\mathbf{r}_{tx,\text{LOS}}^{\text{T}}\cdot\mathbf{d}_{tx,s}}{\lambda_0}\right)\exp\left(\frac{j2\pi\mathbf{r}_{rx,\text{LOS}}^{\text{T}}\cdot\mathbf{v}t}{\lambda_0}\right)$$

  - $d_{3\text{D}}$ is the 3D distance between Tx and Rx
- Then, the channel impulse response is given by:

$$H_{u,s}^{\text{LOS}}(\tau,t)=\sqrt{\frac{1}{K_{\text{R}}+1}}H_{u,s}^{\text{NLOS}}(\tau,t)+\sqrt{\frac{K_{\text{R}}}{K_{\text{R}}+1}}H_{u,s,1}^{\text{LOS}}(t)\delta(\tau-\tau_1)$$

  - $K_{\text{R}}$ is the Ricean K-factor

# CDL Channel Models

- The CDL (**Clustered Delay Line**) channel models are defined for the full frequency range from 0.5 GHz to 100 GHz with a maximum bandwidth of **2 GHz**.
- Three CDL models, **CDL-A**, **CDL-B** and **CDL-C**, are constructed to represent three **NLOS** channel profiles
- Two models, **CDL-D** and **CDL-E**, are constructed for **LOS**
- Each CDL model can be **scaled in delay** so that the model achieves a desired **RMS delay spread**
- Each CDL model can also be **scaled in angles** so that the model achieves desired **angle spreads**



# CDL Channel Model Generation

- The following step by step procedure should be used to generate channel coefficients using the CDL models.
- Step 1: Generate departure and arrival angles
- Step 2: Coupling of rays within a cluster for both azimuth and elevation
- Step 3: Generate the cross polarization power ratios
- Step 4: Coefficient generation

# Generate Departure and Arrival Angles

- For the $n$-th NLOS cluster, the AOA of the cluster $\phi_{n,\mathrm{AOA}}$ is **pre-defined** in the CDL channel models
- Generate the azimuth angle of arrival (AOA) for the $m$-th ray in the $n$-th cluster: $\phi_{n,m,\mathrm{AOA}} = \phi_{n,\mathrm{AOA}} + c_{\mathrm{ASA}}\alpha_m$
- The generation of AOD ($\phi_{n,m,\mathrm{AOD}}$), ZOA ($\theta_{n,m,\mathrm{AOA}}$), and ZOD ($\theta_{n,m,\mathrm{AOD}}$) follows a procedure similar to that for AOA.

| **Ray number $m$** | **Basis vector of offset angles $\alpha_m$** |
|---|---|
| 1, 2 | $\pm$ 0.0447 |
| 3, 4 | $\pm$ 0.1413 |
| 5, 6 | $\pm$ 0.2492 |
| 7, 8 | $\pm$ 0.3715 |
| 9, 10 | $\pm$ 0.5129 |
| 11, 12 | $\pm$ 0.6797 |
| 13, 14 | $\pm$ 0.8844 |
| 15, 16 | $\pm$ 1.1481 |
| 17, 18 | $\pm$ 1.5195 |
| 19, 20 | $\pm$ 2.1551 |



# Generate Departure and Arrival Angles (Cont.)

- Each path is comprised of 20 **equal powered** sub-path components, spaced with increasing angle from the center.
- The summing of the sub-path carriers results in **Rayleigh fading** of each multipath.

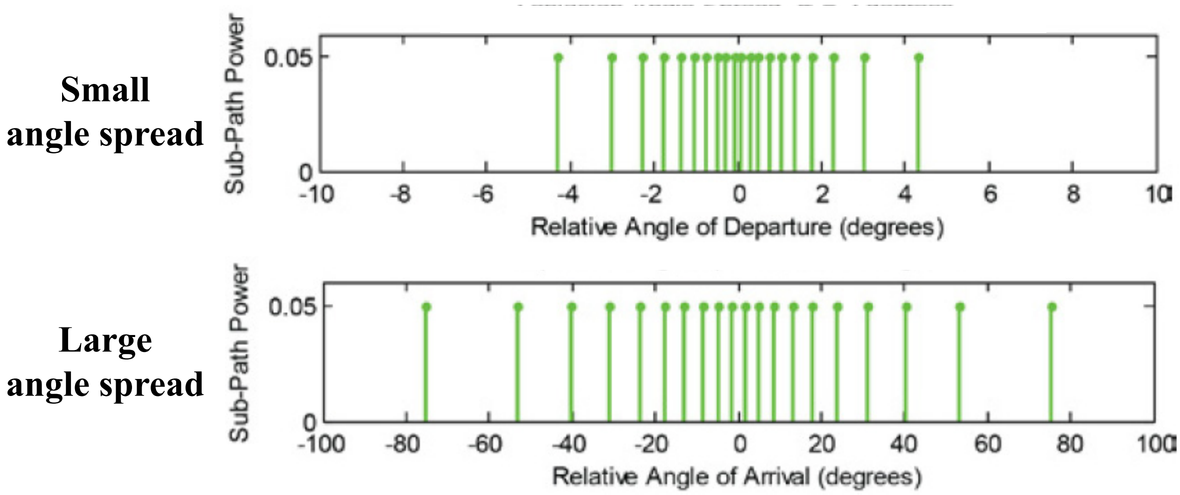

## Generate Departure and Arrival Angles (Cont.)

**CDL-A**

| Cluster # | Normalized delay | Power in [dB] | AOD in [°] | AOA in [°] | ZOD in [°] | ZOA in [°] |
|---|---|---|---|---|---|---|
| 1 | 0.0000 | –13.4 | –178.1 | 51.3 | 50.2 | 125.4 |
| 2 | 0.3819 | 0 | –4.2 | –152.7 | 93.2 | 91.3 |
| 3 | 0.4025 | –2.2 | –4.2 | –152.7 | 93.2 | 91.3 |
| 4 | 0.5868 | –4 | –4.2 | –152.7 | 93.2 | 91.3 |
| 5 | 0.4610 | –6 | 90.2 | 76.6 | 122 | 94 |
| 6 | 0.5375 | –8.2 | 90.2 | 76.6 | 122 | 94 |
| 7 | 0.6708 | –9.9 | 90.2 | 76.6 | 122 | 94 |
| 8 | 0.5750 | –10.5 | 121.5 | –1.8 | 150.2 | 47.1 |
| 9 | 0.7618 | –7.5 | –81.7 | –41.9 | 55.2 | 56 |
| 10 | 1.5375 | –15.9 | 158.4 | 94.2 | 26.4 | 30.1 |
| 11 | 1.8978 | –6.6 | –83 | 51.9 | 126.4 | 58.8 |
| 12 | 2.2242 | –16.7 | 134.8 | –115.9 | 171.6 | 26 |
| 13 | 2.1718 | –12.4 | –153 | 26.6 | 151.4 | 49.2 |
| 14 | 2.4942 | –15.2 | –172 | 76.6 | 157.2 | 143.1 |
| 15 | 2.5119 | –10.8 | –129.9 | –7 | 47.2 | 117.4 |
| 16 | 3.0582 | –11.3 | –136 | –23 | 40.4 | 122.7 |
| 17 | 4.0810 | –12.7 | 165.4 | –47.2 | 43.3 | 123.2 |
| 18 | 4.4579 | –16.2 | 148.4 | 110.4 | 161.8 | 32.6 |
| 19 | 4.5695 | –18.3 | 132.7 | 144.5 | 10.8 | 27.2 |
| 20 | 4.7966 | –18.9 | –118.6 | 155.3 | 16.7 | 15.2 |
| 21 | 5.0066 | –16.6 | –154.1 | 102 | 171.7 | 146 |
| 22 | 5.3043 | –19.9 | 126.5 | –151.8 | 22.7 | 150.7 |
| 23 | 9.6586 | –29.7 | –56.2 | 55.2 | 144.9 | 156.1 |

**Per-Cluster Parameters**

| Parameter | $c_{\mathrm{ASD}}$ in [°] | $c_{\mathrm{ASA}}$ in [°] | $c_{\mathrm{ZSD}}$ in [°] | $c_{\mathrm{ZSA}}$ in [°] | XPR in [dB] |
|---|---|---|---|---|---|
| Value | 5 | 11 | 3 | 3 | 10 |



## Coupling of Rays within a Cluster

- Couple **randomly AOD** angles $\phi_{n,m,\mathrm{AOD}}$ with **AOA** angles $\phi_{n,m,\mathrm{AOA}}$ within a cluster $n$.
- Couple **randomly ZOD** angles $\theta_{n,m,\mathrm{AOD}}$ with **ZOA** angles $\theta_{n,m,\mathrm{AOA}}$ within a cluster $n$.
- Couple **randomly AOD** angles $\phi_{n,m,\mathrm{AOD}}$ with **ZOD** angles $\theta_{n,m,\mathrm{AOD}}$ within a cluster $n$.

# Cross Polarization Power Ratios

- Generate the **cross polarization power ratios** (XPR) $\kappa$ for each ray $m$ of each cluster $n$.
  - XPR is **log-Normal distributed**

$$\kappa_{n,m} = 10^{X/10}$$

  - where $X$ is a pre-defined per-cluster XPR in dB
  - CDL-A: 10 dB
  - CDL-B: 8 dB
  - CDL-C: 7 dB
  - CDL-D: 11 dB
  - CDL-E: 8 dB



# Gain Coefficient Generation

- All clusters are treated as "**weaker cluster**", i.e. no further sub-clusters in delay should be generated.
- Draw random initial phases $\left\{\Phi_{n,m}^{\theta\theta}, \Phi_{n,m}^{\theta\phi}, \Phi_{n,m}^{\phi\theta}, \Phi_{n,m}^{\phi\phi}\right\}$ for each ray $m$ of each cluster $n$
  - Four polarization combinations ($\theta\theta$, $\theta\phi$, $\phi\theta$, $\phi\phi$) (AOD/AOA pair)
  - Uniformly distributed within $(-\pi, \pi)$
- For the **weaker** (**NLOS**) **clusters**, the channel coefficients, for each UE and BS element pair ($u$, $s$), are given by

$$H_{u,s,n}^{\mathrm{NLOS}}(t) = \sqrt{\frac{P_n}{M}} \sum_{m=1}^{M} \begin{bmatrix} F_{rx,u,\theta}\left(\theta_{n,m,\mathrm{ZOA}}, \phi_{n,m,\mathrm{AOA}}\right) \\ F_{rx,u,\phi}\left(\theta_{n,m,\mathrm{ZOA}}, \phi_{n,m,\mathrm{AOA}}\right) \end{bmatrix}^{\mathrm{T}} \begin{bmatrix} \exp\left(j\Phi_{n,m}^{\theta\theta}\right) & \sqrt{\kappa_{n,m}^{-1}} \exp\left(j\Phi_{n,m}^{\theta\phi}\right) \\ \sqrt{\kappa_{n,m}^{-1}} \exp\left(j\Phi_{n,m}^{\phi\theta}\right) & \exp\left(j\Phi_{n,m}^{\phi\phi}\right) \end{bmatrix}$$

$$\begin{bmatrix} F_{tx,s,\theta}\left(\theta_{n,m,\mathrm{ZOD}}, \phi_{n,m,\mathrm{AOD}}\right) \\ F_{tx,s,\phi}\left(\theta_{n,m,\mathrm{ZOD}}, \phi_{n,m,\mathrm{AOD}}\right) \end{bmatrix} \exp\left(\frac{j2\pi \mathbf{r}_{rx,n,m}^{\mathrm{T}} \cdot \mathbf{d}_{rx,u}}{\lambda_0}\right) \exp\left(\frac{j2\pi \mathbf{r}_{tx,n,m}^{\mathrm{T}} \cdot \mathbf{d}_{tx,s}}{\lambda_0}\right) \exp\left(\frac{j2\pi \mathbf{r}_{rx,n,m}^{\mathrm{T}} \cdot \mathbf{v}t}{\lambda_0}\right)$$